博士論文 (要約)

Recovery of Phosphorus from Sewage Sludge Ash and Synthesis of Phosphate compounds

(下水汚泥灰からのリン回収と
リン酸塩化合物の合成に関する研究)

エドウイン　マウリシオ　コルドバ　ウダエタ

博士論文 (要約)

Recovery of Phosphorus from Sewage Sludge Ash and Synthesis of Phosphate compounds

(下水汚泥灰からのリン回収と
リン酸塩化合物の合成に関する研究)

Edwin Mauricio Córdova Udaeta

東京大学大学院工学系研究科
システム創成学専攻

Preface

This research work presents novel processing methods designed to recover phosphorus from Sewage Sludge Ash (SSA) in order to obtain valuable phosphates for useful applications. The first two techniques (named in the document as Method 1 and Method 2, respectively) are presented with the goal of obtaining phosphates suitable for fertilizer applications.

The first method comprises the recovery of Phosphorus from SSA using a carbothermic reaction followed by High Gradient Magnetic Separation (HGMS) and Flotation, and the second method includes the recovery of Phosphorus from SSA using a heat treatment and liquid-liquid separation.

It was shown that the carbothermic reaction increases the magnetization of SSA, and if oxides are added, the phosphate phase obtained can be improved in terms of soil-solubility. In addition, the tests for HGMS separation followed by Flotation indicated iron is removed from the non-magnetic fraction after HGMS, and phosphorus accumulates in the flotation froth; indicating an overall enrichment in phosphorus content when these processing techniques are applied sequentially.

Secondly, this work demonstrated that it is feasible to obtain a silicon substituted phase of calcium phosphate named silicocarnotite (which has a good soil-solubility), by subjecting SSA to the heat treatment described as part of Method 2. In the same manner, the liquid-liquid separation step pointed out that silicocarnotite can be enriched in the organic fraction of a water and kerosene mixture if sodium dodecyl sulfate (SDS) is used as a surfactant.

Both of the aforementioned processing methods were developed to use physical processing techniques that have not been studied as alternatives for the recovery of phosphorus from SSA yet, and are thought to have an advantage over traditional procedures in terms of environmental impact. In addition, the methods proposed are intended to yield a phosphate phase suitable for fertilizer formulations, which primarily require that phosphorus is present in the final product as a soil-soluble phase.

Mauricio Córdova Udaeta

Acknowledgements

First, I would like to thank my parents Edwin Córdova Villegas and Gilda Udaeta Baldiviezo, and my brother Diego Córdova Udaeta for always giving me their love and inconditional support despite the distance, and for always believing in me even though the PhD course seemed really hard at times. I love you all with all my heart!

Secondly, I would like to thank Professor Toyohisa Fujita for all his help, guidance and support during the initial years of the PhD. Likewise, I would like to thank all the support and guidance provided by Associate Professor Gjergj Dodbiba during the latter part of the PhD course which is greatly appreciated.

In addition, I would like to thank my wonderful friends Alejandro Collado, Edison Marrese, Emma Sarath, Jorge Balasz, Carolina Dias Alexiou, Victor Shishkin, Saúl Sotomayor, Lewis Antill and Emil Vatai for all their support during these years, which literally have made possible the completion of the PhD course. I will forever be grateful for your help!

I am grateful for the generous collaboration of laboratory members Kim Yonggu, Dr. Josiane Ponou, Ms. Tomoko Yukoshi, and the rest of members of the Fujita-Dodbiba Laboratory who alongside the staff at the Office of the Department of Systems Innovation have in one way or another helped me a lot along the way, being really patient with me during all these years (specially when I was struggling with japanese!).

I am also grateful for the kind support of Minako Hasegawa, Samuel Soria, Miguel Serrano, Kyoko Kasakura and Miki Shibata who were kind enough to always give me a helping hand and were always present as thoughtful friends.

Lastly, the institutional support of the SEUT program at the School of Engineering, which contributed financially for the completion of the PhD course; alongside the technical support provided by Mr. Kazuhiro Fukawa, Mr. Shigeru Ohtsuka, Mr. Masahiro Fukukawa and Mr. Atsunori Murai is gratefully acknowledged.

Contents

List of Figures

List of Tables

List of Symbols

σ	Mass magnetization, specific magnetization	(emu/g)
ρ	Density	(Kg/m^3)
C_{eq}	Carbon equivalent for the reduction of iron oxide	-
D_{50}	Mass median diameter (average particle diameter by mass)	(µm)
K_a	Dissociation constant of an acid	-
K_b	Association constant of a base	-
m	Magnetic moment	(A m^2)
M	Magnetization	(A/m)
pH	Negative logarithm of the molar concentration of Hydrogen ions	-
T	Temperature	(°C)
V	Volume	(m^3)
Z	Atomic number	-

List of Acronyms

ADP	Adenosine diphosphate
ATP	Adenosine triphosphate
BET	Brunauer-Emmett-Teller theory
CAC	Critical aggregation concentration
CMC	Critical micelle concentration
DLVO	Derjaguin, Landau, Verwey and Overbeek theory
DNA	Deoxyribonucleic acid
DTA	Differential thermal analysis
EDS	Elemental diffraction spectroscopy
EDTA	Ethylenediaminetetraacetic acid
HGMS	High gradient magnetic separation
ICP-MS	Inductively coupled plasma mass spectrometry
ICP-OES	Inductively coupled plasma optical emission spectroscopy
MIBK	Methyl isobutyl ketone
PZC	Point of zero charge
RNA	Ribonucleic acid
RPM	Revolutions per minute
SCE	Silicocarnotite capture efficiency
SDS	Sodium dodecyl sulfate
SEM	Scanning electron microscopy
SSA	Sewage sludge ash
TG	Thermogravimetry
VSM	Vibrating sample magnetometer
WWTP	Wastewater treatment plant
XRD	X-Ray diffraction
XRF	X-Ray fluorescence

List of Chemical Symbols

Ag	Silver
Al	Aluminum
Al_2O_3	Aluminum oxide
As	Arsenic
As	Arsenic
Ba	Barium
BaO	Barium oxide
C	Carbon
Ca	Calcium
Ca^{2+}	Calcium ion
$Ca(NO_3)_2$	Calcium nitrate
$Ca(OH)_2$	Calcium hydroxyde
$Ca_{10}(PO_4)_6SO_4$	Francolite
$Ca_{12}Al_{14}O_{33}$	Mayenite
$Ca_2Al_2SiO_7$	Gehlenite
$Ca_3(PO_4)_2$	Calcium phosphate
$Ca_4Mg_5(PO_4)_6$	Stanfieldite
$Ca_5(PO_4)_2SiO_4$	Silicocarnotite
$Ca_5(PO_4)_3F$	Fluoroapatite
$Ca_9Al(PO_4)_7$	Calcium aluminum phosphate
$Ca_9Fe(PO_4)_7$	Calcium iron phosphate
$Ca_9Mg(PO_4)_6(PO_3OH)$	Whitlockite
$CaAl_2Si_2O_8$	Anorthite
$CaCl_2$	Calcium chloride
$CaCO_3$	Calcium carbonate
$CaNaPO_4$	Calcium sodium phosphate
CaO	Calcium oxide
Cd	Cadmium
$CH_3(CH_2)_{11}SO_4Na$	Sodium dodecyl sulfate
Cl^-	Chloride ion
CO	Carbon monoxide
CO_2	Carbon dioxide
$(CO_3)^{2-}$	Carbonate ion
Cr	Chromium
Cr_2O_3	Chromium oxide
Co	Cobalt
Cu	Copper
Cu^{2+}	Copper ion
Fe	Iron
Fe^{2+}	Ferrous ion
Fe^{3+}	Ferric ion
Fe_2O_3	Hematite
Fe_3O_4	Magnetite

FeO	Iron(II) oxide
H^+	Hydrogen ion
$(H_3O)^+$	Hydronium ion
HCl	Hydrochloric acid
HNO_3	Nitric acid
K	Potassium
K^+	Potassium ion
K_2O	Potassium oxide
KCl	Potassium chloride
KOH	Potassium hydroxyde
Mg^{2+}	Magnesium ion
$Mg_3(PO_4)_2$	Farringtonite
$MgCaSi_2O_6$	Diopside
$MgCl_2$	Magnesium Chloride
$MgNH_4PO_4 \cdot 6\,H_2O$	Struvite
MgO	Magnesium oxide
MnO	Manganese oxide
Mo	Molibdenum
N	Nitrogen
N_2	Nitrogen gas
Na	Sodium
Na^+	Sodium ion
Na_2CO_3	Sodium carbonate
Na_2SiO_3	Sodium silicate
$Na_6[(PO_3)_6]$	Sodium hexametaphosphate
$NaCl$	Sodium chloride
$NaNO_3$	Sodium nitrate
$NaOH$	Sodium hydroxyde
NH_2	Amine group
NH_3	Ammonia
Ni	Nickel
NiO	Nickel oxide
NO_x	Nitrogen oxides
$(OH)^-$	Hydroxyde ion
P	Phosphorus
P_2	Diphosphorus
P_2O_5	Phosphorus pentoxide
P_4	White phosphorus
$[PO_{4-n}S_n]$	Thiophosphate ion
$(PO_2F)_2^-$	Difluorophosphate ion
$(PO_3F)^{2-}$	Monofluorophosphate ion
$(PO_3H)_2^-$	Phosphite ion
$(PO_4)^{3-}$	Phosphate ion
Si	Silicon
SiO_2	Silicon dioxide
SO_2	Sulfur dioxide
SO_3	Sulfur trioxide
SO_x	Sulfur oxides
SrO	Strontium oxide
TiO_2	Titanium oxide

Zn	Zinc
Zn^{2+}	Zinc ion
ZnO	Zinc oxide
Zr	Zirconium

Chapter 1

The importance of phosphorus and the purpose of this study

1.1 General description of Phosphorus

Phosphorus is the chemical element represented by the symbol P. It has an atomic number Z equal to 15, and can be generally considered as a scarce element in our universe, being $3 * 10^7$ times less abundant when compared to hydrogen (Halka et al., 2010) . On planet earth, natural phosphorus can be mostly found as a solid, combined with other elements in the form of phosphates (that is, compounds having the phosphorus combined with oxygen as a ionic species). Estimates rank its relative abundance in Earth' s crust around 0.1% at the 10th or 11th position, close to the abundance of manganese (Fleischer, 1954; Yaroshevsky, 2006).

This element was isolated for the first time in 1669 by Hennig Brand in Hamburg, Germany; and got its name after the greek word "phosphoros" which is translated as "bringer of light" . This can be related to the fact that Brand originally called the substance discovered "cold fire" , and it its thought that under the conditions of his experiments, the most relevant phenomenon he may have observed was the "phosphorescence" (the phenomenon of a substance glowing in the dark), supporting the suitability of the selected name (Yaroshevsky, 2006).

Phosphorus is a relatively highly reactive non-metal element that can form different kinds of compounds. In its elemental form, P atoms can exist arranged in different ways leading to the formation of different allotropes (chemical elements existing in different forms). The most common allotrope for P is "white phosphorus" P_4, consisting of four P atoms arranged in a tetrahedral structure. This molecule is highly reactive, being oxidized spontaneously when exposed to air, oftentimes bursting into flames.

The remaining allotropes include: "red phosphorus", an amorphous arrangement of P atoms; "violet phosphorus" which can be prepared after heating "red phosphorus" to 300 °C; and "black phosphorus", obtainable after heating white phosphorus under high pressure conditions (Daintith, 2009). Additionally, when P_4 is subjected to high temperatures (in the order of 1000 K or more), the allotrope P_2 is found in the gas phase. As a reference, the physical appearance of different forms of phosphorus is presented in Fig.1.1.

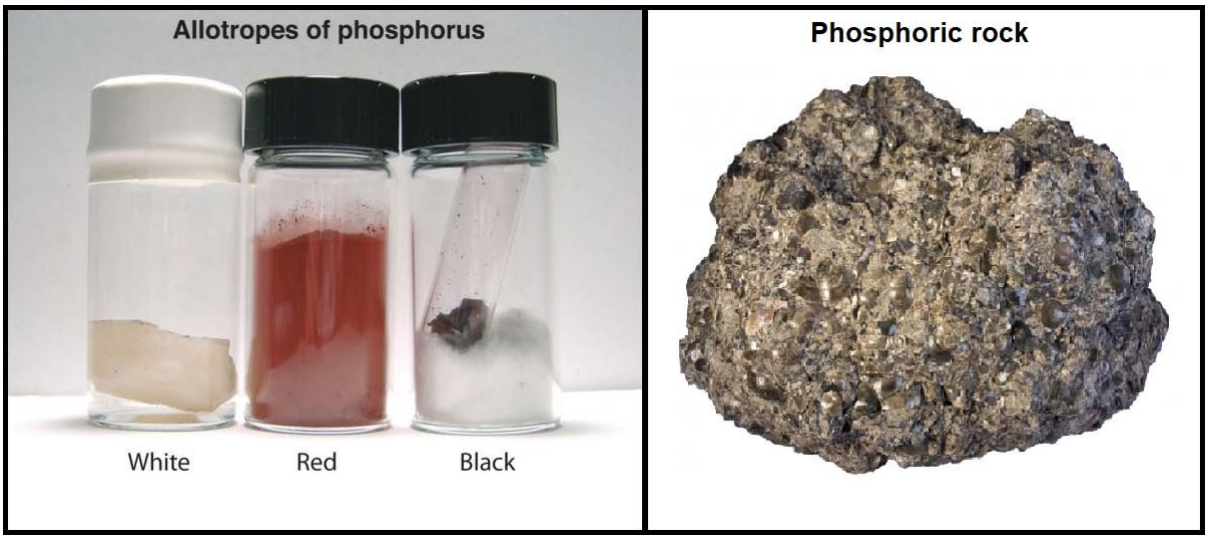

Figure 1.1: Physical appearance of phosphorus. Adapted from Askiitians.com (2020) and Minerals Education Coalition (2020)

When the P atom is bonded to other elements with a coordination number of 4, compounds such as phosphoric acid and a variety of mineral phosphates are formed under normal conditions. In this case, Phosphorus (V) forms one double bond and three single bonds with other atoms (Li et al., 2008). The most representative and important of the oxides formed this way is "Phosphorus Pentoxide" (empirical formula: P_2O_5); which, despite its name, actually exists as P_4O_{10}. This oxide has been used extensively in modern society, given its ability to react with water and yield phosphoric acid (H_3PO_4), which has several uses as an industrial compound.

The rest of the common phosphorus oxides, and more specifically, the ones that occur as condensed phases are phosphorus species that include the phosphate anion $[PO_4]^{3-}$. In addition, compounds where one of the oxygen atoms in the basic tetrahedral unit has been substituted with H, F or S can also form stable phases. For example, there are numerous mineral species including the anion unit $[PO_3H]_2^-$ in phosphites, $[PO_3F]$ and $[PO_2F_2]$in fluorophosphates, and $[PO_{4-n}S_n]$ in thiophosphates (Averbuch-Pouchot and Durif, 1996).

1.2 Phosphorus and its essential role in living organisms

1.2.1 Phosphorus and the structure of nucleic acids

When inquiries about the origin of life are raised, phosphorus is considered as a common roadblock in the quest for answers. Even though phosphorus is scarce in the universe, the observation of its pervasiveness in the solar system has prompted researchers to question how such a minor element became so important for biological processes (Maciá, 2005). In addition to this dichotomy, even at the planetary level, a satisfactory explanation on the situation of phosphorus in the primitive Earth, and moreover to its connection to the origins of life, is still to be found. Some studies propose polyphosphates as candidates for the building of biological molecules since they can be hydrolyzed from mineral P_4O_{10} in a very simple manner (Griffith et al., 1977).

Whichever the case, the essential role of phosphorus for living organisms was established when the work performed by Rosalind Franklin, James Watson and Francis Crick during the 1950s resulted in the elucidation of the arrangement structure of DNA. This event led to the development of the field of molecular biology and was undoubtedly one of the groundbreaking moments for science during the 20th century (Klug, 1968). Nucleic acids such as DNA and RNA are made up of three parts: a deoxyribose (5-carbon sugar), a hydrophosphate group ($(HPO_4)^{2-}$), and a nitrogenous base. This base can either be adenine, guanine, cytosine or thymine. The sugar-phosphate groups are aligned forming a negatively charged "backbone" for the strands of the nucleic acid and continue all along forming the double helix structure (Molnar and Gair, 2013), as it is shown in Fig.1.2

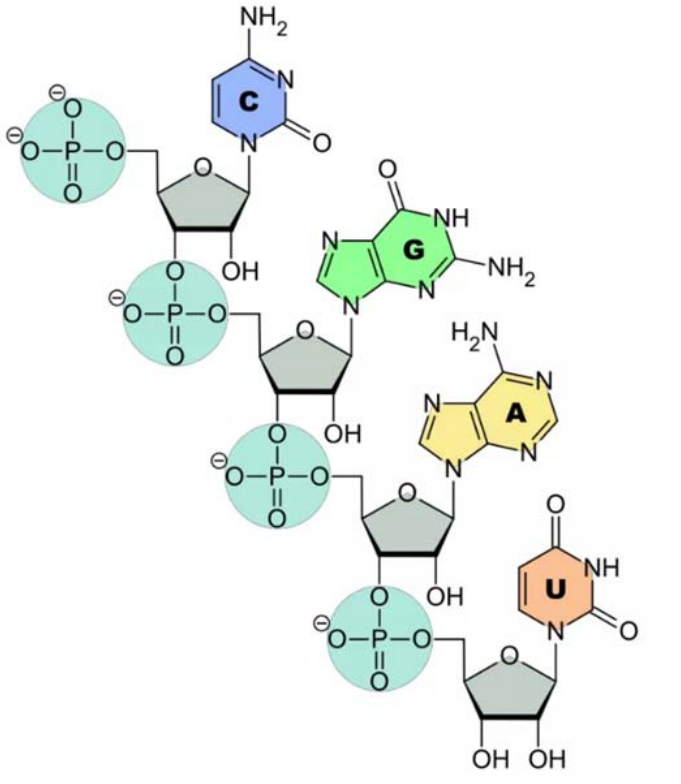

Figure 1.2: Segment of the RNA molecule, showing the phosphate-ribose sugar backbone on the left side. From Bailey (2019)

The critical role of the "phosphate backbone"in the emergence of "living molecules"can be explained as follows: the special properties of the phosphate ion guarantee that a stable molecule could exist over time, while at the same time ensuring said molecule retains a definite reactivity under certain conditions. This makes sense from an evolutionary point of view since the information containing material (nucleotides) must be preserved over time even after undergoing a series of necessary reactions; here, it could be said the phosphate groups act as protectors, stabilizing esters against hydrolysis and nucleophilic attacks in aqueous environments (Arrhenius et al., 1997).

1.2.2 Phosphorus and energy exchange in the cell

In addition to being an intrinsic part of the structure of nucleic acids, phosphorus is crucial in the process by which cells transfer energy. It is known that adenosine triphosphate (ATP) serves as a sort of "unit of exchange" of metabolic energy within living systems, operating in an analogous way money does for human societies (Bolsover et al., 2003). This considered, it is possible to assert that the whole group of complex reactions guiding the energy cycle of a cell would not be possible without phosphorus and the capacity of the phosphate groups to store energy in ATP.

In that regard, the ATP molecule (see Fig.1.3) consists of an adenosine core bound to three phosphate groups at the five-carbon sugar ribose. In this molecule, the "energetic" bonds are the ones linking the phosphates together (phospho-anhydride bonds) given that they can provide the release of energy when hydrated.

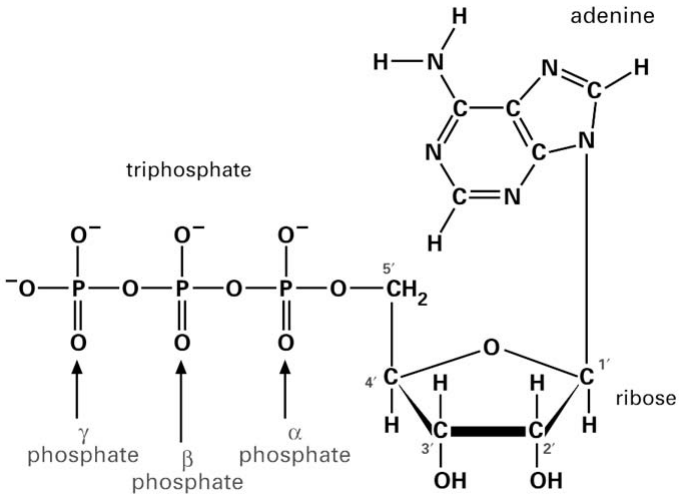

Figure 1.3: The ATP molecule, showing three phosphoryl groups aligned. From Molnar and Gair (2013)

In living cells, the process of energy transfer is part of the metabolism and it involves the aforementioned hydrolysis of the ATP molecule into ADP and the subsequent release of energy. This process is complex in nature and involves the transfer of H^+ ions through the mitochondrial membrane. Nonetheless, it is possible to schematize the releasing/restoring energy reactions as two interlinked process as presented in Eq.1.1 and Eq.1.2:

$$\textit{Hydration (energy release)}: \ \mathrm{ATP} + \mathrm{H_2O} \rightarrow \mathrm{ADP} + \mathrm{Pi} + \text{free energy} \tag{1.1}$$

$$\textit{Dehydration (energy restore)}: \ \mathrm{ADP} + \mathrm{Pi} + \text{free energy} \rightarrow \mathrm{ATP} + \mathrm{H_2O} \tag{1.2}$$

where ATP refers to adenosine triphosphate, ADP to adenosine diphosphate and Pi refers to a released/capture phosphoryl (PO_4^{3-}) group, respectively. The whole process is carried out permanently inside living cells and it is commonly referred to as the ATP-ADP cycle, which is summarized in Fig. 1.4.

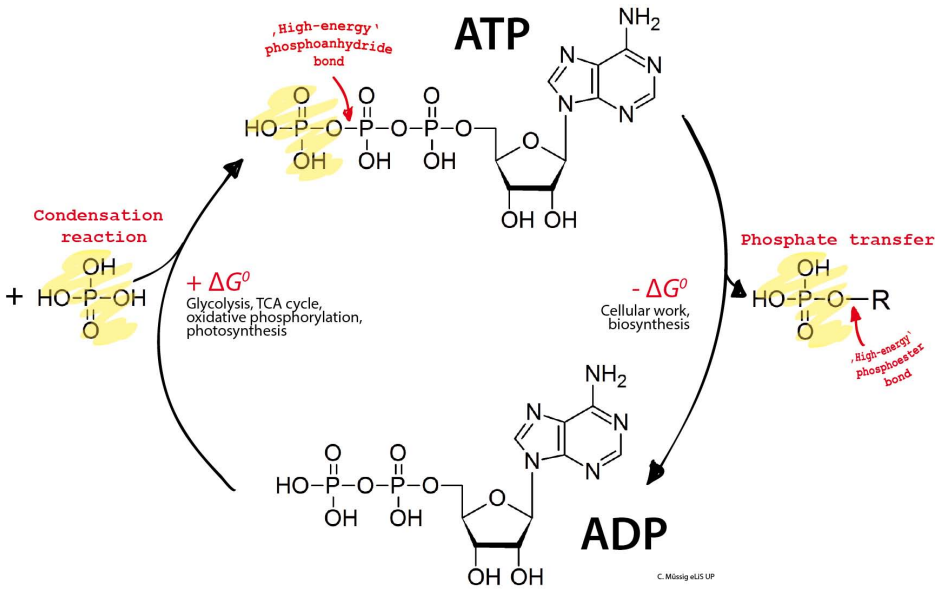

Figure 1.4: The ATP-ADP cycle. From Mussig (2013)

1.2.3 Phosphorus and the structure of bone tissue

The importance of phosphorus is also observed in the formation of living tissue, particularly in the process of bone formation. Given that bone is a living tissue that undergoes different changes throughout its lifetime, a series of reactions and cell interactions are present, for example, the processes involved in bone homeostasis are the formation of bone tissue by osteoblasts, which are in charge of the secretion and synthesis of various substances involved in bone formation and mineralization, and bone resorption by osteoclasts, which secrete enzymes that dissolve the calcium present in the tissue, effectively remodeling the bone matrix (Chang et al., 2019).

In this process, specialized cells known as osteoblasts are responsible for the bone matrix synthesis and the construction of the mineral scaffold of bone tissue consisting of a phosphate mineral called hydroxyapatite ($Ca_5(PO_4)_3(OH)$) and collagen fibers. At the nanoscale, the interactions between collagen molecules and hydroxyapatite (HAP), and as well as the amount of mineral, are known to have a significant role in providing strength and toughness to the bone, making these collagen-HAP composites the basic building blocks of the skeletal system.

The hierarchical assembly of bone goes as follows: cells synthesize the amino acids present in the protein structure of collagen, then, three strands of this molecule assemble to form a strand of tropocollagen. Afterwards, collagen fibrils are formed and bound together via the formation of hydroxyapatite in the gap regions which impart strength to the structure. Finally, these fibrils form different types of arrays of mineralized tissue depending on the type of the bone. For reference, Fig.1.5 and Fig.1.6 show the structures present in human bone at different scales.

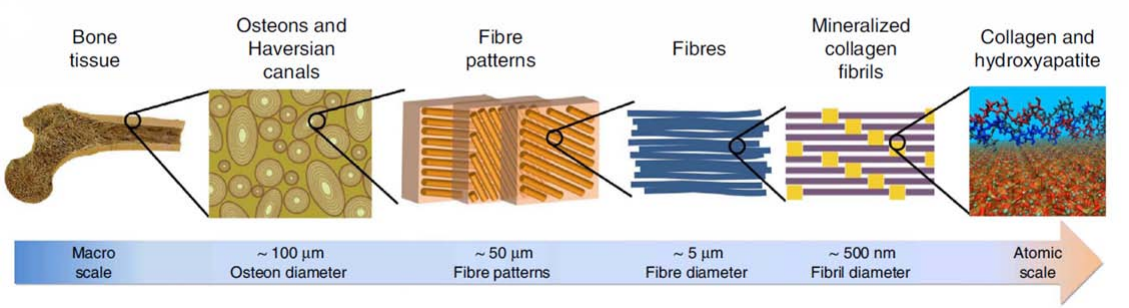

Figure 1.5: Close-up of bone structure, from macroscale bone to the atomic scale. Hydroxyapatite crystals are found as part of the collagen-HAP fibrils. From Nair et al. (2013)

.

The bone matrix is comprised of type I collagen and other non-collagenous proteins. The hardness and rigidity of bone is due to the presence of HAP in the matrix, and calcified bone contains about 25% organic matrix (2-5% of which are cells), 5% water and 70% inorganic mineral (HAP). These numbers reveal the predominance of the mineral matrix, and by extension the predominance of the phosphate ion ($(PO_4)^{3-}$), in terms of its mass abundance in bone tissue.

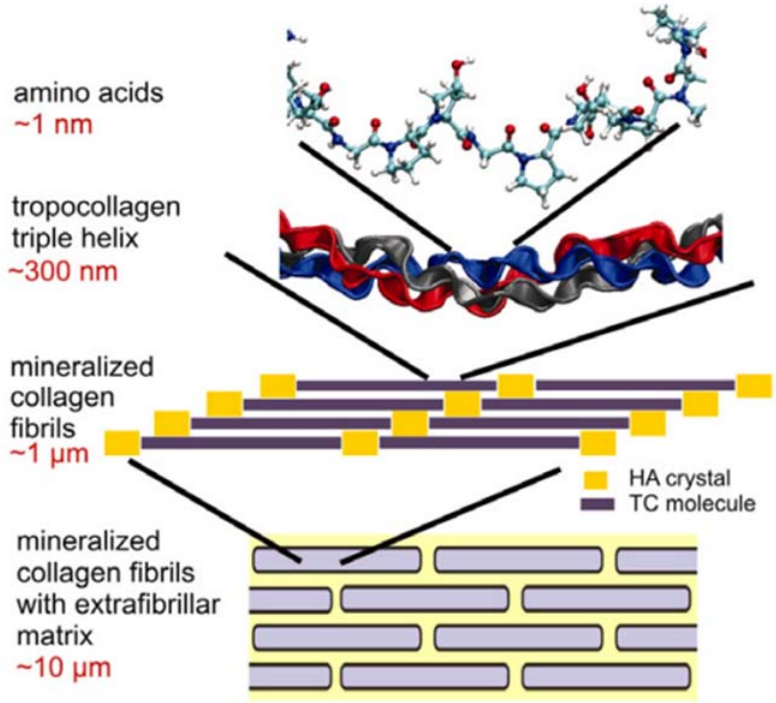

Figure 1.6: Nanostructure of bone, from the atomic scale to microscale. From Buehler (2007)

Based on the information presented, it is safe to say that phosphorus is key to the existence of every single living organism known, both at the molecular level and at the tissue level. Moreover, in order to understand how phosphorus moves from inanimate mineral substances to being bound to living organisms (which virtually manage the flow of phosphorus) the next section is focused on the natural cycles of this element on planet Earth.

1.3 Phosphorus flows in plants and humans

1.3.1 The phosphorus cycle

Phosphorus is constantly being cycled on planet Earth in different ways, from organic to inorganic, from being biologically-bounded to flow mineralized depending on the location and on the type of the available interactions. Principally, the following four components are identified as relevant: tectonic uplift and weathering of phosphorus bearing rocks, erosion and leaching of soils, runoff and riverine transport to the oceans and burial of organic phosphorus as deep sea sediments. The first two scenarios compose the terrestrial phosphorus cycle while the last two comprise the marine phosphorus cycle.

A significant portion of the total phosphorus on the planet is regulated by the marine phosphorus cycle, where it is thought that riverine flux after continental weathering is the process responsible for the majority of phosphorus burial as sediment. This phosphate is commonly found associated with metal oxides and combined inorganically forming minerals such as fluorapatite or rare earth phosphates, yet, evidence suggests marine phosphate to have been biologically available or at least biologically bound before the sedimentation process took effect (Paytan and McLaughlin, 2007).

Although the overall concentration of oceanic phosphorus tends to remain relatively constant over time, anthropogenic sources of this nutrient (see Fig.1.7.) have become an important source of phosphorus input to the oceans in recent times. This situation represents a disturbance on phosphate concentrations at the sediment level that can cause heavy alterations on marine ecosystems (Froelich et al., 1982).

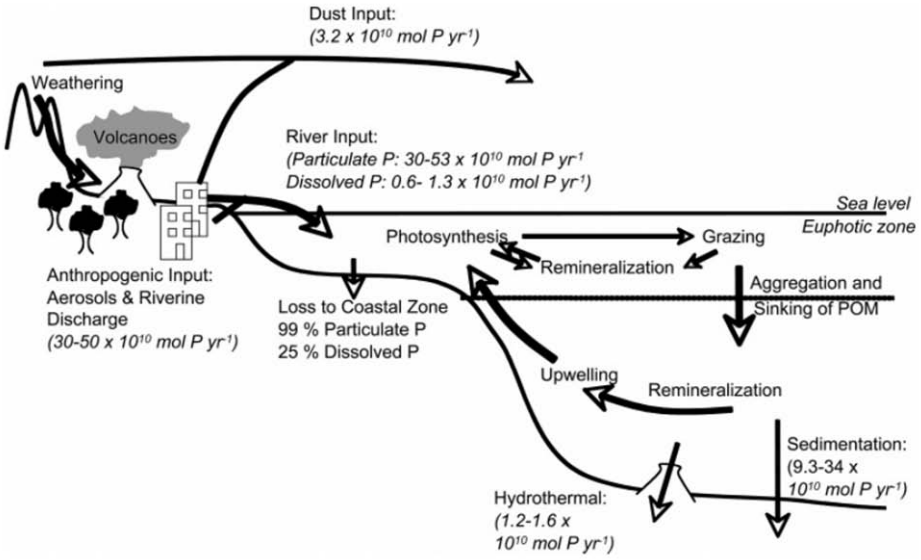

Figure 1.7: Phosphorus cycle in marine environments. From Paytan and McLaughlin (2007)

In the case of the terrestrial phosphorus cycle, the release of phosphate from mineral sources and rock is driven by the exposure to naturally occurring acids of microbial origin and rock weathering. This phosphorus is mostly inorganic and its mobility depends on the pH of the medium after dissolution. After this step, liberated phosphorus will head towards soils where its sorption will be determined by several factors such as temperature, pH, microbial activity and the presence of other chemical elements. Fig.1.8 shows a diagram of the phosphorus cycle in this environment.

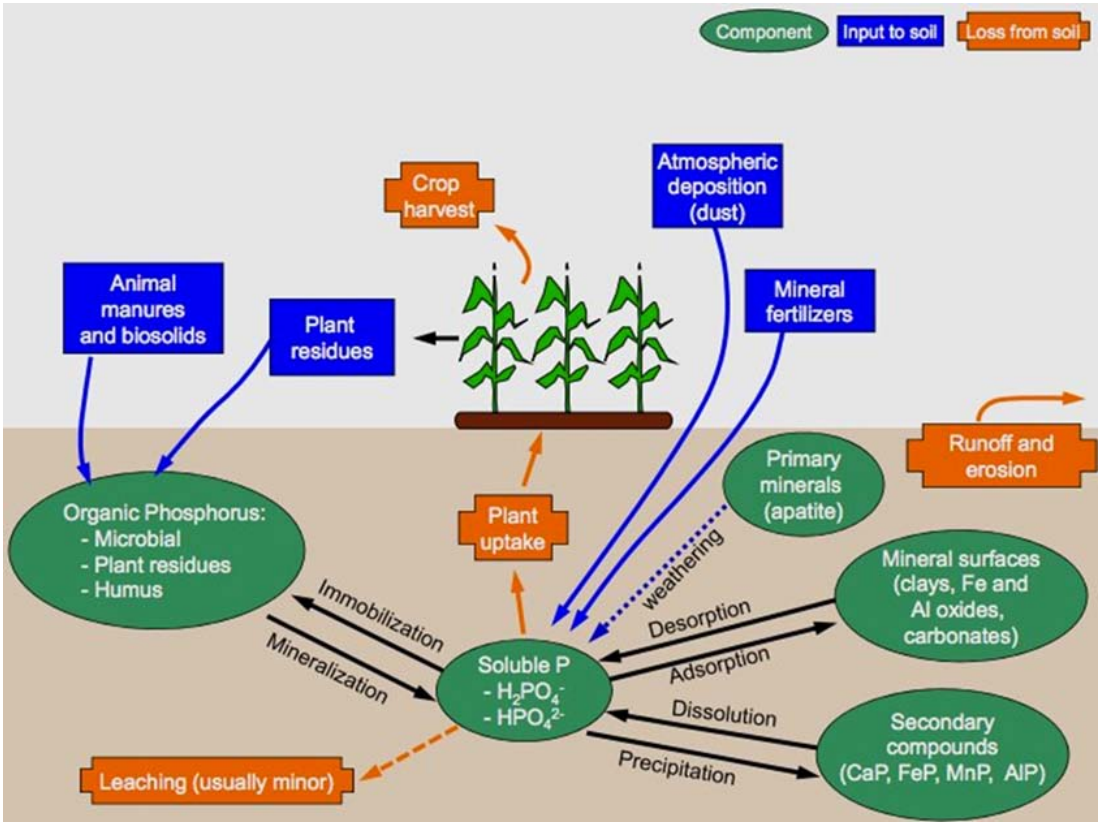

Figure 1.8: Phosphorus cycle in terrestrial environments. From Wikimedia-Commons (2014)

Even though a certain percentage of phosphorus will be stripped away from the soils by natural runoff, capture of phosphorus by plants is the central phenomenon at this stage. Here, the crystal phase of phosphorus is very important, since the environment near root hairs (slightly acidic) causes poorly crystalline P-bearing minerals to release P to soil pore spaces (Filippelli, 2008).

This cycle comprises diverse transformations as P-bearing compounds change from inorganic to organic, from soluble to insoluble and start flowing throughout different environmental matrices. In this light, marine sediments constitute the major sink for phosphoric compounds, followed by soils (inorganic and organic) and mineable rocks (Keyzer, 2010).

The increased quantity need for crop fertilizer not only symbolizes the value of phosphorus as a resource, but its overuse also explains the appearance of imbalances in phosphorus distribution within terrestrial and marine soils. The problem of oxygen depleted marine coastal zones, caused by the runoff of excess nutrients reflects this situation (Elser and Bennett, 2011).

1.3.2 Phosphorus uptake by plants

In the case of plants, phosphorus is considered to be the second most frequently limiting macronutrient for growth after nitrogen, since prompt uptake by crop plant species require phosphorus to exist in a bioavailable form, which is mostly a pH dependent, solubilized species of the orthophosphate ion. This phosphorus migrates to living tissue within the plant and results in a phosphorus content adding up to approximately 0.2% of a plant' s dry weight (Schachtman et al., 1998).

Plant species have different efficiencies when they perform phosphorus acquisition via the rhizosphere, which is a region of the soil directly influenced by the secretions from the root. Here, the formation of organic acids promotes the release of phosphate ions from the solid, which are overwhelmingly susceptible to remain as precipitates under normal pH (Holford, 1997). As a consequence, the uptake process is closely related to the mineral phase of the phosphate and also to the ability of a plant to mobilize P from poorly soluble sources and take the soluble P available in the soil solution (Shenoy and Kalagudi, 2005). This process is depicted in Fig.1.9.

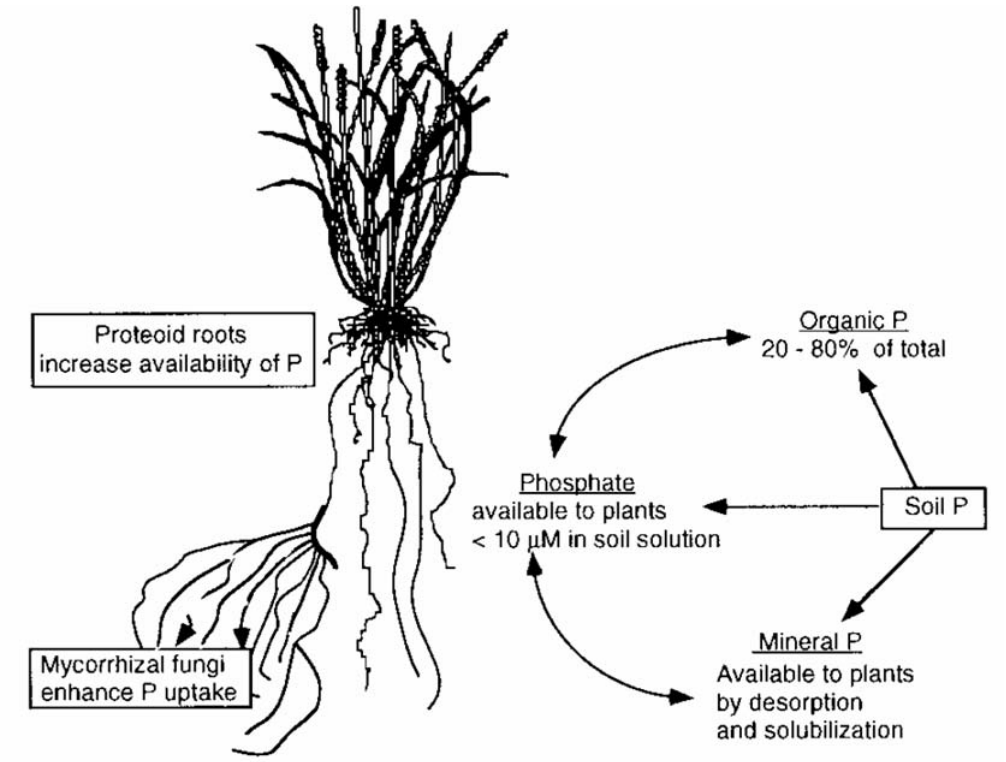

Figure 1.9: Plant acquisition of soil phosphate. From Schachtman et al. (1998)

The overall absorption is initially hindered by physical constrains since phosphate is naturally drawn to sorption sites on the ground where it is immobilized, and thus, removed from the biological cycle (Cornish, 2009). Also, uptake is closely associated with the occurrence of sorption and organic complexation reactions which in turn reduce the actual amount of bioavailable phosphorus present on soils intended for farming, causing an increase in the amount of fertilizer commonly used by agricultural businesses (George et al., 2016).

1.3.3 Phosphorus absorption by humans

Once ingested, phosphorus is absorbed via the gastrointestinal tract, where the vast majority is absorbed in the small intestine by at least two distinct mechanisms: paracellular phosphate transport and active transport. The first route is defined as the transport dependent on passive diffusion, and the second one occurs in conjunction to the sodium-dependent transport (Sierra et al., 2011). On the other hand, studies on homeostasis of this nutrient reveal that a balance between absorption/secretion of phosphorus is performed in the gastrointestinal tract, whereas filtration/absorption takes place in the kidneys, followed by a shifts into and out of bone, as shown in Fig. 1.10.

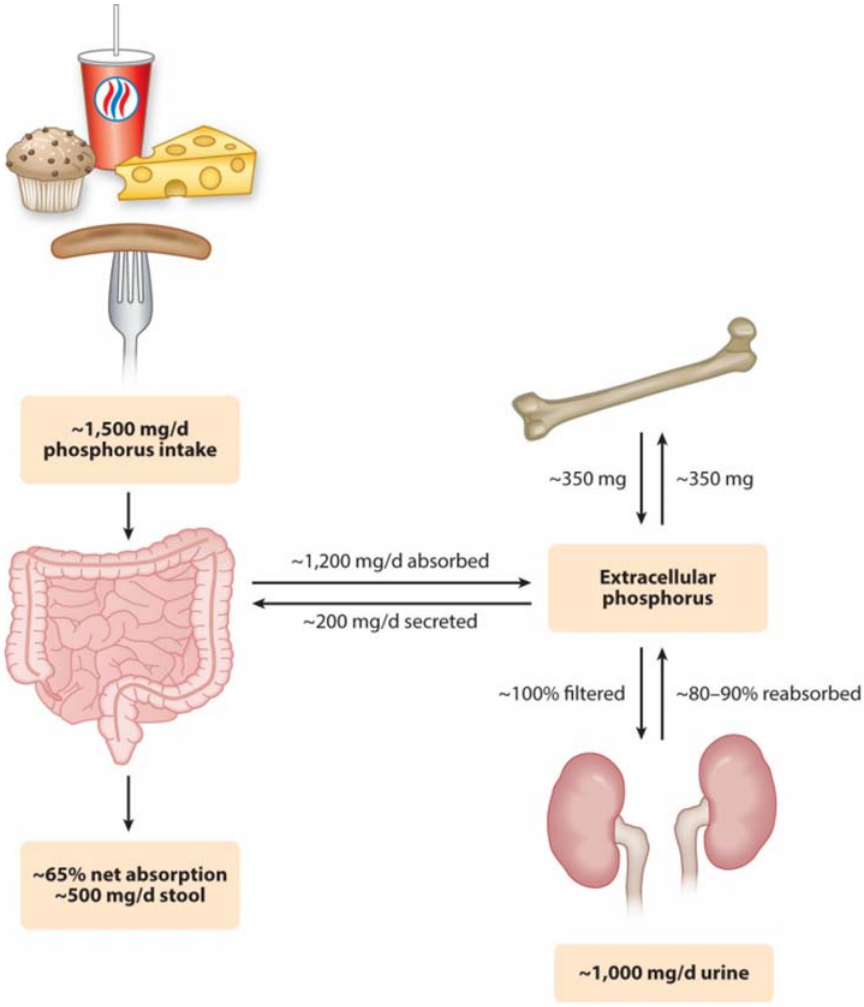

Figure 1.10: Phosphorus absorption in humans. From Chang and Anderson (2017)

The role of phosphorus in human nutrition is well known, as P-bearing compounds are considered of essential importance for a balanced nutrition. Given the ubiquity of organic-phosphorus in nature, virtually all foodstuffs contain some form of phosphate in their structure. In that regard, dairy products, meat, grains, eggs and fish can be considered as common sources of dietary phosphorus (Navarro-Alarcon et al., 2012), alongside the phosphate additives commonly used by the food industry in their formulations (see Appendix A), which guarantees the average human can access this nutrient in a relatively straightforward way.

Furthermore, it is estimated that a healthy adult has an average of 700g of phosphorus in the body, with 85% existing as bone tissue in the crystal phase of hydroxyapatite ($Ca_5(PO_4)_3(OH)$), 14% as part of soft tissues and a very small amount existing extracellularly (that is, phosphate not combined with living matter). Additionally, the deficiency of phosphorus in the diet can lead to diverse complications and health issues. For instance, hypophosphatemia (a reduced amount of phosphorus) at the cellular level can cause diseases such as muscle weakness, poor heart function, a reduction in the efficiency of tissue oxygenation and other types of respiratory dysfunctions (Takeda et al., 2004). Moreover, evidence suggests that a lack of phosphate in the human diet can result in malnourishment, and is commonly associated with conditions such as rickets and other nutritional problems (Kraft, 2015), highlighting the essential role phosphorus plays in human life.

1.4 The fertilizer industry and phosphorus

1.4.1 Historical development of fertilizers

It is likely that at some point in history our ancestors noted that the areas where dead remains of animals and plants were located, newer plants grew consistently without much effort. Then, this observation could have led to the conclusion of the soil having some special properties and prompted further investigation to reap these benefits. For example, there is evidence of the usage of livestock manure and water management to enhance crop yields by groups of humans in Neolithic sites (Bogaard et al., 2013), while it is well known that advanced civilizations like the Egyptians knew substantially about the fertility of the Nile mud and used it in their harvests.

For the most part of history, these "natural" sources of nutrients for the soils remained essentially unchanged as civilizations developed, since the nutritional requirements of the average human were low, and increases in population was rather slow. Nonetheless, as population growth was dramatically accelerated, new sources of phosphorus alongside other nutrients were sought, especially in Europe where cities were being rapidly urbanized.

It is around the mid to late 19^{th} century when the notion of mineral composition of the soil affecting crop yields begins to gain acceptance, leading to the establishment of the early fertilizer factories in the world. Additionally, the extraction of guano in South America and the mining of phosphate rock started during that time, meaning societies could now rely on importing specific minerals from distant locations in order to cover the need for nutrients in their soils, globally accelerating the production cycle.

As more time passed, advances in soil science allowed scientists to identify the elements considered "nutritive" for plants, resulting in the acceptance of the modern framework for the study of nutrients in plants, which states the following (Frauenkron et al., 2009):

- A deficiency of the "nutritive" element makes it impossible for the plant to complete its life cycle.
- The effects of said deficiency are specific for each element.
- The element in question is involved in plant nutrition because of its physicochemical properties.

In addition, the role of the nutrient carrier was acknowledged, meaning that even though the elements can be located in the soil, plants are able to assimilate each nutrient if they are present in certain ionic forms; for example, C can be assimilated via CO_2 and P via the $H_2PO_4^-$ ion. Hence, the modern classification of Phosphorus as a plant nutrient puts it in the category of oxo complexes where plant uptake promotes the formation of esters and other organic-P forms (Frauenkron et al., 2009).

Unsurprisingly, manufacturing fertilizers in the current age have become a multidisciplinary and lucrative industry that relies on sophisticated methods for the synthesis of specialty chemicals aimed at the selective enrichment of productive soils, resulting in a plethora of fertilizer preparations aimed at covering the nutrient needs of each particular application.

1.4.2 Phosphate rock resources

The natural phosphorus cycle has been altered by humanity since phosphate rock started to be exploited as a mineral resource in the 19th century, and this "resource" was without a doubt one of the most critical for sustaining the impressive growth of global population in the last two centuries. Humanity uses phosphorus in an "open" circuit where P contained in plant and animal cells is captured just to posteriorly leave in the excreta, leading to an accumulation of this nutrient in the wastewater streams, especially in urban areas (Childers et al., 2011) as the main use for P resources relies on agriculture fertilizer.

Geographically speaking, mineral deposits containing phosphate rock can be found around the globe; however, the bulk of their natural occurrence is located in West Africa, China and the United States. In addition, Fig. 1.11. clearly shows that Morocco is the country with the most abundant reserves in the world by a considerable margin (Cooper et al., 2011).

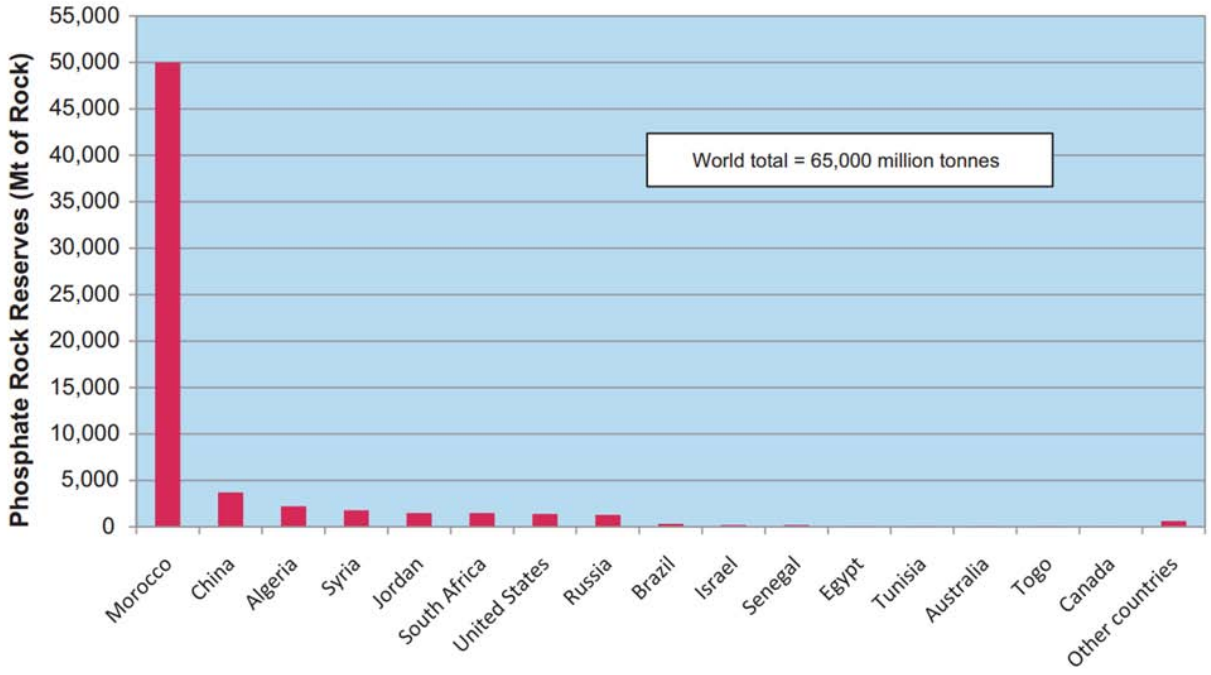

Figure 1.11: Distribution of world reserves of phosphate rock. From Cooper et al. (2011)

The term "phosphate rock" is loosely defined and mostly refers to naturally occurring geological materials that contain one or more phosphate minerals suitable for industrial processing. In general terms, calcium apatites (calcium phosphates) are defined as the main component of "phosphate rock". For example, minerals such as fluorapatite $Ca_5(PO_4)_3F$, francolite $Ca_{10}(PO_4)_6SO_4$ and hydroxyapatite $Ca_5(PO_4)_3OH$ are considered valuable for phosphorus production, and there are refining processes focused on the profitable exploitation of each one of them (Chandrajith and Dissanayake, 2009).

In terms of phosphorus demand, several studies (Chen and Graedel, 2016; Cordell and Neset, 2014; van Dijk et al., 2016; Van Vuuren et al., 2010; Villalba et al., 2008) have tackled the flows of the human phosphorus cycle and have pointed out the following challenges for the sustainable and long term management of this natural resource:

- Because population growth will continue to increase in the following years, more P will be required in order to guarantee the food supply, especially in the emergent economies such as China and India. In addition, most of the per capita demand will increase as the total caloric intake per capita increases.
- P resources are at risk for complete depletion because among other reasons, the currently known reserves are not being mined efficiently and there is a lot of phosphate runoff due to erosion and poor management once it is applied as fertilizer into the soil, with some estimates predicting a global shortage of phosphate in the years 2050 - 2100.
- Since the location of natural reserves of phosphate rock is extremely unequal, future scenarios where only a handful of countries (i.e. Morocco, China, USA and Russia) control phosphorus supply are to be expected. Therefore, gaining access to these resources can quickly turn into a geopolitical issue in which monopolies or oligopolies, controlled by governments or corporations can exert pressure at the expense of farmer' s needs.
- In order to reduce the dependency on continuous mining of phosphate rock, a few alternatives are available, namely: optimizing the mining operation, improve the intake of P by plants, prevention of losses from agricultural systems, reduction of livestock production and phosphorus recycling from waste products. Nonetheless, worldwide application of these alternatives by the agricultural industry at large remains a challenge.

These findings reveal the critical situation of phosphorus resources around the world and point out the necessities for corrective measures directed to the improvement of usage of the resource and the implementation of measures aimed at the sustainability of phosphorus resources for the years to come. On the other hand, the chemical fertilizer cycle starts with the beneficiation of phosphorus rock using conventional mining techniques, followed by its transformation to phosphoric acid, from which the actual fertilizer is produced when it reacts with calcium, often jointly with sodium and potassium. This process is not sustainable in the long run, as researchers have made a prediction (Cordell et al., 2009) for the ore production to reach a "peak" in quantity, as phosphate rock can be compared to another non-renewable resources, such as oil (see Fig. 1.12). This means that in a similar fashion to the present situation for oil, the rate of global production of high-grade phosphate rock will eventually reach a maximum point in the near future, where the demand will outpace the possible output available, forcing the use of lower and lower grade ores, increasing the costs of fertilizers and consequently of food.

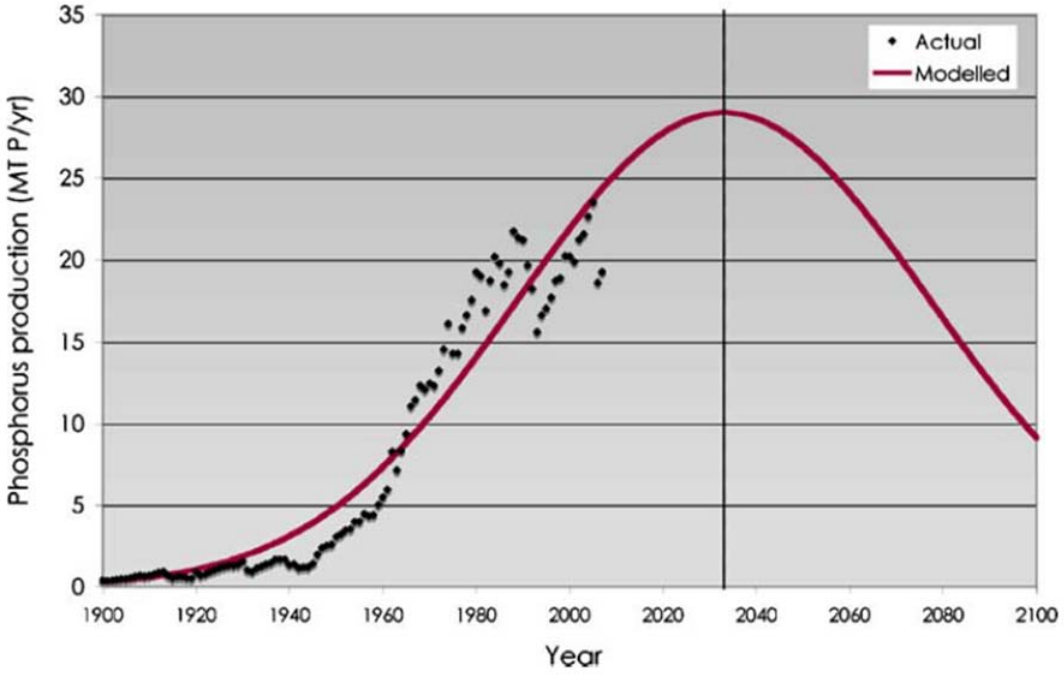

Figure 1.12: Projection illustrating "peak phosphorus", showing that the estimated time for the "peak" to arrive is the year 2030. From Cordell et al. (2009)

The geopolitical implications of this can become very serious compounded by the effects of climate change and overpopulation. Hence, research efforts are being performed to develop alternatives directed at tackling the issue of phosphorus resources. Among these efforts, phosphorus recycling appears as an interesting alternative due to its relatively simple application cost and it potential as a source of economic incentives to sustainable economies.

1.5 Phosphorus recycling

1.5.1 The need for phosphorus recycling in urban settings

In general terms, phosphorus has not been considered a typical candidate for recycling circuits, perhaps because historically the supply of phosphate required for agricultural purposes was reliant on raw sources or could have been subjected to "unintentional recycling" performed in-situ by farmers or local agricultural managers. Also, since the bulk of phosphorus is immobilized in osseous tissue, it could be that any problem related to the intake of this element was masked by other health issues, except perhaps for rickets in children and the elderly. This comes as a surprise since, there are several places where a sustainable scheme for phosphorus recycling can be implemented. For instance, it is feasible to implement recycling from food waste using a proper anaerobic treatment or improve the collection of phosphorus coming from urban wastewater and subsequently use these as sources for phosphate used in biofertilizers (Koppelaar and Weikard, 2013).

The lack of national policies focused on the sustainable management of phosphorus for human consumption is a serious concern, moreover when considering that growth in human population worldwide is expected to reach high levels in the next decades, reaching a projected 11.2 billion people in the year 2100 (Bongaarts, 2016).

One of the consequences is that the requirements of available phosphate for food production and demand will continue to rise in the future (Metson et al., 2012), putting more pressure on the search of sustainable alternatives for phosphorus supply. For example, Fig.1.13 displays the volatility of phosphate rock as a commodity, which was exacerbated in the year 2008 when a sharp increase of around 800% was felt in the prices of phosphate rock, severely disrupting the whole food supply worldwide and consisting in a prime example of the dependency, and thus the fragility of the current management of this resource.

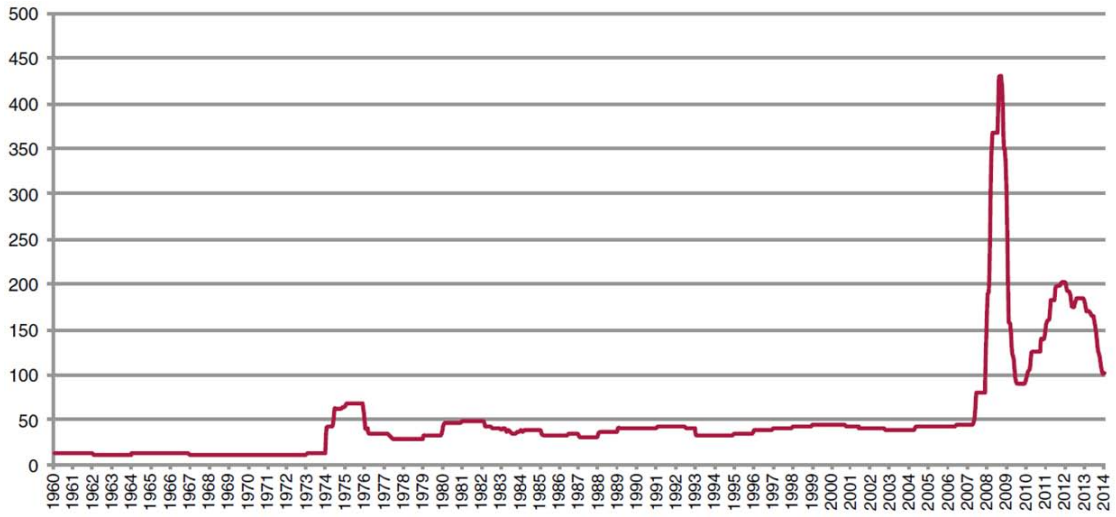

Figure 1.13: Commodity price for phosphate rock in the period 1960-2014. The peak observed in the year 2008 indicates the volatility in the market for this resource. From Cordell and White (2015)

Despite the urgency for alternatives for a comprehensive recycling policy for phosphorus, the traditional mindset for agricultural uses of phosphorus acts in a way that resembles an "open circuit" where first, phosphate rock is mined in the regions where the industry is located, then the process of rock beneficiation occurs in specialized facilities and the phosphate is ready for combination to prepare fertilizers. Afterwards, the fertilizer product is used in crop fields until depletion by harvesting; if there is a need for more phosphate, the cycle starts again with the mining of fresh phosphate rock.

This situation is illustrated in Fig.1.14, where it can easily be observed that the nature of the current "open circuit" for the usage of phosphorus coming from fresh mineral ores, promotes the extensive consumption by an ever increasing human population and makes the whole situation a complex problem which has to be addressed.

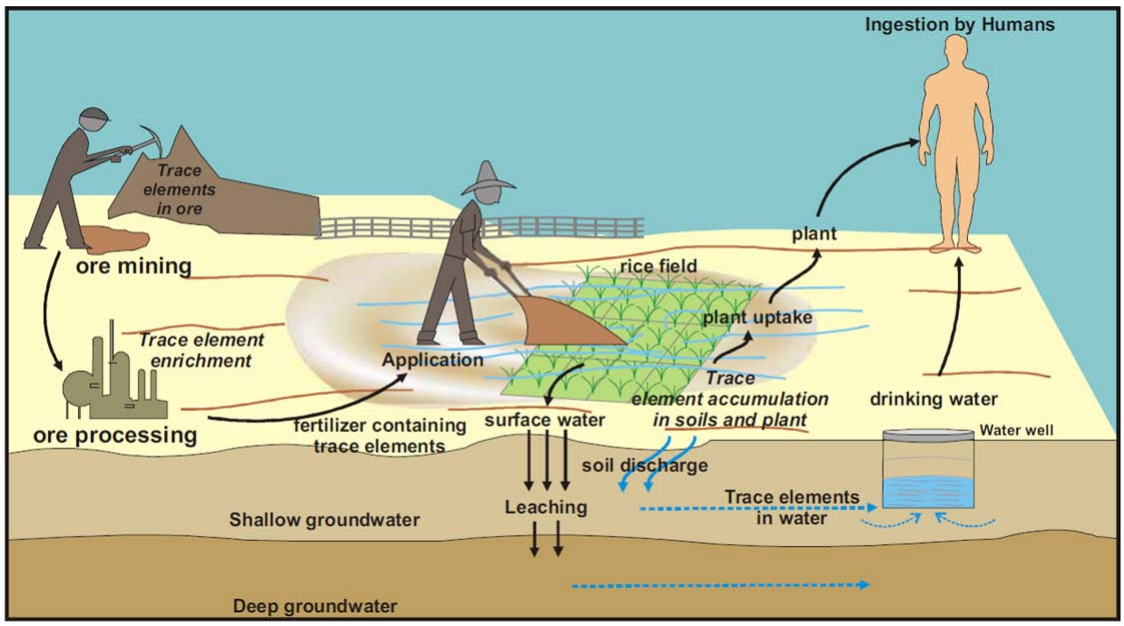

Figure 1.14: Conceptualized geochemical pathways for the "open circuit" of phosphate rock, highlighting heavy metal ingestion by humans. From Chandrajith and Dissanayake (2009)

Consecutive repetitions of this process by the agricultural industry can lead to serious problems in the future, since excessive addition of phosphate ore-based fertilizers to the soil can also cause a buildup of unwanted elements, for example: heavy metals such as arsenic (As), cadmium (Cd) and chromium (Cr) (Mclaughlin et al., 1996), possess a risk for posterior plant uptake by crops due to the similarity of their cations with phosphate ions (Chen et al., 2007; Peralta-Videa et al., 2009).

Considering that humans typically uptake only 1/3 of their total intake of phosphorus, it can also be observed in Fig.1.14 that the endpoint of the current "open cycle" will inevitable lead to the accumulation of phosphorus in waste streams (sewage) coming from urban settlements, where the larger the population, the larger the quantity of phosphorus being released.

In urban settings, the main source of phosphorus flows comes from human consumption, either directly as food or indirectly as a material commonly found on products such as detergent; hence, phosphorus can be recovered from urban sewage containing both P bound to organic and inorganic components (e.g. excreta, detergents and food) via

the use of several techniques. Nevertheless, difficulties arise when the amount of another contaminants is taken into account, namely: pathogens, hormone residues and most importantly, heavy metals (Withers et al., 2015). In this case, there is evidence of major crops performing uptake of heavy metals from the soil (Angelova et al., 2004; Gupta et al., 2014) which may result in the subsequent uptake by human populations and cause health problems over time.

1.5.2 Phosphorus recycling from wastewater

Direct recovery from wastewater represents one of the most straightforward path to take for phosphorus recycling, as treatment techniques can be implemented directly at a large scale at Waste Water Treatment Plants (WWTPs), using their existing infrastructure and processing capabilities.

In this regard, research efforts have been performed to recycle phosphorus from supplementary sources such as wastewater or sewage sludge (Jaffer et al., 2002; Schütte et al., 2015), though disadvantages exist when such sources are employed, as they have been associated with the presence of organic pollutants and heavy metals in soils (Nanzer et al., 2014). Then, in general the current research for recycling from this stream include:

- The use of ion exchange processes, which involves a reversible migration of ions from a liquid to a solid phase, to recover phosphates. In this case the removal is not very efficient since wastewaters tend to have multiple anions competing for active sites, physically hindering the exchange resin.
- The use of precipitation processes after exposure to activated sludge. After P uptake occurs by the sludge, liquor can be separated and the P-rich sludge precipitated in a different compartment, resulting in a compact mixture that can go further processing
- The use of membrane processes, such as an osmotic membrane bioreactor, in which the ionic species are removed by a combination of forward and reverse osmotic routes.

Nonetheless, the simplest approach for a direct recovery of P from wastewater relies on struvite ($MgNH_4PO_4 \cdot 6\,H_2O$) formation, as it forms naturally in the form of "scale" in pipes used to transport wastewater. These methods work well and have the advantage of struvite being a fairly soluble phosphate for plants; nonetheless as it was shown before, they also suffer from the interference of other ions present in wastewater, which reduce their efficiency. As a collateral issue, these methods require the addition of magnesium salts (e.g. $MgCl_2$) and rely heavily on pH regulations carried out using NaOH so they can easily cause a rise in the operational costs incurred by WasteWater Treatment Plants.

1.5.3 Recycling potential for urban settings in Japan

In the case of Japan, the vast majority of phosphorus entering the country does it through imports which amount to around 630 kilotons of P per year (ktP/y), as presented in Fig.1.15. It can also be observed in Fig.1.15 that of all the phosphorus imported, the main targets for recycling are the phosphorus imported as foodstuff, which is used either to serve as animal fodder or to be used for human consumption as food; and the phosphorus that enters the country imported as part of other mineral resource like iron ore and coal for the steelmaking industry (Ohtake and Okano, 2015). This is because the rest of the phosphorus flows end up as finalized products of the chemical industry or more importantly, as phosphorus scattered across the country accumulated in soil due to the application of fertilizers by farmers.

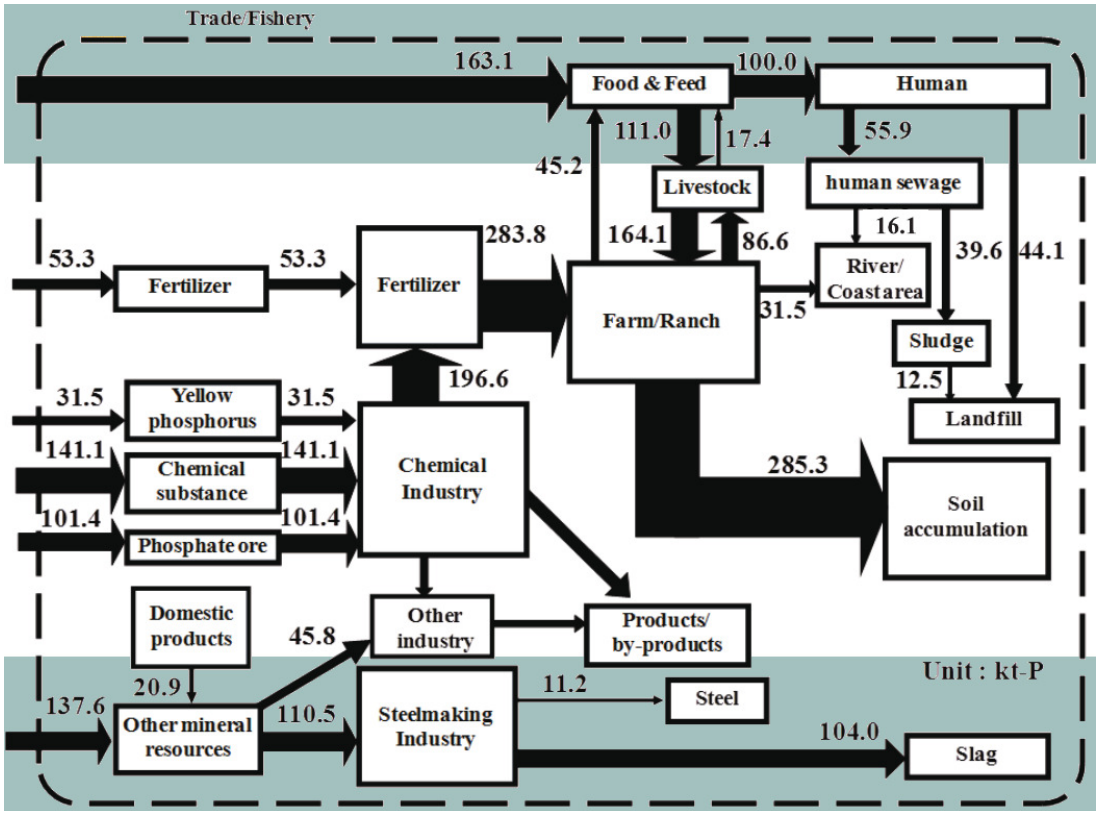

Figure 1.15: Diagram representing the phosphorus flows in Japan for the year 2005. The shaded areas represent the flows where recycling has the largest potential for application, being the top area the flow for human consumption, and the bottom area the flow for other mineral resources used in industry. Adapted from Ohtake and Okano (2015)

On the other hand, it can be observed that the estimate for human consumption in Japan is roughly 100 ktP/y, indicating that phosphorus flows coming from urban settings may be close to that value, assuming that more than 90% of the population in Japan is living in urban locations (United Nations Population Division, 2018). Also, Fig.1.15 indicates that phosphorus streams going out after human consumption can be classified into phosphorus going to human sewage and phosphorus going directly to landfills. Then, if the installations commonly found in urban settings (e.g. wastewater treatment plants, garbage collection services) are to perform the recovery of phosphorus, it is possible to consider a value close to 100 ktP/y as the total recycling potential for phosphorus recovery in urban settings in Japan, where around 60 ktP/y are in sewage sludge, and 40 ktP/y are in other forms.

1.6 Introduction to Sewage Sludge Ash (SSA)

1.6.1 Treatment of Sewage Sludge

The role water treatment plants perform in modern society is of utmost importance. These installations consist of treatment facilities, storage reservoirs, pumping stations and distribution pipelines, which are required for the production and delivery of treated water to the final user. They are responsible for the removal of unwanted materials dissolved and/or transported in conjunction to water. Whether this stream comes from urban or industrial installations, the aforementioned role remains unchanged as it can be inferred water treatment plants are just concerned about the "production" of cleaner/useable water using specialized equipment and techniques (Asano, 2007).

In this regard, Fig.1.16 shows the standard block diagram used at a typical sewage treatment plants. It can be observed that, in the particular case of water treatment plants dealing with sewage, after primary and secondary treatment, the remaining solids (mostly suspended and colloidal materials) are required to agglomerate and be removed from water using physical and chemical means. Initially, the process involves several treatment units aimed at the formation of a uniform mixture, including equipment such as: mixing tanks, digesters, thickeners and blenders; then, the bulk of the solids is separated using a flocculation/sedimentation process.

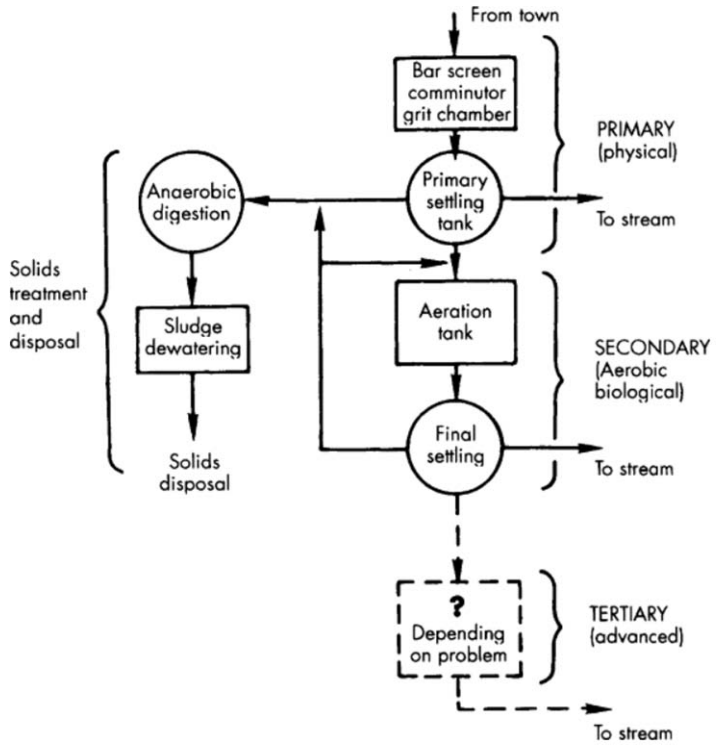

Figure 1.16: Block Diagram for a complete wastewater treatment plant. From Peirce et al. (1998)

Afterwards, biological treatment is applied to the sediments from the primary treatment in order to further promote the degradation of organic matter. This is usually carried out by installations for aerobic and anaerobic treatment, resulting in the formation of settled sludge at the bottom and clarified water upwards, which is pumped to

a different area for further treatment or recirculation. As for the remaining sludge, a dewatering process is applied first, where installations such as belt filters, hydro cyclones and centrifuges may be used, resulting once again in the separation of solid and liquid phases, the latter being commonly returned to the raw sewage flow of the plant or to a different area (Cheremisinoff, 2002).

Once the dewatering step has concluded, the solids produced (commonly known as "wet cake"), require further treatment as their volume can be still very large, and more importantly, they can contain a significant amount of pathogens due to the large amount of organic matter in their composition, which is regarded to be close to that of classical biomass (Ferrasse et al., 2003), in addition to some estimates putting it at around 30% in carbon content on a dry basis (Ros et al., 2006). This means the wet sludge generated at the exit of WWTPs cannot be disposed directly into landfills nor be disposed at sea, because of the very high risk of spreading pollutants, therefore specialized facilities are required for the final treatment of sludge.

Taking that into account, wastewater treatment plants are in the need to find a proper way to manage the "wet cake" they produce, considering the environmental legislation they are subjected to and their own operational costs. Hence, the following section discusses the incineration process of sewage sludge in more detail.

1.6.2 Incineration process and formation of Sewage Sludge Ash

In recent years, the worldwide trend for the management of large volumes of dewatered sludge is to use incineration as the final step before disposal. Incineration is attractive because as a whole, it reduces the total volume of excess material, promotes the destruction of toxic compounds, reduces odor generation and allows real scale installations to recover a substantial amount of energy as heat (Fytili and Zabaniotou, 2008). The incineration process of sludge can be carried out in different ways. The usual classification of these technologies is summarized in Fig.1.17

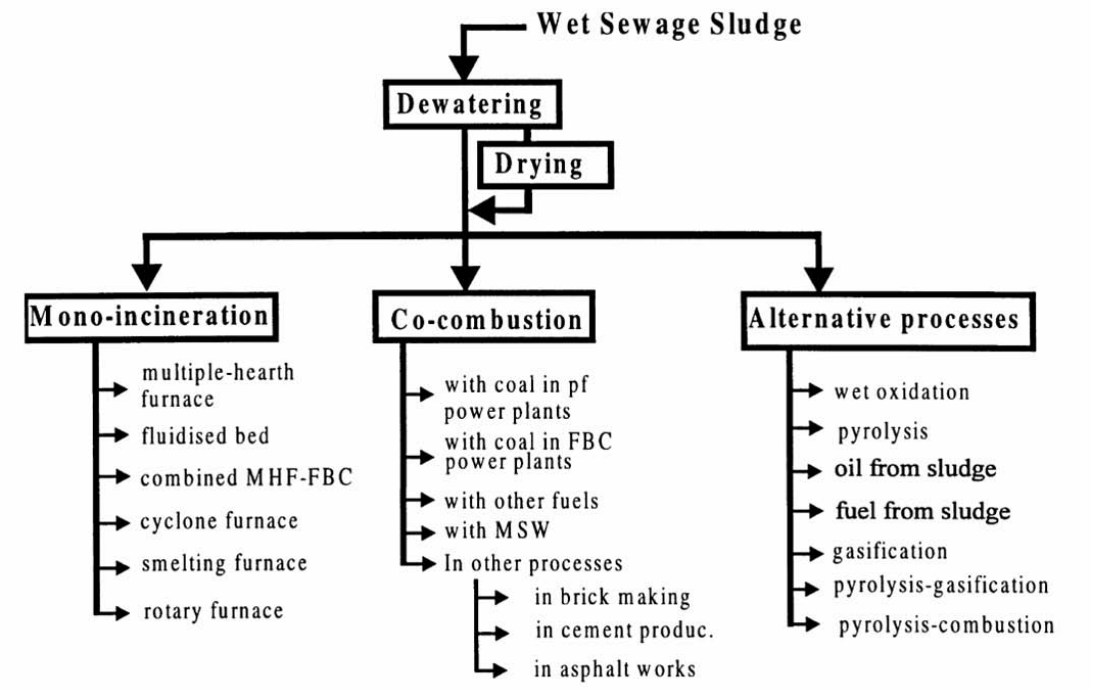

Figure 1.17: Different routes for thermal processing of sludge. From Werther and Ogada (1999)

The selection of a particular technique depends on the nature of the sludge and the accessibility of supplementary fuels on-site. In the case of multiple hearth furnaces, for example, the cost associated with the supplementary fuel needed for reliable combustion is often cited as a common drawback (Vesilind and Ramsey, 1996).

On the other hand, fluidized bed combustors have been used and improved since the beginning of the 20th century, where they were first deployed as alternative to direct (or multi-staged) combustors. A fluidized bed installation usually consist on a closed compartment filled with a bed of sand, where hot air is introduced from the bottom at pressures of 0.25 to 0.35 bar in order to fluidize the sand particles; the air flow being carefully controlled to prevent the sludge from floating on top of the bed (Cheremisinoff, 2002).

During operation, the "fuel" (in this case, dewatered sludge) is introduced into the combustor from a different opening, and heated to temperatures in the range 700 - 1000 °C, depending on the incineration scheme. Due to the high temperature of the system, the sludge particles disintegrate and volatile compounds are released, organic matter is combusted and bigger incombustible pieces fall through the fluidized sand for later removal (Stasta et al., 2006).

Fluidized bed systems, such as the one depicted in Fig.1.18 have been proven advantageous for a variety of reasons, namely: the increase of surface area for combustion material to exchange heat, the effect of "energy sink" from the filling (which reduces the cost of re-ignition after shutdown and reduces the effect sudden changes in the feed's composition have on combustion stability), and a resilience increase in terms of equipment maintenance because the bulk of the sand particles act as a buffer that reduces the thermal shock affecting the refractory material over time (Werther and Ogada, 1999).

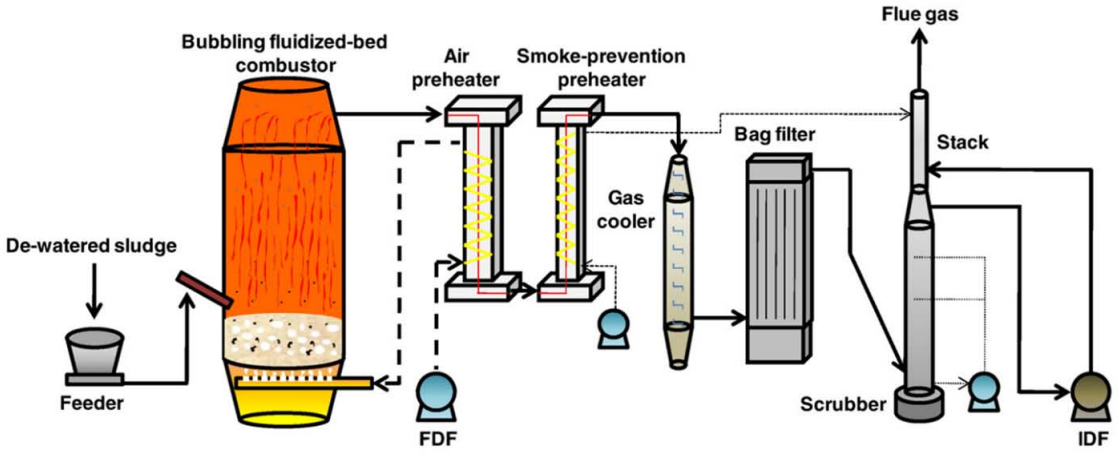

Figure 1.18: Schematic diagram of a conventional incineration plant, equipped with an atmospheric bubbling fluidized bed combustor. From Murakami et al. (2009)

In addition, current research trends focus on the improvement of the efficiency during the incineration process of sludge, via alternative pathways like pyrolysis and gasification (Samolada and Zabaniotou, 2014). When sewage sludge is heated in the absence of oxygen, it is possible to obtain liquid along with a carbonaceous solid holding calorific value, evidence suggesting the yield of this process being highly dependent on the temperature of the pyrolysis (Fonts et al., 2009). Correspondingly, studies on gasification have pointed

out the feasibility of obtaining syngas from sewage sludge, either directly (Groß et al., 2008), using a supercritical water influx (Acelas et al., 2014; Amrullah and Matsumura, 2018), or when steam (Nipattummakul et al., 2010) is added during the process.

In the particular case of Japan, the percentage of sewage sludge from urban areas disposed through incineration can be as high as 55% (Werther and Ogada, 1999). In a typical installation, sewage sludge is dewatered using physicochemical methods (such as pressurized filtration and air convection), and then used as dried sludge, being subsequently pumped into a fluidized bed boiler filled with hot silica sand. Since the temperature of silica sand is very high, the remaining water and volatile compounds escape the sludge along with the combustion gases generated by organic matter combustion. As this process is exothermic, treatment facilities are equipped to recycle the released energy by using heat exchangers and moisture removal systems interconnected in a closed-cycle fashion, improving the overall efficiency.

This way, Fig.1.19 shows a scheme of the processes used for Sewage Sludge Gasification and generation of Sewage Sludge Ash (SSA), proposed by the Bureau of Sewerage of Tokyo Metropolitan Government.

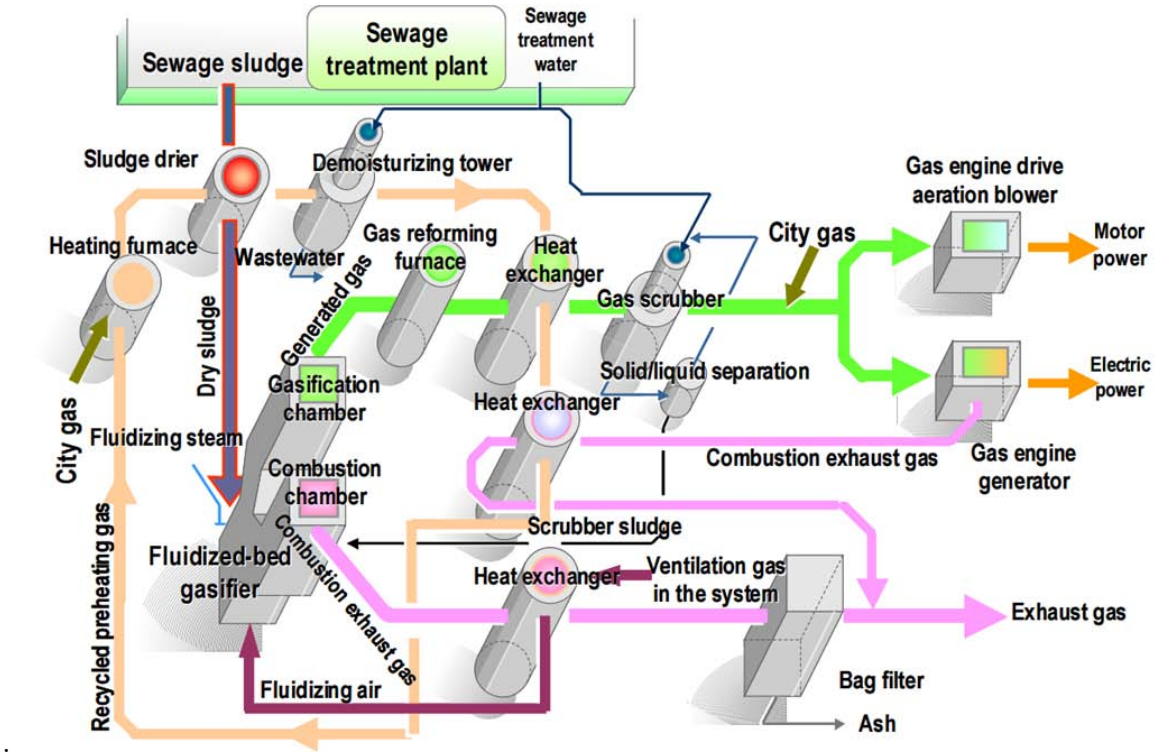

Figure 1.19: Sewage sludge gasification and incineration energy system. From Takahashi (2007b)

It can be seen that the only exits of material are exhaust gases and ashes collected by the bag filters as it is necessary for the treatment plant to comply with local regulations about the maximum concentrations allowed for these emissions, considering that exhaust gases are expected to contain compounds like NO_x, SO_x, CO, CO_2 and particulates. On the other hand, the composition of the ashes generated this way is generally not regulated, and has been traditionally considered to be useful mostly as cement filler material (provided the requirements from the cement industry are met).

1.6.3 Properties of Sewage Sludge Ash

Even though the facilities described in Section 1.6.1 are designed to optimize the combustion process and thus reduce the amount of residual material, solid residues are expected to be generated. Frequently, an arrange of physical particle collectors (e.g. filter bags and cyclones), or an electrostatic precipitator, are installed after the combustion system in order to collect coarse particles of mineralized materials and heavy metals; also including minute amounts of silica coming from the attrition caused by the turbulent fluidization of the sand bed itself. An illustration of these processes is presented in Fig. 1.20.

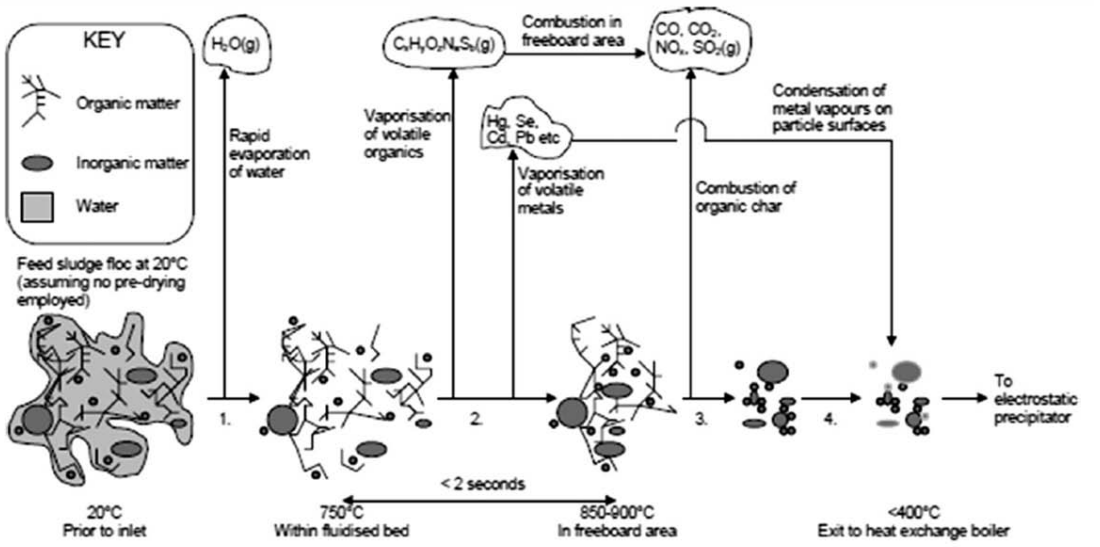

Figure 1.20: Illustration of the physicochemical processes most likely occurring during the incineration of sewage sludge. From Donatello and Cheeseman (2013)

The "ashes" collected at the exit of the flue stack are solid particles comprised of mineral species coming from the sludge, as well as crystal formed after the condensation of metal vapors on top of their surface. In addition, if the initial contents of the sludge feed and the way the incineration process is carried out are considered, the composition of the final ash is bound to vary, for instance, their energetic value and organic content will be different, as evidenced on Fig.1.21 where the differences of ashes subjected to different incineration processes can be noted visually.

Nonetheless, in the case of fluidized bed incinerators working in real scenarios, research efforts performed in different geographic locations around the world (Krüger et al., 2014; Smol et al., 2015), have pointed out that SSAs produced by thermal processing plants have an specific gravity in the range 1.8 - 2.9, a mean diameter of 50 - 260 µm, an average BET surface area in the range 2500 - 23100 m^2/kg, and a similar composition.

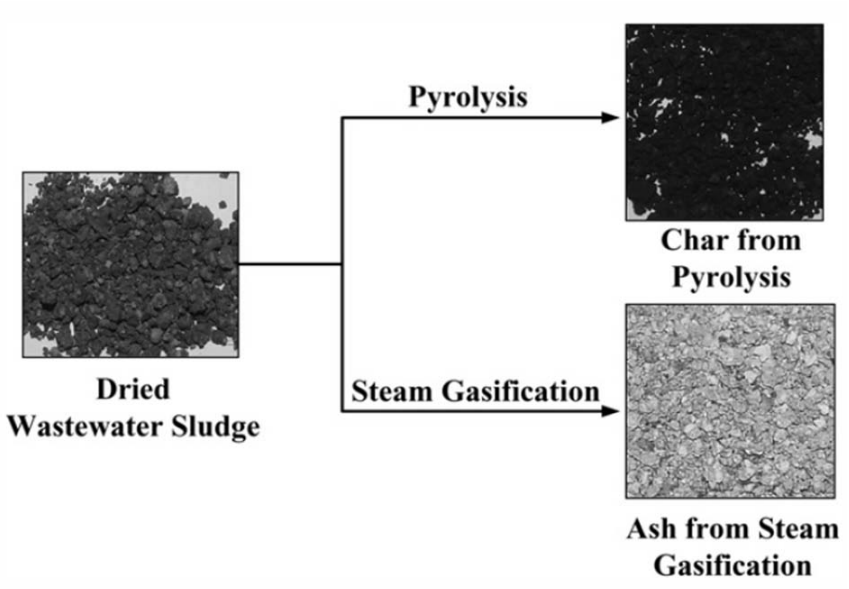

Figure 1.21: Products obtained depending on the incineration process. From Nipattummakul et al. (2010)

Thus, the main constituents of SSA are often minerals oxides of silicon (Si), calcium (Ca), iron (Fe), phosphorus (P) and aluminum (Al), in crystal configurations based on their stability at the incineration temperatures (around 700 - 1000 °C), resulting in the most abundant elements being found as iron oxides, phosphates and silicates. Additionally, heavy metals such as zinc (Zn), copper (Cu), barium (Ba) and chromium (Cr) are commonly present, and some SSAs even have traces of unconventional elements like zirconium (Zr), molibdenum (Mo) or silver (Ag). The aforementioned information is summarized in Table 1.1.

Table 1.1: Typical characteristics of Sewage Sludge Ash (SSA). Adapted from Lynn et al. (2015)

Composition (Summary)		
Main Elements	**Value (mean)**	**Unit**
Si	113368	mg/kg
Fe	68454	mg/kg
P	60697	mg/kg
Ca	54493	mg/kg
Al	44885	mg/kg
Na	17126	mg/kg
Mg	13894	mg/kg
Metals		
Zn	3355	mg/kg
Cu	2260	mg/kg
Mn	1404	mg/kg
Cr	750	mg/kg
Pb	373	mg/kg

In order to comply with environmental regulations, treatment plants are required to treat all the emissions (either solid, liquid or gas) before they are released to the outside environment. Regarding air emissions, it is common to make us of wet collection devices such as scrubbers using alkaline solutions to neutralize potential acid rain inducing gases (for example, NO_x and SO_x). In general terms, airborne emissions generated from treatment plants are considered of higher quality than of brown coal, however the ashes generated tend to present high concentrations of heavy metals.

Heavy metals that end up as part of the sewage discharge in urban settings come from industrial effluents and diffusion from households, along with the contribution made by corrosion and erosion of sewerage pipes. Researchers have pointed out the prevalence of zinc, nickel, copper, cadmium, lead, chromium and in some cases mercury in sewage streams (Asano, 2007; Smith, 2009). This means these elements will go through the treatment process, aggregate with the organic matter, precipitate, undergo combustion, and remain in the solid state until their final disposal as ashes.

Studies have shown (Gad, 2005) that heavy metals have a potential for a lasting, harmful effect on humans, since they can be bound to the blood stream and bioaccumulate. Also, disruption on the normal functioning of the cells may occur as heavy metals can react with enzymes and cell membranes, affecting specific organs or diverse anatomical sites. Because unplanned disposal of solids containing heavy metals may lead to an eventual deterioration of the soils, which in turn augments the risk of increased metal uptake by food crops grown on contaminated areas, a matter of concern arises and strategies must be devised.

Nonetheless, research efforts are being made to valorize SSA as a resource because of the comparatively high concentration of phosphorus. In addition, because SSA is composed only of mineral species, it has a relative advantage over the direct use of sludge for fertilizer, since the latter can contain pathogens even after treatment. Still, the main limitations for the direct application of SSA on crop fields are the presence of heavy metals (Werther and Ogada, 1999) and the low plant biovailability of phosphate ions due to the P-bearing phases (Vogel et al., 2013) in SSA. Therefore, if SSA is properly treated, and the "undesired" elements are removed, it could be considered as a useful source of cheap, recycled phosphorus, which can in turn be reused in diverse ways. In that light, Section 1.7 introduces the methods currently being studied around the world to recover phosphorus from SSA.

1.7 Current state of the technology for Phosphorus recovery from SSA

Even though using SSA directly onto agricultural land as a supplementary source of phosphate ions for the soil seems as a plausible alternative to alleviate the present phosphate rock demand, there are two main concerns with this practice that may hinder its sustainability in the long term, as evidence has revealed that there is a risk of gradual release of heavy metals into the soil, if said elements are not previously removed (McBride et al., 2004). On the other hand, the low soil-solubility (bioavailability) of the phosphate in the SSA when it is used "as is" (Raymond et al., 2018) can also reduce the value of SSA as a phosphorus resource, which in addition makes maximizing the purity of the phosphate an important part for any candidate recovery process being devised, as only a smaller percentage of the phosphate will eventually be dissolved in the solid.

Taking that into account, any method focused on the recovery of phosphorus from SSA should not only aim at obtaining the largest "yield", in terms of recovering the largest amount possible of phosphorus from SSA; but also should consider the soil-solubility of the phosphate phase present, and moreover, the potential remnants of unwanted metals that may still remain in the solid after the recovery process.

Therefore, it is possible to divide the lines of research in the recovery of phosphorus from SSA in the following categories (Donatello and Cheeseman, 2013):

- Thermochemical methods of recovery, which subject the SSA to high temperatures and promote the separation of heavy metals using particular reagents and reactions.
- Leaching methods of recovery, based on the dissolution of phosphorus at lower pH values and the differential solubility of the each ion.
- Methods based on other processes.

1.7.1 Thermochemical methods for the recovery of Phosphorus from SSA

In the industrial process of steelmaking, phosphorus is considered to both positively and negatively affect the properties of the steel. For example, a low P content is desired in steels that require high ductility, whereas for steels that are expected to have an increased strength, P can be a requirement as it can strengthen ferrite (Hong Tian et al., 2009). Hence, the bulk of the literature found on phosphorus behavior at high temperatures is devoted to the proper management of P content in steels, where the addition of CaO as a dephosphorization agent is used.

Given the capacity of slag systems to capture phosphorus is greatly increased by the addition of CaO, the vast majority of the available literature is related to the study of the $CaO{-}FeO{-}P_2O_5{-}SiO_2$ system to different degrees. Likewise, the rate of dissolution of lime is affected by the viscosity of molten slag, as well as the mass transfer of phosphorus from hot metal to the slag system (Gao et al., 2013). Fig.1.22 shows the $CaO{-}FeO{-}P_2O_5{-}SiO_2$ system, highlighting the existence of definite phases based on the composition of these species:

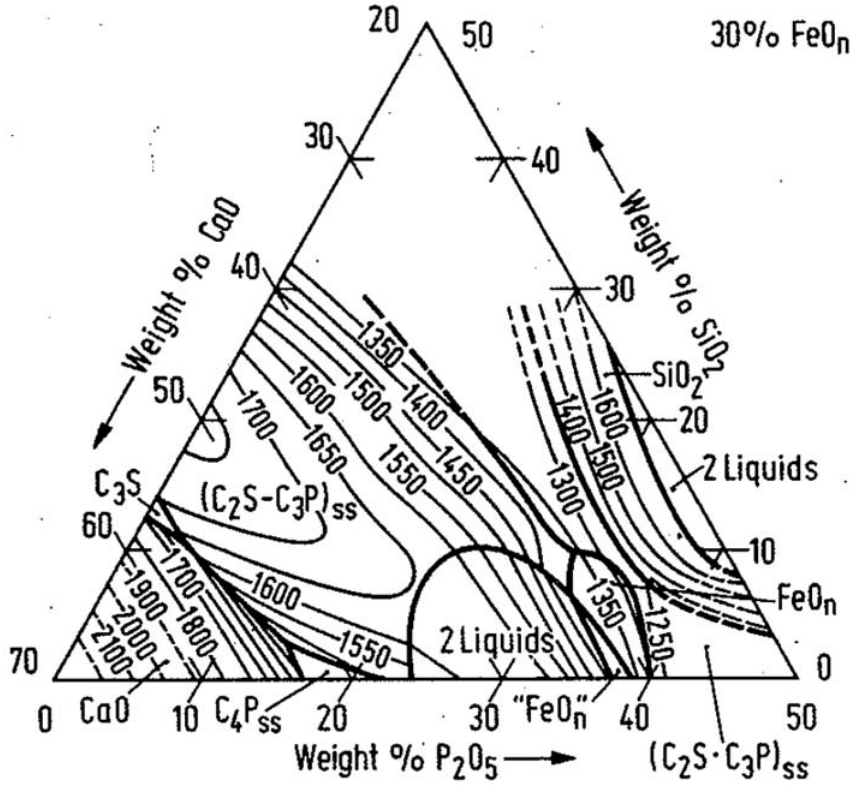

Figure 1.22: Diagram of the system CaO−FeO−P_2O_5−SiO_2 for 30%FeO content. From Stahleisen. and Verein Deutscher Eisenhuttenleute (R.F.A) (1995)

Thus, based on the similarities in their percentage composition, it is presumed SSA and steelmaking slag may have an analogous behavior if exposed to the same conditions. When SSA is subjected to high temperature treatment, a series of chemical reactions take place. Based on particular conditions (temperature and composition of the mix), it is possible to devise a scheme aimed at the increase of purity with respect to phosphate content, while at the same time performing the removal of heavy metals.

One research work (Adam et al., 2009) has proposed a possible recovery route for Phosphorus from SSA. The main idea behind this process is the addition of alkaline earth chlorides like $MgCl_2$ and $CaCl_2$, which act as chloride (Cl^-) donors to SSA, followed by the ulterior burning of said mixture to temperatures in the range 800 - 1000 °C, in order to promote the formation of volatile metal chlorides that are separated from the solid phase.

This technique seems more suitable for a system that is designed to handle the volatilized chlorinated compounds and is able to dispose of them accordingly. Second, the final products have their phosphate content mostly as Mg-bound phosphates like farringtonite $Mg_3(PO_4)_2$ and stanfieldite $Ca_4Mg_5(PO_4)_6$, highlighting the Mg-binding effect of the chlorine donors. Further analysis of these species showed their solubility in citrate increased to 97% when compared with the untreated SSA, which stood at 25 - 40%. Fig.1.23 shows the flowsheet used in this method:

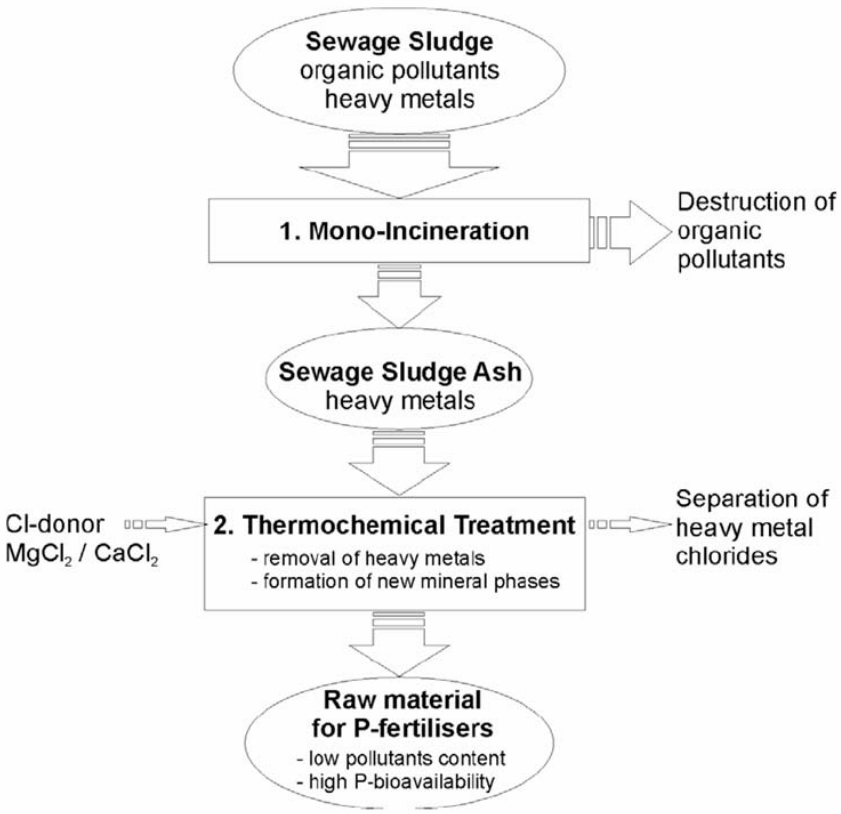

Figure 1.23: Recovery of phosphorus from SSA using Cl^- donor salts. From Adam et al. (2009)

On another approach (Stemann et al., 2015), SSA was mixed with diverse sodium salts and treated at 1000 °C, towards achieving similarities to the Rhenania process, where $CaNaPO_4$ is formed from pure $Ca_3(PO_4)_2$ (Jantzen et al., 1979) as described by Eq.1.3.

$$2\,Ca_3(PO_4)_2 + 2\,SiO_2 + 2\,Na_2CO_3 \longrightarrow 2\,(Na_2O \cdot 2\,CaO \cdot P_2O_5) + 2\,CaO \cdot SiO_2 + 2\,CO_2 \quad (1.3)$$

Results showed the phosphate existing in the SSA does indeed behave in a similar way to pure $Ca_3(PO_4)_2$, producing Ca/Na combined phases as predicted by the equation above. Moreover, if during calcination a reducing agent is added (for example, a source of carbon), Na_2SO_4 can be employed as the selected sodium salt, instead of Na_2CO_3 which is considered more expensive. The final products are reported to have a dependence on the amount and type of Na-salt used, with the best performing citrate solubilities reaching values of around 80%.

Due to the increase in the prices of phosphate rock observed in the last decade, companies and experts in sustainability science have started to take more interest in phosphorus recycling technologies that could be viable for real-scale application. Examples of the thermochemical technologies with potential applications are:

- ***The ASH DEC®*** process, based on the addition of chlorides to remove the heavy metal contents (Amann et al., 2018). This process deals only with SSA and has only been implemented on a trial basis and tests are still ongoing for pilot plants. **Advantages:** Reduced energy demand, reuse of waste material, good removal of heavy metals from the solid residues. **Disadvantages:** Mandatory SO_2 and chlorine emissions, low availability on alkaline soils, costs of added reagents.

- ***The RecoPhos®*** process, aimed at the production of P_2 using the reaction described by Eq.1.4 for calcium phosphate (Rapf, 2012).

$$Ca_3(PO_4)_2 + 3\,SiO_2 + 5\,C \longrightarrow 3\,CaSiO + 5\,CO + P_2 \tag{1.4}$$

  Advantages: High purity of the material obtained, high P recovery, possibility of using the remaining slag as a cementitious material. **Disadvantages:** Low plant availability on acidic soils, high initial expenditure -as it needs to be installed along the sewage sludge incineration process, high demand for reduction agents (i.e. coke as a source of carbon)

- ***The Mephrec®*** process, that uses sludge and SSA as raw materials and subjects both to metallurgical treatment, recovering phosphate rich products. This technology has been executed on a large plant scale (Amann et al., 2018). **Disadvantages:** Scalability, reduction of energy sources, reduced gaseous emissions.

It is clear that the thermochemical processing of SSA has a promising outlook and it might be possible to see a wider adoption of the techniques described in the future. Likewise, leaching methods are considered as promising prospects for industrial application and are described in the following sections.

1.7.2 Leaching methods for the recovery of Phosphorus from SSA

The beneficiation of phosphorus from phosphate rock is the standard way of industrially obtaining this product since the beginnings of the 20th century. Processing is needed because phosphate ore is commonly composed of calcium phosphates, such as fluorapatite ($Ca_3(PO_4)_3 \cdot CaF_2$) and the average content on the ore is of about 13% phosphorus.

The existing impurities are minerals of iron, aluminum, silica, sodium, potassium and depending on the mining sites, some radionuclides like uranium and radium (Habashi and Awadalla, 1988). The wet process route for the commercial production of fertilizers involves the leaching of calcium phosphate from the phosphate ore using sulfuric acid as expressed by Eq.1.5 to promote the formation of *phosphoric acid* (H_3PO_4) and *gypsum* ($Ca_2SO_4 \cdot 2\,H_2O$).

$$Ca_3(PO_4)_2 + 3\,H_2SO_4 + 6\,H_2O \longrightarrow 2\,H_3PO_4 + 3\,CaSO_4 \cdot 2\,H_2O \downarrow \tag{1.5}$$

In general terms, the production process yields satisfactory results, however depending on the initial composition of the ore, many impurities are bound to appear in the leachate. Also, the presence of $CaSO_4 \cdot 2\,H_2O$ demands for an extra step in processing aimed at its removal. Aside from raw phosphate ore, it is possible to perform the leaching process onto secondary phosphorus sources. For example, solid material coming from the steelmaking industry (see Section 2.1.4), is a candidate for a contributory source of phosphates.

Therefore, it is possible to consider SSA as a type of "mineral ore" where the solid contains a meaningful amount of P combined with other minerals, and depending on the solubility of their ions the leaching process is bound to occur.

One of the most straightforward ways to recover phosphates from SSA, relies in promoting the release of phosphate ions from solid SSA using a mineral acid in order to obtain a concentrated leachate. This is based in the fact that under different pH conditions, phosphate ions $(PO_4)^{3-}$ in solution are combined with hydrogen and form the hydrogen phosphate ion $(HPO_4)^{2-}$, the dihydrogen phosphate ion $(H_2PO_4)^{-}$ and phosphoric acid H_3PO_4 respectively, being this balance of ions regulated by the well-known rules of chemical equilibrium. In that regard, Fig.1.24 presents typical ion speciation diagrams for phosphorus, summarizing the thermodynamic calculations performed onto the activities of the aforementioned species in solution.

These diagrams highlight that under acidic conditions the phosphate in the SSA (initially combined with Ca, Mg, Al or Fe) will be gradually released into solution. Moreover, at pH values lower than 2, the majority of the phosphate ions present, are going to be combined as H_3PO_4, and the formation of any kind of P-bearing precipitate will be negligible, resulting in a leachate having large concentrations of phosphorus. However, the main drawback any leaching technology faces is related to the fact that heavy metals normally present in the solid tend to be dissolved under similar pH conditions; thus, researchers have tried different approaches to circumvent this issue, resulting in the suggestion of diverse methods.

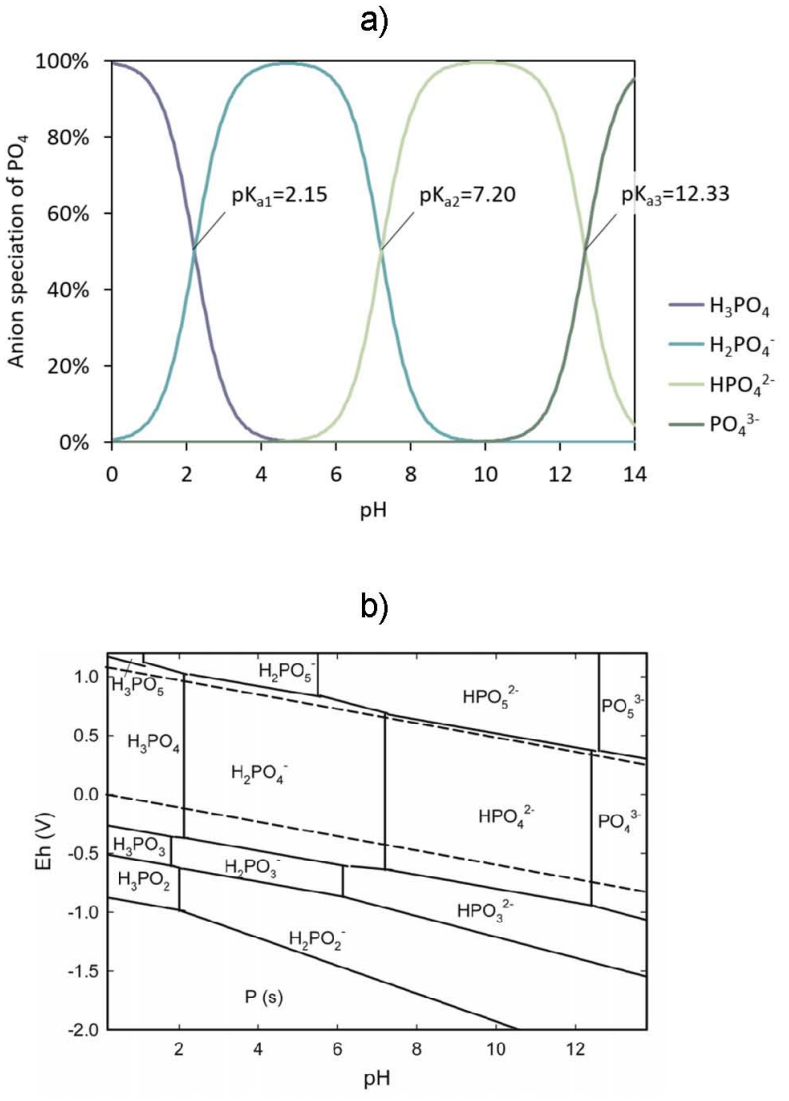

Figure 1.24: Speciation of the phosphate $(PO_4)^{3-}$ ion. a) As a function of pH, b) As expressed by an Eh-pH diagram. From Everaert (2018) and Pasek (2008)

One study suggested the controlled release of phosphate after being dissolved from SSA, under the pH range = 3 to 4, based on the premise that pervasive interferences like Cu and Zn ions have greater solubilities than of phosphate under those conditions (Schaum et al., 2007). A different method proposes the dissolution of all the species available at pH values lower than 2, and then proceed to remove the heavy metal ions phosphate via sulfide precipitation, finally promoting the subsequent precipitation of calcium phosphates by the addition of lime water (Franz, 2008). The combined approach seems to be of promise since the body of literature published counts many applications of this technique to different SSAs around the world (Takahashi, 2007a).

Diverse adaptations of leaching processes are still at the laboratory scale; however, it is relevant to discuss two processes based on leaching that have moved on to the pilot plant scale:

- ***LeachPhos***, developed and patented by BSH Umweltservice GmbH. This method dissolves phosphate from the SSA using H_2SO_4, followed by filtration to separate the remaining solids. The liquid is then processed using $Ca(OH)_2$ to recover phosphorus as calcium phosphate ($Ca_3(PO_4)_2$) (see Fig.1.25). **Advantages:** High purity of the material obtained, possibility of using on ashes with low P content. **Disadvantages:** High amount of waste generated (no scheme for reuse), slow processing due to the sequential removal of heavy metals.

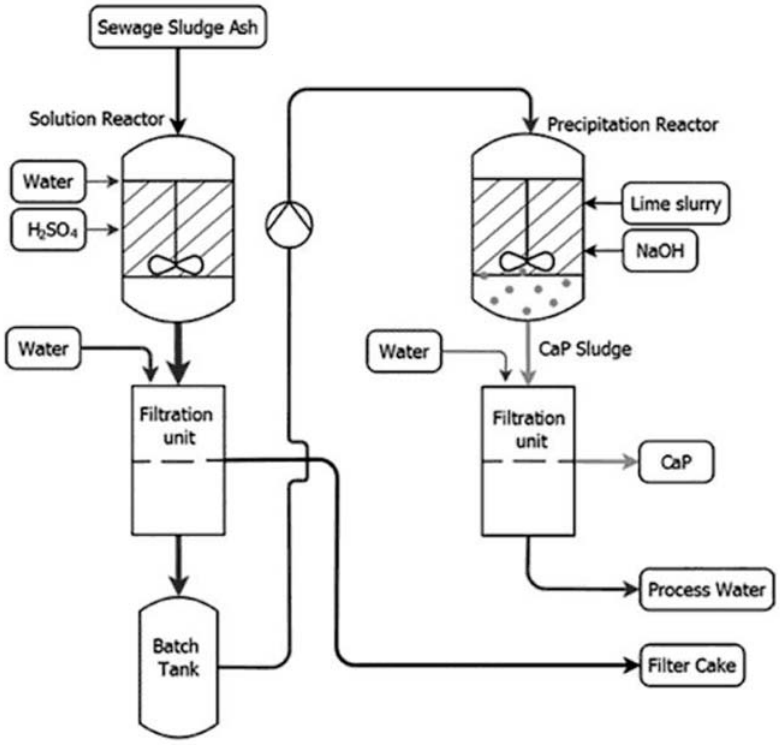

Figure 1.25: Diagram of the LeachPhos process. From Lema and Suarez (2017)

- ***EcoPhos***, based on the digestion of SSA with phosphoric acid, followed by treatment with ion exchange columns (aimed at the removal of Al, Fe, Mg, Ca), and further concentration of the obtained liquid using temperature (see Fig.1.26). **Advantages:** Very high purity of the material obtained, possibility of recovery secondary Fe, Al, Mg products. **Disadvantages:** High amount of chemicals and materials needed in the ion exchange step, increased costs associated to maintenance and installation of more process units.

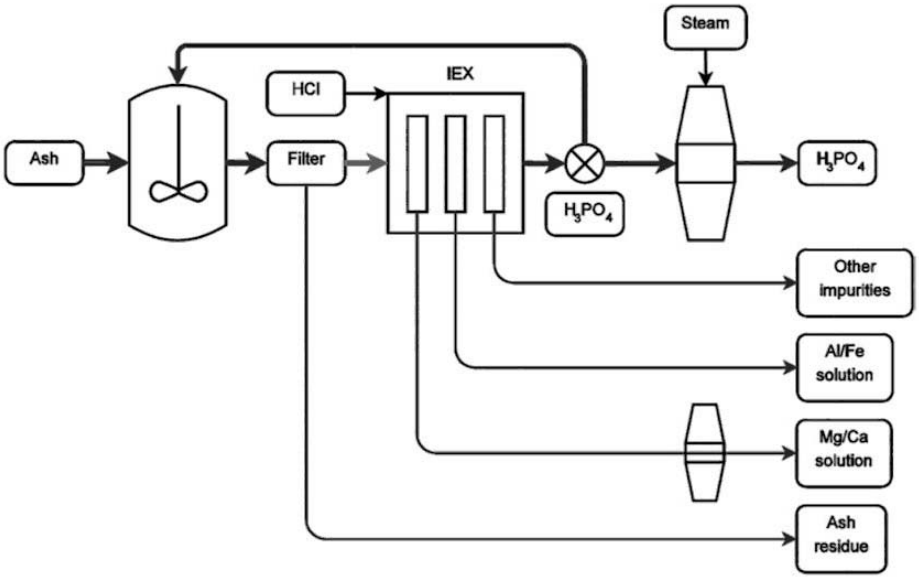

Figure 1.26: Diagram of the EcoPhos process. From Lema and Suarez (2017)

1.7.3 Other approaches for the recovery of phosphorus from SSA

Aside from the main trends in research for phosphate recovery from SSA, a few other techniques are currently under investigation. The main idea behind these alternative approaches is to improve the efficiency of the final products, to decrease the amount of reagents required, or to apply a completely different processing method altogether:

For example, an alternative process is related to thermochemical treatment where the mixing of SSA with a calcium source to promote the formation of both a calcium phase rich in alumina and another calcium phase rich in phosphorus (Imai, 2019). Here, the process is carried out at higher temperatures and results in calcium phosphate phases with a high bioavailability.

One of the alternative methods related to wet leaching, proposes the use of an electrodialytic cell to separate the phosphate and the heavy metal ions dissolved in the solution coming from SSA (Guedes et al., 2016). In this approach, a cell with three compartments separated by ion exchange membranes that isolate the ash suspension in the middle and have the "anolyte" and "catholyte" respectively on each side of said cell is used, as observed in Fig.1.27.

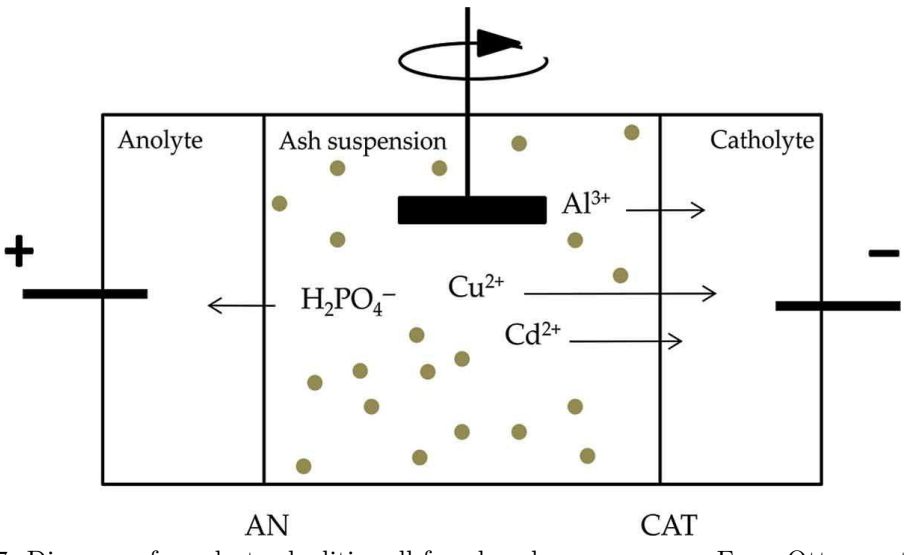

Figure 1.27: Diagram of an electrodyalitic cell for phosphorus recovery. From Ottosen et al. (2014)

1.7.4 The need for physical separation methods for the recovery of phosphorus from SSA

Naturally, this means that at the moment, the processes designed for the recovery of phosphorus from SSA rely entirely on costly transformations which may require the use of specialized equipment, reducing the effectiveness of the method as a whole. This way, the disadvantages in terms of costs for such methods can be described as:

- The large amounts of thermal energy required for the thermochemical method, and the large amount of electrical energy for the electrodyalitic method where the concentration of ions will depend on the current provided to the system.
- The large quantity of acid needed for the leaching methods, in addition to the similarly large quantity of base required for neutralization of the leachate. The costs here can be further compounded considering that the purification of the leachate will require supplementary reagents like EDTA (Fang et al., 2018) or sulfides (Franz, 2008).

This shows that there is a need for the development of alternative methods that can overcome these deficiencies. The desired qualities of said methods are to perform a quick recovery process, and to be simple enough so it could be implemented in a real scale without the requirements of a complicated setup or the design of specialized machinery. For this purpose, the alternative presented by physical separation methods that rely on straightforward transformations appears as an interesting option.

In this regard, since SSA can be considered as a type of “mineral ore” where the target element for enrichment is phosphorus, the physical separation methods commonly used for the concentration of unrefined ores in the mining industry are attractive. Moreover, because mining operations are capable of handling large volumes of ore, and the beneficiation systems can be implemented with relatively simple equipment which increase the appeal of these techniques from an economical viewpoint.

1.8 Objective of this research and structure of the thesis

1.8.1 General Objective

The purpose of this research work is to develop novel processing methods designed for recovering phosphorus from Sewage Sludge Ash (SSA) in order to obtain phosphates for useful applications. In this regard, the first two methods are intended to obtain phosphates suitable for fertilizer formulations, which mostly require the presence of soil-soluble phosphates;

1.8.2 Structure of the thesis

The structure of the thesis work presented here can be summarized as follows:

- Chapter 1 shows a general introduction of the importance of phosphorus, and the need for recycling phosphate from SSA.
- Chapter 2 presents the recovery of phosphorus from SSA using a carbothermic reaction followed by High Gradient Magnetic Separation (HGMS) and flotation (Method 1).
- Chapter 3 presents the recovery of Phosphorus from SSA using a heat treatment and liquid-liquid separation, which is named as Method 2.
- General conclusions are included in Chapter 4, in addition to an overview of the main findings of this work and proposed process diagrams

The first two methods rely on *physical* processing techniques commonly used for mineral processing, and are relatively easy to scale up in WWTPs and have not been studied as alternatives for the recovery of phosphorus from SSA as of yet. In addition, the method presented in Chapter 2 includes a carbothermic reaction aimed at increasing the magnetization of SSA, whereas Chapter 3 includes a heat treatment step where the phosphate in SSA is adjusted to form a soil-soluble phosphate.

For instance, since SSAs commonly have iron oxides in their composition, then it might be possible to use the technique of High Gradient Magnetic Separation (HGMS) to remove the iron oxides and therefore increase the percentage of phosphorus as proposed in Chapter 2.

In a similar manner, it could be feasible to take advantage of the difference in the surface properties of phosphates (which are positively charged under certain pH conditions), to promote their concentration using physical methods like liquid-liquid separation as explored in Chapter 3, or flotation which was investigated in the latter part of Chapter 2.

Chapter 2

Recovery of Phosphorus from SSA using a carbothermic reaction followed by High Gradient Magnetic Separation (HGMS) and Flotation

2.1 Introduction

As shown in Table 1.1, SSAs commonly have a fair amount of iron in their composition. Hence, it is proposed in this research work that the physical process of magnetic separation could be applied to remove the ferrous materials from the SSA. In this case, it is posited that performing a carbothermic reduction reaction for the iron present in SSA (which exists as an oxidized, weakly magnetic form), will increase the overall magnetization of the sample, and thus facilitate the effectiveness of iron removal via a magnetic technique known as High Gradient Magnetic Separation (HGMS).

Following the magnetic separation step, the physical separation procedure of flotation for the phosphorus rich "non-magnetic" fraction is presented. For this purpose, phosphate is enriched in the upper part of a foamy accumulation (known as "flotation froth"), consisting in the hydrophobic agglomeration of bubbles and solid particles. The process of flotation was considered based on the reported affinity for anionic collectors described for similar materials containing phosphate (Sis and Chander, 2003).

Thus, an overview of the steps taken for the development of the aforementioned method are presented below:

1. The characterization of the sample of *as-received* SSA using common analysis techniques.
2. The implementation of a carbothermic reaction using SSA, carbon and other oxides as raw materials, in order to increase the mass magnetization of the SSA and to improve the soil-solubility of the phosphorus phase obtained after heating.
3. The study on the removal of iron from the reacted SSA using High Gradient Magnetic Separation, in order to collect two different fractions: the "magnetic-fraction" (enriched in iron content), and the "nonmagnetic-fraction" (enriched in phosphorus content).

4. The evaluation of the increase in concentration of phosphorus in the froth for the *"best-performing"* nonmagnetic fraction using a flotation process.

2.1.1 Brief introduction to the magnetization of solid materials

In a very simplified manner, and due to the nature of this work, a brief explanation on the magnetization of materials is in order. On the road to define the effect a magnetic field will have over a solid particle, it is possible to define the "magnetization" as the magnetic moment per unit volume of a solid using Eq.2.1.

$$M = m/V \tag{2.1}$$

The magnetic moment m is a vector quantity and itself a function of the flux density, the dipole length and the permeability of the medium. Depending on the alignment of the moments of the individual atoms of a sample, a strong or weak magnetization will occur. A very useful quantity in engineering is the magnetic moment per unit mass, which is a general way to describe how magnetizable a substance can become when subjected to a given magnetic field, and is represented by Eq.2.2:

$$\sigma = m/mass \tag{2.2}$$

Naturally, the highest the value of σ for a material, the higher the alignment its atoms achieve when subjected to a magnetic field. Nonetheless, there is a practical limit to the magnetization a substance can attain, called the saturation magnetization (Jiles, 1991). This value can be very useful to compare the behavior of materials under similar conditions and to establish the nature of their magnetization.

Measuring the saturation magnetization of solids

For a material to be considered "magnetic" some conditions are to be fullfilled, in a very simplified way the main requirement is having a "net magnetic moment" in terms of the arrangments of the dipoles formed at the atomic and crystalline structure of a solid. In this light, materials can be classified as ferromagnetic when an appreciable fraction of the aforementioned dipoles are arranged in a favorable direction, resulting in magnetization existing in the absence of external magnetic fields.

On the other hand, only a partial fraction of the magnetic moments in ferrimagnetic materials have a partial preference arrangment, meaning that there are dipoles arranged in a different direction which counteract (and reduce) the effect on net magnetization. Lastly, when the magnetic moments of the dipoles are ordered in an antiparallel arrangment and cancel each other, resulting in a net magnetization similar to those of paramagnetic materials (Miyazaki and Jin, 2012)

In this regard, the most familiar example of a ferrimagnetic material is magnetite Fe_3O. More explicitly, the chemical composition of magnetite is actually $FeO \cdot Fe_2O_3$, showing that there are two types of iron ions: the ferrous ions Fe^{2+} with a charge of (2+) and the ferric ions Fe^{3+} with a charge of (3+). This way, Fe ions are located in either of two different coordinate environments: A tetrahedral one, where the Fe ion is surrounded by 4 oxygen ions, and the octahedral one, in which it is surrounded by 6 oxygen ions.

This indicates that, of the 16 ferric ions in the unit cell of magnetite, half are in one type of position and the other half are in the other. Moreover, the tetrahedral structure promotes the orientation of moments opposite to the orientation of the octahedral one, resulting in a complete cancellation of the contribution of the ferric ions to the magnetic moment. The net moment therefore arises entirely from the 8 ferrous ions which occupy octahedral sites. (E.Y.Tsymbal, 2005)

On the other hand, when a magnetic field is applied to a previously demagnetized ferromagnetic specimen, its magnetization will gradually increase. This way, it can be observed in Fig.2.1 that starting from point O, the magnetization increases relatively fast at first, and then the increase becomes less pronounced until it reaches a constant value at point A. At this point, the specimen is considered to be "saturated" in terms of magnetization, while the curve just described is known as the initial magnetization curve. Then, the saturation magnetization Ms is equal to the spontaneous magnetization of the material.

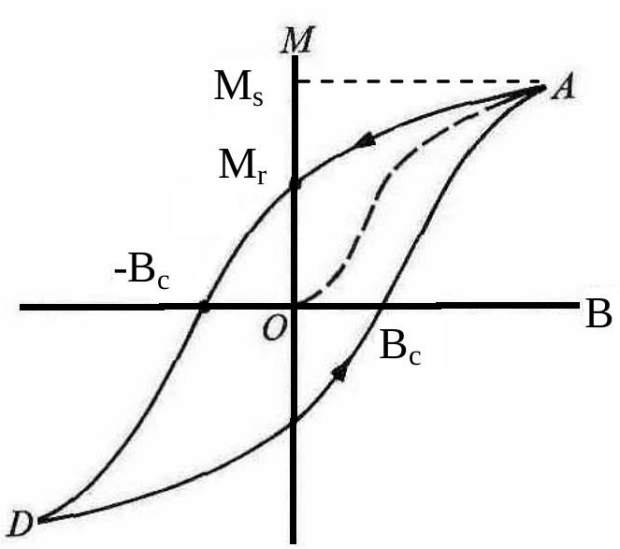

Figure 2.1: Magnetization curve for solids. The The coercivity Bc is the reverse magnetic field that reduces the magnetization M to zero. The remanence Mr is the value of M at B = 0 wheras the saturation magnetization Ms is the limit of M at a large magnetic field B. From E.Y.Tsymbal (2005)

Experimentally, the determination of the magnetization curves for materials can be carried out using a low-cost alternative known as the Vibrating sample magnetometer (VSM), which is a device presented in the late 50's by Foner (1959). The working principle behind the VSM machine is the generation of currents based on the effect of the voltage induced in the pickup coil, which is proportional to the magnetic moment obtained when a controlled magnetic field is exerted on a solid sample. These currents are then typically measured using a lock-in amplifier where the piezoelectric signal is taken as a frequency reference. Likewise, it is also possible to sweep the external magnetic field on a controlled range to obtain a hysteresis curve similar to the one described in Fig.2.1.

2.1.2 High Gradient Magnetic Separation (HGMS)

Among mineral processing techniques, magnetism based separation methods are part of the most prominent as their implementation at large scale facilities started during the 1970s, especially in the kaolin beneficiation industry where its efficiency has been proven repeatedly during the years (Lofthouse, 1981). In addition, recent developments in the field are concentrated into fabricating systems able to capture nanoparticles that can be used to perform treatment tasks and remove contaminants from wastewaters, or purify chemical products.

The pioneer work in the study of this topic performed by Svoboda (2001) has established that HGMS is essentially a deep filter bed with an external magnetic field, where the principles that govern the filtration phenomena should apply reasonably well to HGMS separation. That means the probability of a particle being attracted to a magnetically influenced wire is determined by the collision conditions, which in turn depend on hydrodynamic considerations. In addition, theoretical studies on the operational principles of HGMS (Uchiyama et al., 1976) have demonstrated that when a stainless ferromagnetic mesh is used to capture magnetic particles their effectiveness is increased at the portion perpendicular to the slurry flow, as the drag force acting on the particles competes with the capturing magnetic force, as can be observed by the diagrams presented in Fig.2.2

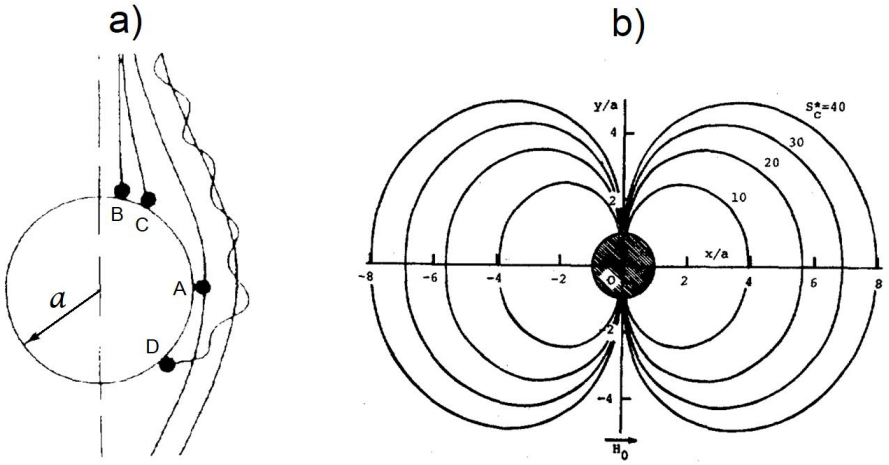

Figure 2.2: Schematic diagram of the magnetic capture of particles by a magnetized wire. a) Collision mechanism in deep-bed filtration. A: interception, B: Inertia adherence, C: Sedimentation, D: Diffusion. Adapted from Svoboda (2001); b) Contour of capture cross section of an isolated ferromagnetic wire, where H_0 represents the direction of the magnetic field. From Uchiyama et al. (1976)

This highlights that the ideal matrix used for the magnetic capture should promote perpendicular contact of the particles that are wanted to be captured, instead of promoting the capture of said particles via a simple mechanical filtration. This situation (promoting magnetic capture instead of filtering) can be achieved if the perturbation to the one-directional magnetic field caused by the ferromagnetic wires is large enough to result in a "magnetic gradient", that is a function of the proximity of the particles to the wire.

In the practical sense, this resulted in the adoption of a metallic mesh matrix, similar to the one depicted in Fig.2.3, where an example of an experimental stream type magnetic canister, consisting of an arrangement of metallic wires in a repeating pattern which promote the appearing of large perturbations to the magnetic field is presented.

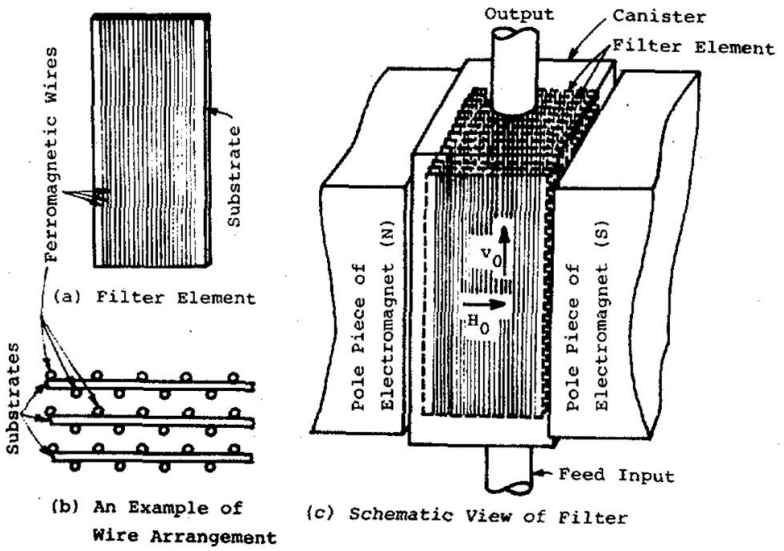

Figure 2.3: Parallel stream type magnetic filter canister. From Uchiyama et al. (1976)

In a similar fashion, it was observed that magnetic capture is also influenced by the size of the magnetic wires comprising the matrix. In this regard, earlier work (Chen et al., 2016) pointed out that a fine matrix such as a wired mesh matrix tends to give a high recovery while a coarser matrix gives a high concentrate grade, since a sharply shaped magnetic pole is bound to produce a higher gradient in the magnetic field, indicating that the role exerted by the matrix in the removal performance should be acknowledged.

2.1.3 Flotation

Flotation is one of the most widely used mineral separation methods (Mesa and Brito-Parada, 2019), as every year large volumes of the most important minerals are processed worldwide in order to increase the concentration of several elements important for the development of modern societies (Wills and Finch, 2016). The main idea behind flotation processes is the ability of air bubbles to selectively adhere to specific minerals in a slurry comprised of solids and water, whereby the particles able to have bubbles attached to their surface will move upwards and agglomerate in a concentrated zone where they can be collected as the *froth*, whereas the particles that are not able to have air attached to their surface will remain at the bottom as the *tails* (Sutherland, 1948).

Specifically, the basis of froth flotation is the difference in wettability between materials, caused by the surface properties of the solids. Hence, it is possible to classify particles in two categories: particles that are hydrophilic (prone to get wet), and particles that are hydrophobic (water repellent). This process is illustrated in Fig.2.4.

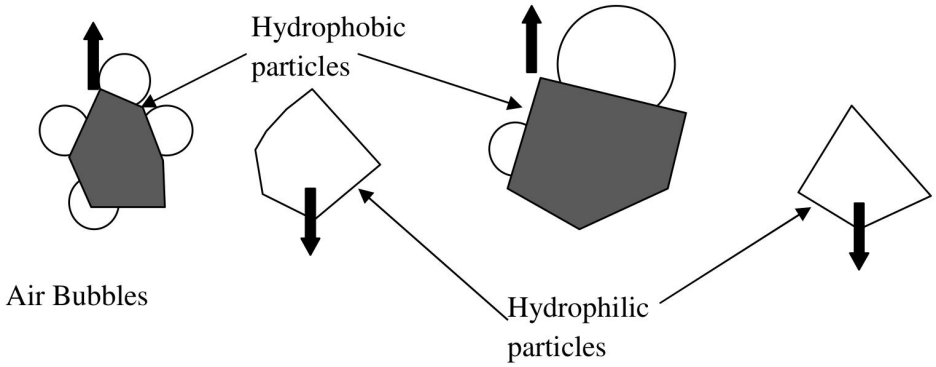

Figure 2.4: Adhesion of bubbles onto hydrophobic particles during the flotation process. From Kawatra and Eisele (1992)

Mineral particles can either be naturally hydrophobic, or the hydrophobicity can be induced by chemical treatments designed to influence the charge on the surface of the particles, in order to achieve the desired hydrophobicity. This way, the study of the different reagents used to facilitate the formation of froths and to increase their stability is an active area of research (Farrokhpay, 2011). Hence, in preparation for the flotation process a chemical step is used, where the reagents required for achieving different levels of hydrophobicity are applied. In that light, the more hydrophobicity of a particle, the more chance this particle has to remain in the froth.

In consequence, once the interaction of bubbles and solid particles has started, it is possible to model (see Fig.2.5) the process by which particles attach to bubbles and a stable froth.

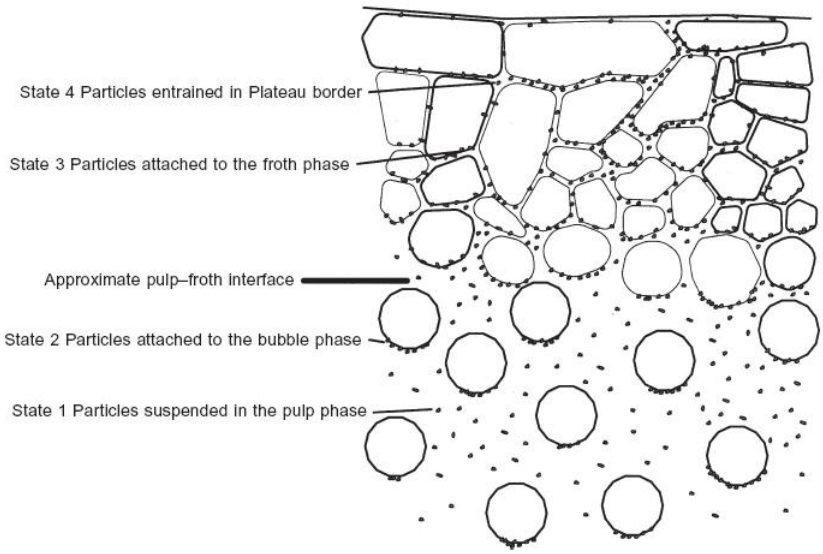

Figure 2.5: States of froth formation during flotation. From King (2001)

From Fig.2.5, the required steps by which the particles ascend and are captured in the top fraction of the forth can be inferred and summarized as follows:

1. A particle reaches a certain level of hydrophobicity
2. The particle is suspended in the pulp
3. The particle collides with a bubble. Then, it adheres to the bubble
4. The particle must not detach from the bubble
5. The particle must keep attached even moving towards the surface
6. The particle must not detach when moving in the froth

The flotation process is usually carried out in a specialized "flotation cell", schematized in Fig.2.6. This cell is designed to promote the migration and recovery of the froth and the accumulation of the deposited material existing in the tails. Inside, slurry is being constantly agitated and mixed with microbubbles on the inside that are generated at the bottom (see Fig. 2.6) that usually stand at approximately 1 mm in diameter. The heavier particles in the slurry are naturally dragged towards the bottom of the cell due to gravity and keep in constant interaction with the bubbles, as it is likely that at a certain point a bubble will be able to "carry" many particles while ascending, achieving separation. In addition paddles and weirs are commonly attached to the inner surface of the cell to improve the mixing and the process of bubble adhesion.

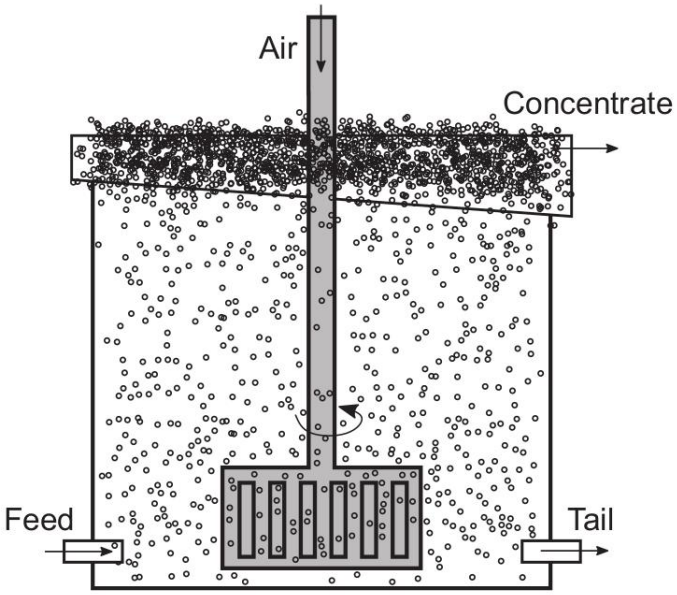

Figure 2.6: Diagram of a flotation cell. From Mesa and Brito-Parada (2019)

Atop the cell is the froth phase where bubbles are collected, agglomerate, and form a stable heterogeneous mixture, whereas the bottom includes the area where the hydrophilic particles remain. The pulp phase in the middle corresponds to a mixing zone where particles collide and bubble capture is increased. At the pulp phase, the relative speeds of the settling and capture are expected to be balanced since, at the bubble phase, the bulging mass of captured particles gets heavier and heavier as time passes, whereas at the froth phase bubbles join and form polyhedral big bubbles that move throughout a single film of water. In addition, it is possible to define an "entrained phase" as the middle zone between these two main areas.

Because of the turbulent nature of the flotation process, most industrial applications of flotation cells require weirs used to help with the removal process of the froth and to control the formation of agglomerated bubbles. Additionally, batch flotation operations rely on simplified models that take into account mass balance considerations, particle size, bubble area and chemical variables. Depending on the particular application, such models are available for different minerals and, in the case of phosphorus many empirical (Fortes et al., 2007; Liu et al., 2019; Partridge and Smith, 1971; Sis and Chander, 2003) studies are available in the literature.

2.1.4 Similarities between steelmaking slags and SSA as sources of recyclable phosphorus

Considering that phosphorus is commonly found as a byproduct in steelmaking slags, several research efforts have been performed (Lin et al., 2014; Morita et al., 2002) to concentrate the phosphorus present in this material as a mean for phosphorus recycling. In these cases, the effectiveness of concentrating the phosphorus from steelmaking slags using the difference in the magnetic properties between the phases of the "magnetic" fraction (rich in ferrous materials) are captured and the "non magnetic" fraction (rich in phosphorus) is explored, with several degrees of success based on the nature of the slag, the particle size and the usage of modifier agents before and during the separation (Menad et al., 2014).

For example, the process for phosphorus recovery from steelmaking slags was explored using different techniques such as gravity assisted magnetic separation using large fields (close to 2 T) generated by a superconducting magnet (Yokoyama et al., 2007). In this case, it was seen that the size of the particles have an important effect on aggregation, being the smaller particles (mean size < 30 µm) the most affected, and thus causing a reduced effectiveness of the capture, which had to be handled using SiO_2 as a dispersant.

Another process investigated was the use of capillary action from a slag mixture onto a prefabricated "absorber" (Koizumi et al., 2016). Here, a predetermined tablet containing CaO, Fe_2O_3 or $CaCO_3$ was prepared to promote the diffusion of the Fe_2O_3 rich liquid fraction of the slag into the absorber, while at the same time allowing for the capture and subsequent grow of solid crystals rich in P_2O_5 content on the surface of the absorber, resulting in an overall separation as presented in Fig.2.7.

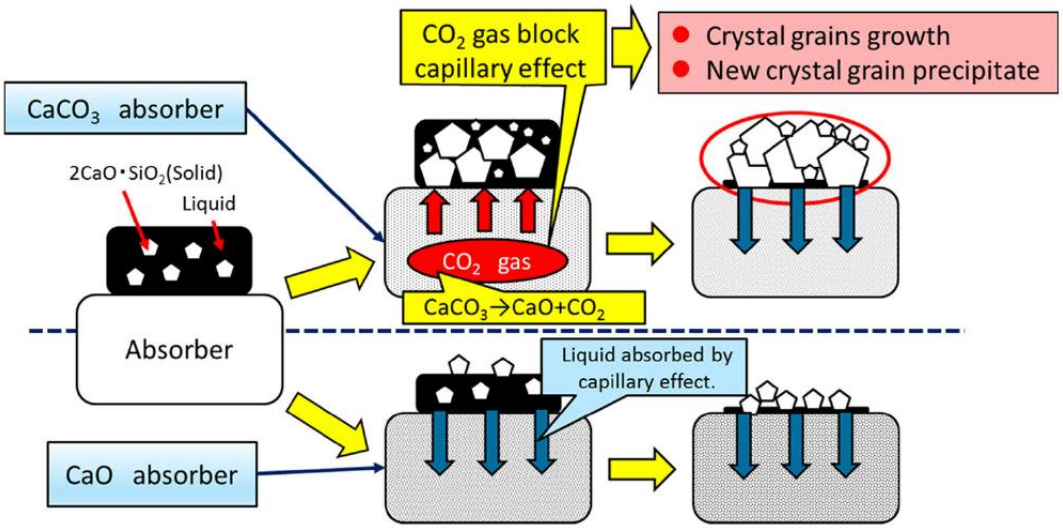

Figure 2.7: Diagram of the absorption process of Fe_2O_3, and the deposition of P_2O_5 containing crystal onto the surface of a prefabricated "absorber" tablet. The top section of the figure illustrates the favorable effect of CO_2 formation from $CaCO_3$ inside the "absorber". From Koizumi et al. (2016)

It was observed that the effect of capillary action on the absorption of the liquid fraction (rich in Fe_2O_3) was carried out efficiently into the absorber, which then could be used as a recycled Fe resource for reprocessing in a blast furnace. Moreover, the best results were obtained when the "absorber" tablet contained $CaCO_3$, as the generation of CO_2 obstructed the unwanted absorption of small $2\,CaO \cdot SiO_2$ solids via capillary action, which resulted in P_2O_5 recoveries of around 90% in the surface of the "absorber" tablet.

Similarly, Fujita and Iwasaki I. (1989) have shown that in the case of steelmaking slags containing amounts of dicalcium silicate along with Phosphorus, it is possible to transform the iron phase into a strongly magnetic material using thermal treatment. In this case, small amounts of coke were added to the slag and then heated to 1723 K under a nitrogen atmosphere, promoting the formation of magnetic ferrites, like wustite. In addition, P_2O_5 present in the slag performed rejection from the matrix prompting the use of cationic flotation as the selected mineral technique to achieve further purification.

2.2 Methodology

The sample of Sewage Sludge Ash (SSA) used in this study was provided by Tokyo Metropolitan Sewerage Service Corporation and was initially subjected to characterization analyses. The particle size distribution was determined using laser diffraction (NIKKISO Microtrac MT3000), the mineral composition and crystal phase structures were determined using a XRF machine (RIGAKU SuperMini WDXRF) and an XRD machine (RIGAKU SmartLab, PDXL ver. 2.3.1.0, Database: PDF-2/Release 2010 RDB), along with SEM/EDS imaging (JEOL JSM-7500FA), which provided additional information of the physical characteristics of the raw sample, which will be referred in this document onwards as the *as-received* SSA sample.

For the thermogravimetric analyses a TG-DTA machine (RIGAKU ThermoPlus EVO TG8120) was used, and with the aim of obtaining the magnetization values, standard Vibrating Sample Magnetometer (VSM) equipment (TAMAKAWA CO., LTD) was employed. Electric current/magnetic field equivalence was determined using a Tesla meter (MAGNA MG-801), and equipment calibration was made using a nickel standard, which is common routine for VSM measurements.

For the HGMS separation trials, we adapted a custom made cell (based on ERIEZ L model 4 separator) to fit the same VSM machine described in an earlier paragraph (see Fig.2.8). This cell used plastic sheets supported with threads on both ends, packed with a stainless steel mesh matrix inside. Sample feeding and collecting was achieved using a set of hoses and a funnel plugged to the cell. This setup allowed us to obtain a reliable magnetic field from the coil array of the VMS, and use it to generate high gradient fields around the steel matrix and thus inside the customized cell.

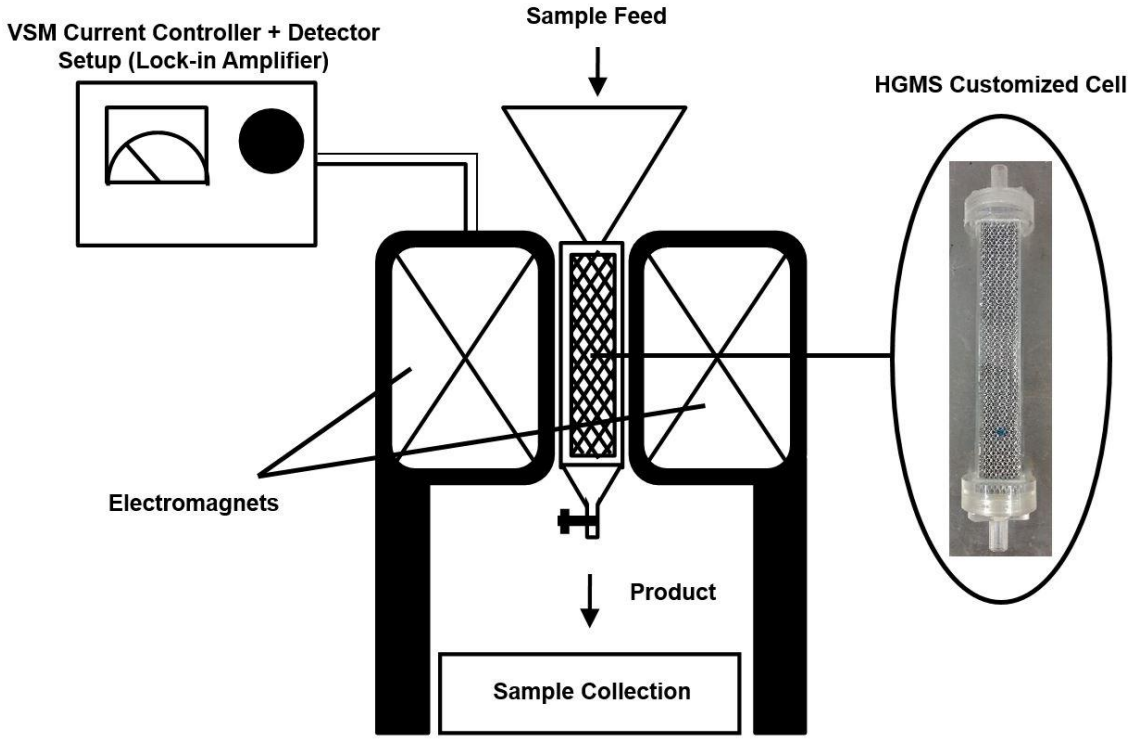

Figure 2.8: Diagram of the HGMS experimental setup, where the magnetic field is generated and controlled by a VSM machine, which has been adapted to suspend the HGMS cell in the middle. The inset photograph shows a close-up of the customized cell used.

Introductory experiments for HGMS separation were performed using 3 liquid samples containing untreated ("As-received") SSA. Each one of them had 5% on a mass/mass basis of SSA, a dispersion agent, and were diluted with desalinated water. In order to assess the effect of the dispersion agent used, the first one had 0.1% Na_2SiO_3, the second one had 0.1% $Na_6[(PO_3)_6]$, and the third one had 0.015% of Sodium Dodecyl Sulfate (SDS) (Nacalai Tesque Inc. and Wako Pure Chemical Industries, respectively).

Each one of these mixtures went through the adapted HGMS system at a rate of 10 mL/s, and separated using magnetic fields of 0.1 T, 0.2 T and 1 T; afterwards, both "magnetic-rich" and "nonmagnetic-rich" fractions were captured, filtrated, dried and analyzed by XRF and XRD.

Aiming at the increase in the percentage of iron removal, samples of as-received SSA mixed with ground activated charcoal (Nacalai Tesque Inc.) were prepared. Thermogravimetric analysis was performed on these, using carbon percentages of 5%, 10%, 15% and 20% on a mass/mass basis. With the results, larger specimens of the mixtures were heated using capped aluminum ceramic crucibles (AS-ONE 3W, 100 mL) and an electric furnace (AS-ONE HPM-1G) for 30 min. at 540 °C and 680 °C under an air atmosphere, these temperatures were chosen to ensure carbon combustion (see Fig. 10). Also, additional samples with the same composition underwent the same heating procedure, but this time using an inert (N_2, flow equal to 5 L/min) atmosphere.

After assessing the changes in mass magnetization values for these samples, and considering the costs of using large amounts of carbon associated with a hypothetical scale-up of the process, only the heated samples with a content of 5% carbon were subjected to subsequent HGMS separation trials. These trials used 0.015% of SDS as a dispersing agent and magnetic field strengths of 0.1 T and 0.2 T.

In order to evaluate the effect of oxide addition, three different samples of SSA were prepared. The first one had only 5 wt.% carbon added, the second one had the same amount of carbon added and also an additional 5% of $Ca(OH)_2$, and the third one had a content of 5% carbon plus a content of 5% of Fe_2O_3. These mixtures were then heated to 800 °C for 30 minutes, using an inert atmosphere (N_2, flow equal to 5 L/min). Afterwards, the samples were analyzed using XRF and XRD techniques and were subjected to similar HGMS separation experiments; using field strengths of 0.1 and 0.2 T, and once again using 0.015% of SDS as a dispersion aid. Likewise, a sample of untreated, "As-received" SSA went through the same treatment and acted as a blank reference for the procedure.

Finally, flotation tests were carried out at two different pH values (pH = 8 and pH = 10) for selected "nonmagnetic-rich" fractions obtained after magnetic separation trials. Flotation was carried out using a Denver type flotation cell (ODA Machinery Co. LTD), equipped with a bubble generator (ADD-X 101), and the pH measurements were done using a pH-meter instrument (HORIBA LAQUA F-72). The mixes prepared had all the following mass/mass percentages: 10% non-magnetic-fraction materials, 0.01% SDS as a dispersant, 36 ppm MIBK (Methyl Isobutyl Ketone, Wako Pure Chemical Industries) as a frother, and desalinated water as a solvent. Flotation parameters were the following: air flow equal to 4 L/min, propeller speed equal to 1500 RPM and an agitation time of 5 minutes.

2.3 Results and Discussion

2.3.1 Characterization of the sample of Sewage Sludge Ash used in the experiments

Particle size and composition

The sample of sewage sludge ash (SSA) comes from one of the water reclamation centers that processes sludge coming from urban areas in Tokyo, Japan. In this processing plant, wet sludge is dewatered using a series of treatment steps before being sent to a gasification chamber and pyrolyzed, then it is reformed at temperatures ranging from 800 to 900 °C (Takahashi, 2007b).

In terms of composition, the main elements detected by XRF expressed as oxides on a mass/mass basis for the As-Received SSA are: calcium (20.7% CaO_2), iron (16.3% Fe_2O_3), silicon (24.3% SiO_2), and a significant phosphate content of around 18.5% P_2O_5; also, relevant amounts of aluminum, potassium, and barium were detected. Interestingly, the content of heavy metals for this particular SSA was reflected mostly as the presence of zinc and chromium, which accounted for percentages of 1.2% ZnO and 0.2% Cr_2O_3, respectively. These results are in concordance with the ones reported in the literature (Donatello et al., 2010; Guedes et al., 2014; Krüger et al., 2014), and are summarized in Table 2.1.

Table 2.1: Chemical Composition (as oxides) of the sample of *As-received* SSA.

Element oxide	Content, (wt.%)
CaO	20.7
Fe_2O_3	16.3
SiO_2	24.3
P_2O_5	18.5
Al_2O_3	8.4
K_2O	3.2
TiO_2	2.0
BaO	1.7
SO_3	1.3
ZnO	1.2
MgO	1.0
CuO	0.6
MnO	0.3
Cr_2O_3	0.2
SrO	0.2
NiO	0.1
Cl	<0.1

The SSA sample provided consisted of fine, soil-like particles, greyish in color, that originated from the exit of one the Jet mills located at the processing plant. This explains the median size detected by the particle size analysis, which was found to have a D_50 value of 3.33 µm as observed in Fig.2.9.

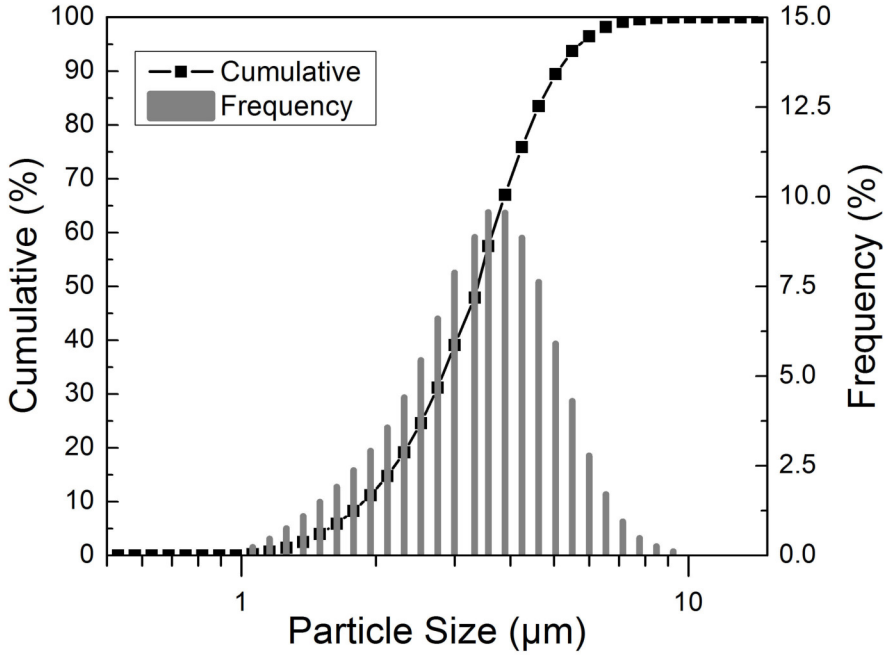

Figure 2.9: Particle size distribution for the As-received SSA. The value for D50 stands at 3.33 [µm]

Crystalline phases, SEM imaging and mass magnetization

The results from the XRD analysis of the as-received SSA are presented in Fig.2.14. Here, it was revealed that SSA contains a phase of well-defined quartz (SiO_2), which probably comes from the usage of a silica bed for the burning of the dried sludge. On the other hand, the XRD results highlighted the existence of a somewhat diffuse spectra that pointed out the presence of phases close in nature to Calcium Aluminum Phosphate ($Ca_9Al(PO_4)_7$) and a phase identified as ($Ca_{2.589}Mg_{0.411}(PO_4)_2$). The latter is a phosphorus phase thar resembles whitlockite ($Ca_9Mg(PO_4)_6(PO_3OH)$), which is a phosphate commonly found in SSA, often occurring due to the tendency of the Mg^{2+} ion to replace and be in combination with Ca^{2+} ions during the formation of calcium phosphates at high temperatures (Qian and Jiang, 2014).

This situation stresses the need for a separation method for phosphate existing in this SSA, since the presence of aluminum in soils can reduce plant' s uptake of other nutrients, such as P, Ca, K, N, and become a limiting factor in the production from field crops (Kabata-Pendias, 2011). Remarkably, no clear iron phosphate phase was detected in the SSA, despite the high concentration detected by the XRF analysis (around 16%).

Furthermore, SEM/EDS analysis reinforced the notion of phases of Ca, P and Al existing in combination in the sample, while at the same time suggesting that the iron phase only exists as smaller particles in the crystalline phase of hematite, as evidenced in Fig.2.10

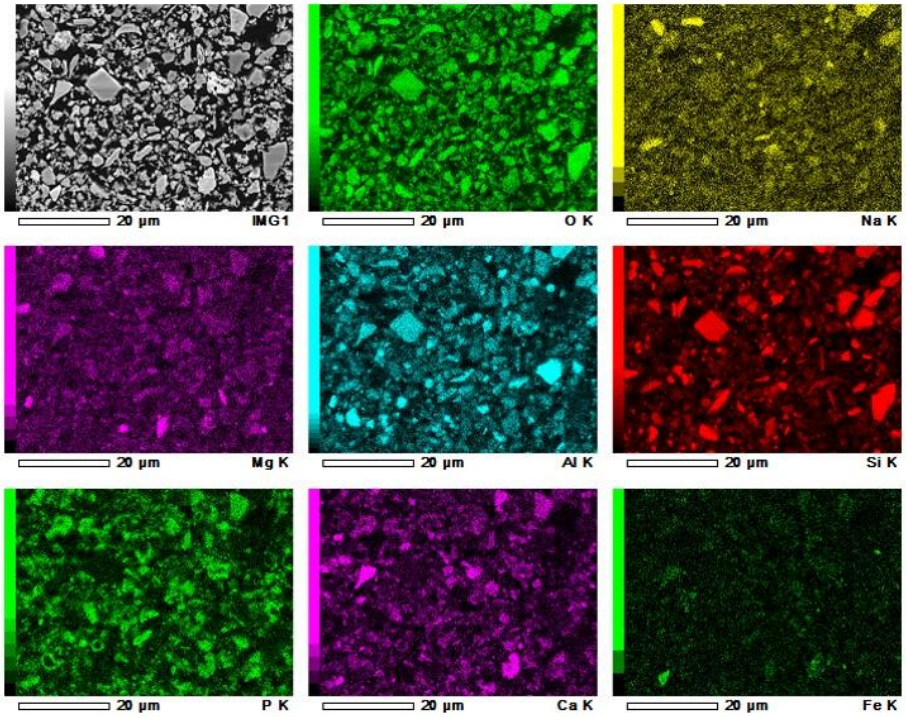

Figure 2.10: SEM/EDS images for the As-received SSA. The stark contrast between the iron phase (lower right) and the rest of the elements suggest Fe_2O_3 particles are not combined with the rest of the elements.

Lastly, when the as-received SSA was subjected to a mass magnetization analysis using VSM, the results showed that magnetization values for the SSA increase rapidly until a magnetic field of 0.2 T, then the rate of increase in magnetization diminishes until a field of 0.4 T is reached and saturation takes place. At this point the observed magnetization is considered to have reached a maximum value and was measured to be 1.0 emu/g. Though relatively small, this value for maximum magnetization represents an important magnetic feature of the bulk sample, since it was qualitatively observed that a small ferrous magnet is able to attract particles from the SSA when placed in its vicinity.

2.3.2 Carbothermal reaction of SSA aimed at the increase of mass magnetization

The carbothermic reduction of Fe_2O_3 present in SSA

Preliminary experiments using *as-received* SSA samples (untreated ash samples) and subjecting them directly to the HGMS separation method described in Section 2.2, pointed out a small dependency on the dispersion agent used. When Na_2SiO_3 and $(Na_6(PO_3)_6$ were the dispersants, ut was observed that virtually no difference in Fe_2O_3 content could be achieve between the ”magnetic” and ”non magnetic” fractions.

Similarly, this behavior was observed to have no dependence on the strength of the magnetic field used, as phosphate contents showed practically no increase in concentration across all the different conditions studied in these introductory experiments. Therefore, phosphorus recovery from SSA via the use of *direct* magnetic separation is deemed to be extremely difficult to achieve. This claim is also supported by previous research (Franz, 2008), where it was suggested that the main phases containing combined phosphorus tend to increase their physical volume as a glass-type material when hydration occurs, thus leaving the comparatively smaller iron particles physically hindered from any kind of magnetic capture.

This is the reason why, in order to attain an increase in the amount of captured Fe_2O_3, a heating process using a reducing atmosphere, prior to HGMS separation was proposed. Moreover considering that previous results (Fujita and Iwasaki I., 1989) suggested that the heating of steelmaking slags containing phosphorus in the presence of coke, may be beneficial for the means of iron removal using HGMS. This way, it was proposed that the Fe_2O_3 existing in the SSA could undergo a carbothermic reduction via Eq.2.3, which has been previously suggested (El-Geassy et al., 2013) as a valid transformation for the formation of the highly magnetic phase of Fe_3O_4 from the rather weak ferromagnetic phase of Fe_2O_3.

$$3\,Fe_2O_3 + C \longrightarrow 2\,Fe_3O_4 + CO \tag{2.3}$$

Therefore, in order to observe the effect of the concentration of carbon used for the aforementioned reaction, a set of Differential Thermal Analysis (DTA) curves obtained for the combustion of carbon mixed at different percentages with SSA samples is presented in Fig.2.11

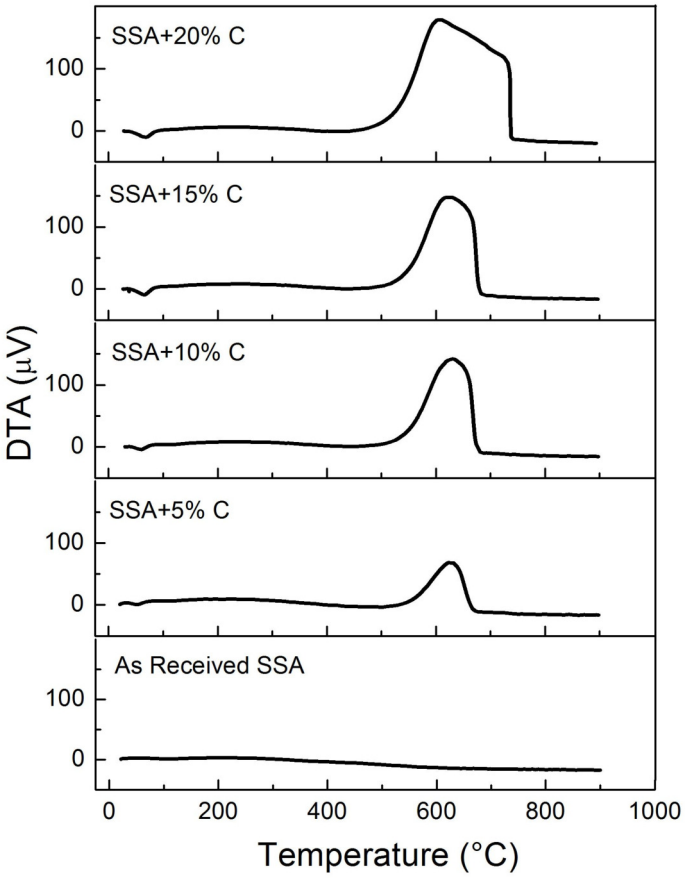

Figure 2.11: Differential Thermal Analysis (DTA) curves for SSA samples mixed with carbon heated under air atmosphere. (Standard used: Al_2O_3, Heating Rate: 10.0 °C/min.).

The different concentrations of carbon (5%, 10%, 15% and 20% of powdered activated charcoal) were considered to carry out the reaction described by Eq.2.3 and refer to the amount of carbon added per 100 g of SSA (that is, 5 g carbon per 100 g SSA and so on). Likewise, in terms of iron content in SSA, these carbon concentrations correspond to values of *carbon equivalent* (C_{eq}) of 1.5, 3.0, 4.5 and 6.0, respectively. The definition of C_{eq} is based on the work by Morita et al. (2002), and is defined as the ratio of carbon used in the mix for carbothermic reaction, required for the complete reduction to Fe of the Fe_2O_3 found in SSA (see Appendix B for details on the calculation).

The apparent excess in the values of the *carbon equivalent* is observed in the experiments because the carbon added is expected to only generate a reducing atmosphere before quickly leaving the crucible as gaseous CO, meaning that the amount of Fe_2O_3 actually leading to the formation of Fe_3O_4 may be limited if there is not enough carbon to react before the formation of gaseous carbon oxides.

The results presented in Fig.2.11 suggest that the combustion process for carbon starts at around 540 °C, reaches a peak at around 600 °C and continues until 680 °C for carbon concentrations of less than 20%. At this concentration the combustion process merely sustains itself with the excess carbon present and does not further contribute to the main reaction, as the maximum DTA potential detected remains practically the same for samples even with a carbon content higher than 10%. Hence, it was decided that the maximum amount for carbon addition to be used in further tests should be 15%.

Measurement of mass magnetization after treatment

When two batches of SSA mixed with different carbon percentages were first heated for 30 minutes at 540 °C and 680 °C, respectively; and then subjected to magnetization measurements, the results indicated that their mass magnetization remained close to the one for *as-received* SSA. This can be evidenced in Fig.2.12, since the curves are very similar in nature and maximum magnetization (that is, where magnetic saturation occurs) is essentially the same situated between 0.9 and 1.0 emu/g when a magnetic field equal to 0.4 T is employed.

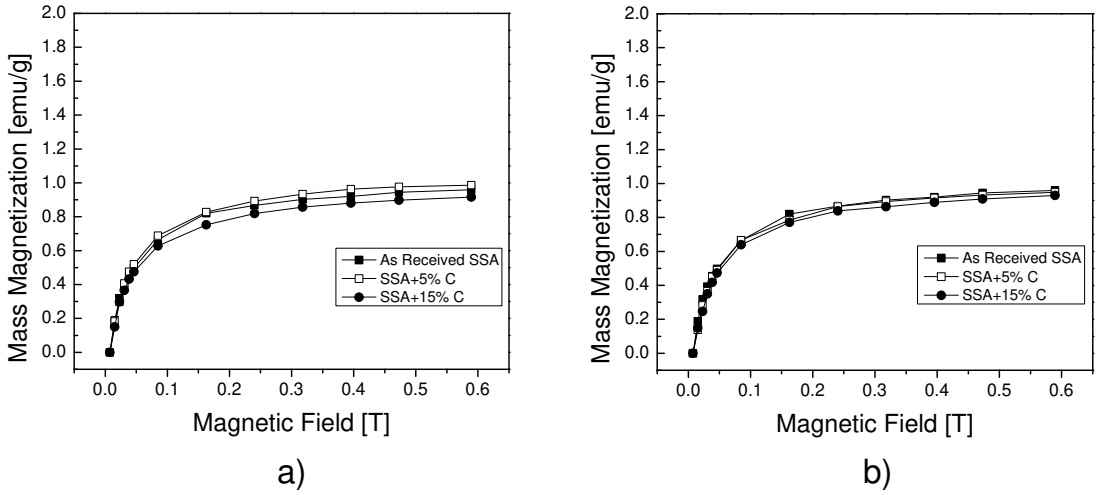

Figure 2.12: Mass magnetization curves for samples of SSA + Carbon heated for 30 minutes under an air atmosphere. a)Heating temperature: 540 °C, b) Heating temperature: 680 °C.

It is possible that these results arise because the iron already existing in the sample is oxidized to form non-magnetic Fe_2O_3, as it was also qualitatively observed that the samples acquire an orange tint after heating under an air atmosphere. In comparison, when a nitrogen atmosphere was used instead of air, an increase in mass magnetization was observed. Referring to this, the samples heated at 680 °C acquired higher magnetization values than the samples heated at 540 °C, suggesting that the reduction process is carried more efficiently at higher temperatures.

Additionally, it was observed that the carbon contents in the sample also affected the magnitude of the increase, as the samples that had a carbon content of 15% achieved the highest increase in magnetization, reaching maximum saturation values of 1.5 emu/g for the sample heated at 540 °C and 1.7 emu/g for the sample heated at 680 °C Fig.2.13. However, from the point of view of a real scale process, using a percentage of carbon as high as 15% to increase magnetization may seem economically unfavorable, furthermore when it is considered that the second highest magnetization increase was achieved when the samples had only a 5% carbon content, giving maximum magnetization values equal to 1.1 emu/g when the sample was heated at 540 °C and 1.6 emu/g when it was heated at 680 °C.

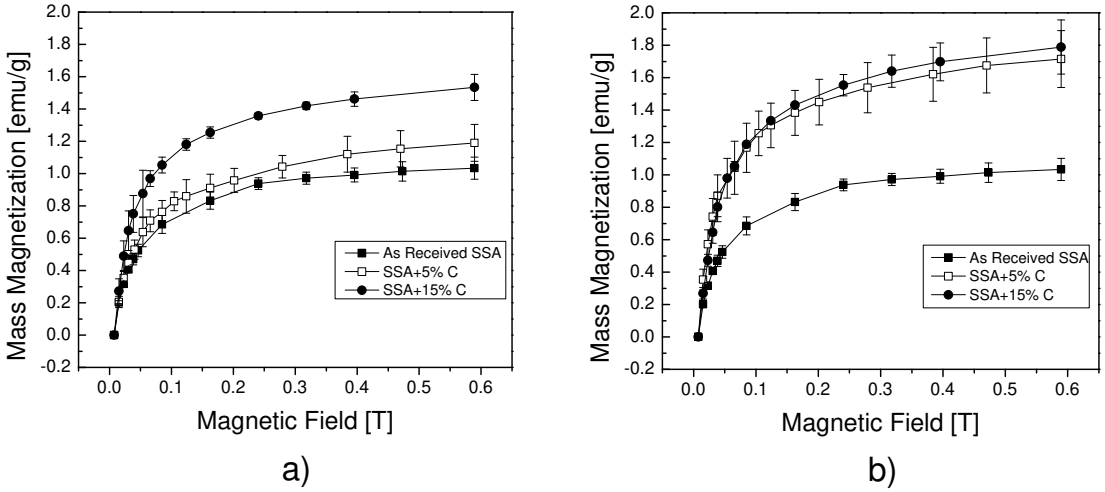

Figure 2.13: Mass magnetization curves for samples of SSA + Carbon heated for 30 minutes under a N_2 atmosphere. a)Heating temperature: 540 °C, b) Heating temperature: 680 °C.

Addition of Ca and Fe oxides during the thermal treatment

In another approach, since the phosphate phase detected in this particular SSA is comprised mostly of an aluminum-type mineral, it is highly desirable to obtain a change in crystalline phase (for the sake of a higher soil-solubility that will increase plant bioavailability (Wollmann et al., 2018)) while at the same time having an increase in mass magnetization (for the sake of improving iron capture by HMGS). Therefore, samples with an added oxide, either a calcium oxide or an iron oxide were prepared and subjected to the same procedure described in Section 2.3.2 paragraph to tackle this issue.

Hence, mixtures were prepared using 5% of either $Ca(OH)_2$ or Fe_2O_3 as the added oxide plus 5% carbon as the reducing agent. Afterwards, said mixtures were heated to a temperature of 800 °C, for 30 minutes using an inert (N_2) atmosphere. After cooling and grinding, the samples were recovered and XRD characterization was performed. Consequently, the results obtained for these analysis are shown in Fig.2.14.

It can be observed that the quartz phase remained unchanged in every case, regardless of the oxide added to the SSA, whereas aluminum remained combined with phosphorus as $Ca_9Al(PO_4)_7$. Nonetheless, a previously non detected phase corresponding to the mineral stanfieldite ($Ca_3Mg_3(PO_4)_4$) was identified for all the samples containing carbon.

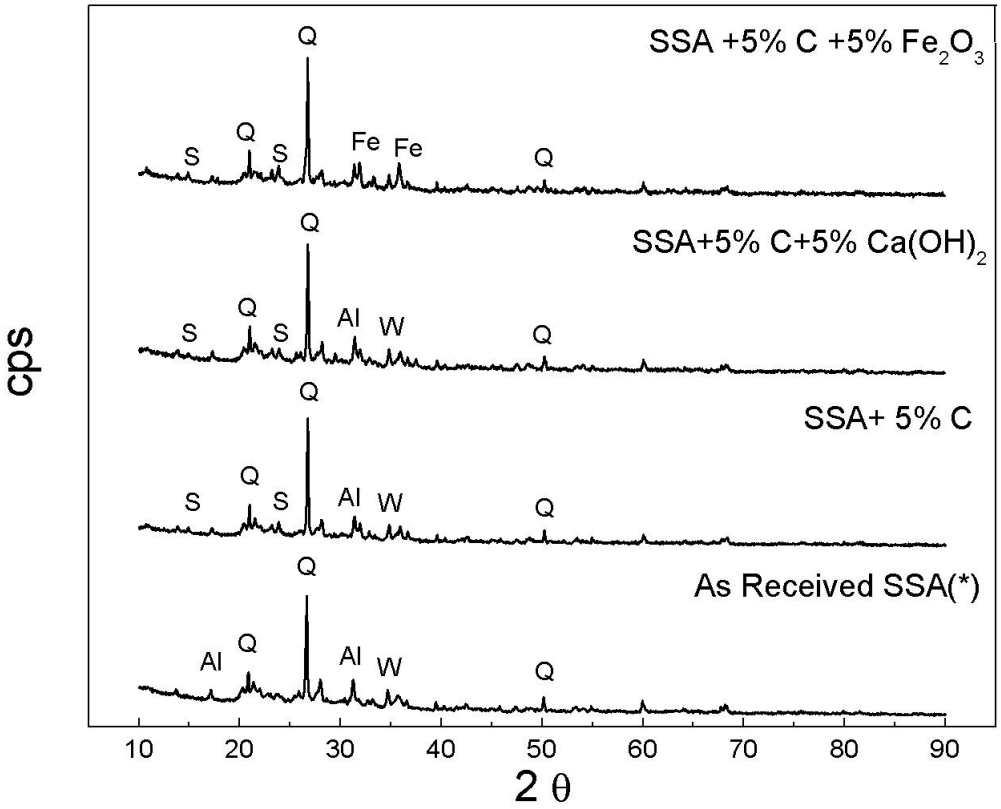

Figure 2.14: XRD spectra for samples after heating at 800°C under a N_2 atmosphere for 30 min. Phases identified are: Q=Quartz (SiO_2), Al=Calcium Aluminum Phosphate ($Ca_9Al(PO_4)_7$), W=Whitlockite ($Ca_{2.589}Mg_{0.411}(PO_4)_2$), S=Stanfieldite ($Ca_3Mg_3(PO_4)_4$), Fe=Calcium Iron Phosphate ($Ca_9Fe(PO_4)_7$). As received SSA(*) refers to the XRD data obtained for the original SSA sample without any treatment at all, and is shown in this figure for reference only.

Furthermore, for the sample where 5% Fe_2O_3 was added, the calcium aluminum phosphate phase was no longer identified and a calcium iron phosphate ($Ca_9Fe(PO_4)_7$) phase was revealed instead. This suggests that the presence of additional iron in the mixture during the carbothermal reaction promoted the formation of a Ca-Fe-P phase during the heating step, displacing aluminum and thus, increasing the bioavailability of the existing phosphorus phase.

2.3.3 High gradient magnetic separation and flotation experiments

Results of the HGMS experiments

The separation experiments using HGMS carried out for the samples with oxide addition previously described in Section 2.3.2 resulted in two fractions recovered. One of the fractions consisted of the materials captured when the magnetic field was turned on and was denominated the "*magnetic-fraction*", and the other was comprised of the materials captured when the magnetic field was turned off, receiving the name of "*nonmagnetic-fraction*". It can be observed in Fig.2.15 that the separation procedure done by HGMS yields notoriously different amounts of "magnetic-rich" and "nonmagnetic-rich" material captured, in accordance with the strength of the magnetic field used.

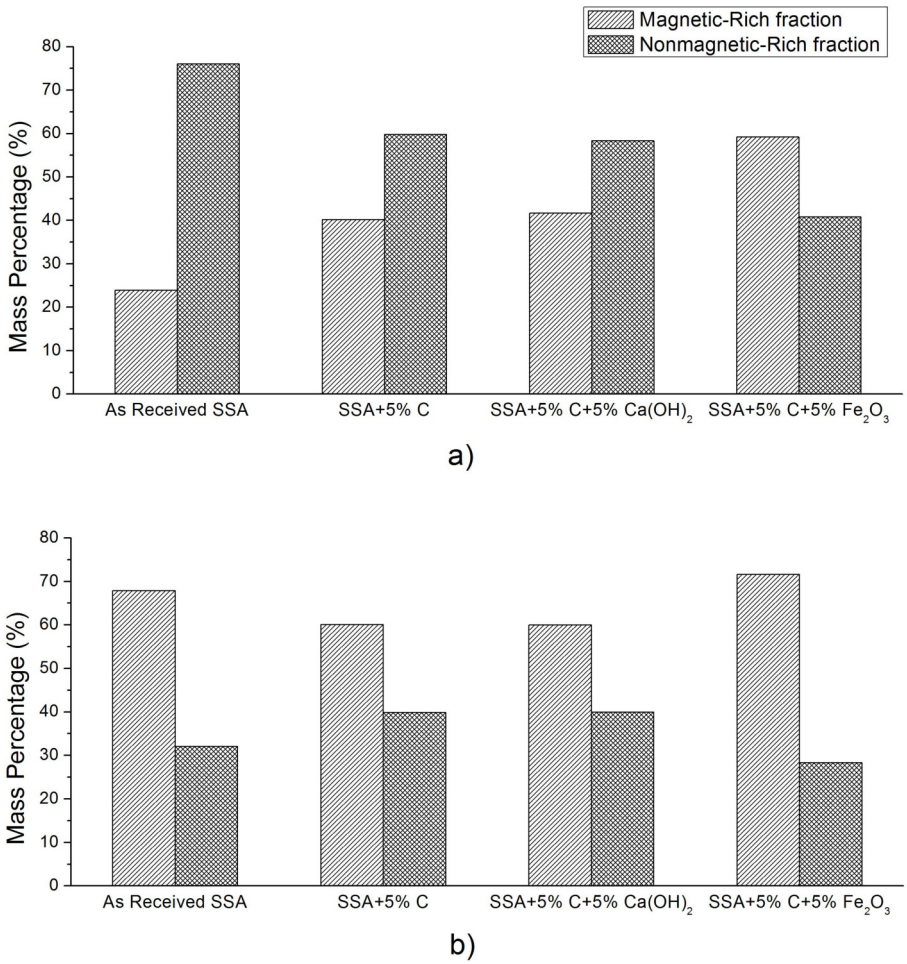

Figure 2.15: Mass recovered (expressed as percentage) after HGMS separation tests. The samples consisted of SSA heated with carbon and added oxide under a N_2 atmosphere for 30 min. Magnetic field used: a) 0.1 T ,b) 0.2 T.

This result is encouraging from the point of view of separation efficiency since it not only suggests that the magnetic materials are responsive even when a small magnetic field such as 0.1 T is being applied, but also that the mesh inside the cell is effectively generating magnetic gradients forcing the capture of particles.

When the separation was carried out at 0.1 and 0.2 T the differences in P_2O_5 measured between the "magnetic-fraction" and "nonmagnetic-fraction" were situated in the range of around 1% relative to each other, showing a slight improvement over the performance observed for the preliminary tests carried out using HGMS for untreated SSA, which had values of less than 1% in relative difference between each fraction (data not shown).

However, for the heated sample containing Fe_2O_3 a larger relative difference close to 7% in P_2O_5 content was detected between the "magnetic" and "nonmagnetic" fractions, being the latter the fraction with enriched phosphorus content. This value is significantly higher than the ones obtained previously, and this is probably attributed to the presence of calcium iron phosphate stated lines above. This behavior is pointed out in Fig.2.16

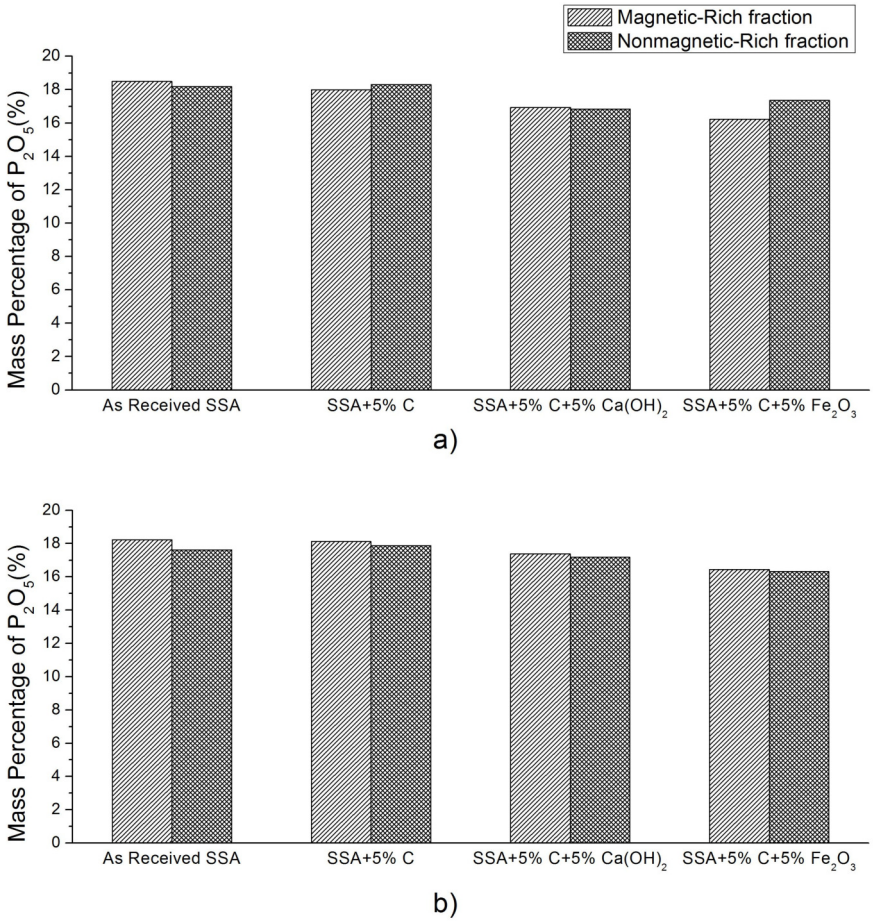

Figure 2.16: Phosphorus concentrations (expressed as precentage of P_2O_5) for the fractions obtained after HGMS separation. Magnetic field used: a) 0.1 T, b) 0.2 T.

The presence of $Ca_9Fe(PO_4)_7$ is favorable for the concentration of phosphate species in the "non magnetic-rich" fraction, because the magnetization values reported for materials in the CaO-P_2O_5-Fe_2O_3 system are generally small (Kumar and Chen, 1994), meaning that the HGMS separation will capture more easily the comparatively more magnetic hematite or magnetite, instead of $Ca_9Fe(PO_4)_7$. This is because magnetic susceptible iron phases in calcium phosphates can only be partially substituted in apatitic structures (Desport et al., 2011; Sato and Nakahira, 2013), or in the structure of $Ca_3(PO_4)_2$; which in addition may undergo oxidation towards Fe_2O_3, further reducing their magnetization (Lazoryak et al., 2003).

Moreover, research has shown that the magnetization of calcium phosphates containing iron is extremely dependent on the concentration of Fe_2O_3, with values of 0.5 emu/g (Singh and Srinivasan, 2010) and less than 1.5 emu/g (Kumar and Chen, 1994) were reported for concentrations of 10% Fe_2O_3 and 30% Fe_2O_3, respectively. These concentrations are almost 2 and 6 times larger than the amount of added Fe_2O_3 used in our experiments and as such, suggest that as long the concentration of added Fe_2O_3 to the SSA sample is less than 10% the effects of $Ca_9Fe(PO_4)_7$ magnetization can be considered negligible.

Based on the observations presented above, it was decided that the "nonmagnetic-rich" fraction recovered from the SSA sample heated with 5%C and 5%Fe_2O_3, was the "*best-performing*" in terms of increased plant bioavailability and P_2O_5 concentration enrichment when subjected to HGMS separation. Considering that this sample constitutes the most suitable candidate for posterior flotation experiments, further flotation tests on the rest of the samples was discarded.

Flotation of the "best-performing" sample obtained after HGMS

After performing the flotation of the sample, both "froth" and "tails" were retrieved and their composition analyzed using XRF. In this regard, Fig.2.17 shows the results obtained when the "nonmagnetic-fraction" of the selected sample was subjected to flotation trials, after being subjected to HGMS separation at 0.1 T.

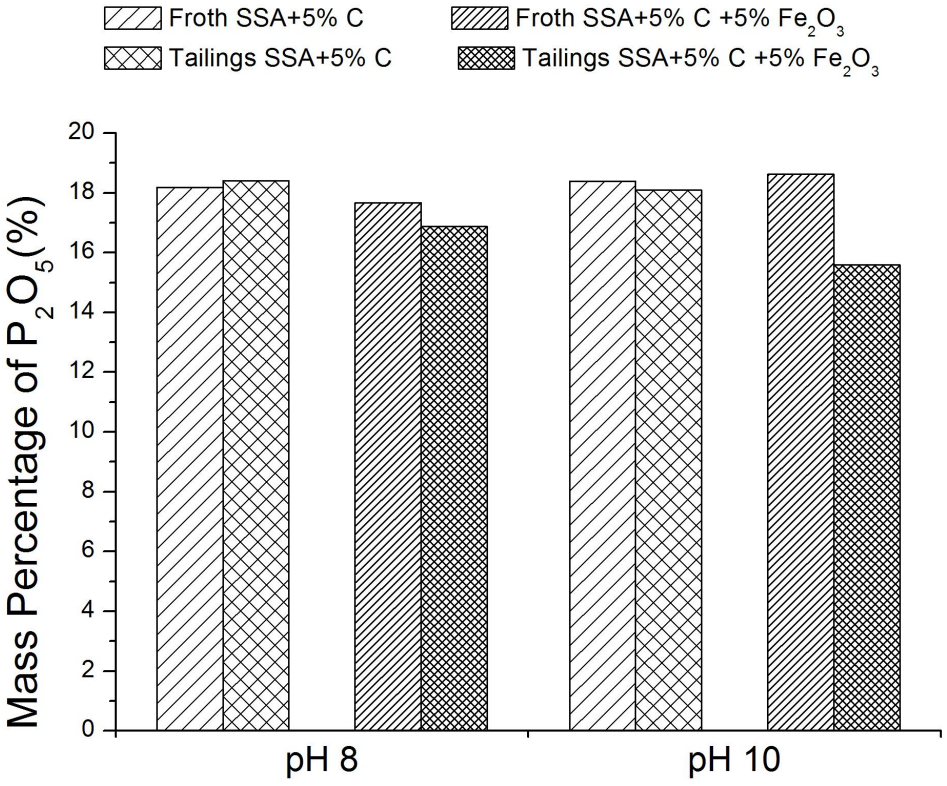

Figure 2.17: Concentration of phosphorus (as P_2O_5) after flotation experiments of the "non-magnetic" fraction after HGMS separation. The flotation experiments were carried at two different pH.

It can be clearly observed that the sample with Fe_2O_3 addition yielded the largest difference in P_2O_5 content between froth and tailings. In this case, when flotation was carried out at pH 10, the froth contained 19% more P_2O_5 when compared with the P_2O_5 in the tailings. Conversely, when the procedure takes place at a pH equal to 8, the froth' s P_2O_5 content is observed to be only 4.6% higher than of the tailings.

In comparison, the samples of "nonmagnetic-rich" SSA plus 5% carbon heated at 800 °C in N_2 but without Fe_2O_3 addition, used for comparison purposes only showed a minor difference (i.e. less than 2%) in relative P_2O_5 concentration in the froth, with a small decrease at pH = 8 and a slight increase at pH = 10, indicating that Fe_2O_3 addition before the carbothermal reaction had also a beneficial effect promoting phosphorus removal by flotation.

2.4 Conclusions

The sample of Sewage Sludge Ash (SSA) used in this study has a mineral composition typically found in sewage sludge samples coming from incineration plants around the world, with a phosphorus content expressed as 18.5% P_2O_5 on a weight basis, and a global magnetization value close to 1.0 emu/g, which indicates the weak mass magnetization for the *as-received* sample of SSA. This small value is probably due to the presence of an oxidized form of iron oxide (Fe_2O_3) detected as hematite, which is found in a comparatively high concentration (16.3%) in the SSA sample, and was confirmed by SEM/EDS characterization in the form of small particles.

On the other hand, XRD analysis of this SSA sample showed that phosphorus is initially combined with Al, Mg, Ca, and other elements in the crystalline phases of calcium aluminum phosphate ($Ca_9Al(PO_4)_7$) and whitlockite ($Ca_{2.589}Mg_{0.411}(PO_4)_2$), indicating that the direct use of this SSA for fertilizer applications may not be adequate from the point of view of soil-solubility as the release of the combined aluminum is detrimental for the soil.

Attaining phosphate enrichment by subjecting SSA to *direct* high gradient magnetic separation (HGMS) was proven difficult, as the experiments using a customized HGMS cell equipped with a wire mesh, resulted in concentrations of Fe_2O_3 and P_2O_5 remaining essentially equal in both the "magnetic-fraction" and "nonmagnetic-fraction" obtained after HGMS. To overcome this problem, it is required to increase the mass magnetization of the iron existing in the sample. For this purpose, the transformation of hematite to magnetite via a carbothermic reaction was proposed.

Thus, when adding carbon as a reducing agent and heating SSA samples under an inert atmosphere for 30 minutes to carry out the carbothermic reaction, it was observed the magnetization of SSA can be enhanced, achieving values of 1.5 emu/g at 540 °C and 1.7 emu/g at 680 °C for samples prepared using 15 wt.% of carbon. Similarly, samples with a content of carbon equal to 5 wt.% displayed magnetizations of 1.1 emu/g when the heating temperature was 540 °C and 1.6 emu/g when it was equal to 680 °C.

Using such comparative "low" temperatures for the carbothermic reaction and the formation of soil-soluble phosphates is promising, since this reaction is bound to reduce the amount of thermal energy required for the processing of SSA, in opposition to traditional thermal processing methods (see Section 1.7) that require temperatures higher than 1000 °C.

Accordingly, our experiments showed the formation of stanfieldite ($Ca_3Mg_3(PO_4)_4$) is observed for SSA mixtures containing 5% carbon and heated at 800 °C for 30 minutes under a N_2 atmosphere. Additionally, when 5% Fe_2O_3 is added before heating, the initially detected crystal phase of $Ca_9Al(PO_4)_7$ dissapears, as the presence of $Ca_9Fe(PO_4)_7$ is observed instead. This result is useful from the point of view of soil-solubility since the phosphate phase to be recovered now contained only magnesium and iron, replacing the undesired phase of aluminum.

As for the HGMS separation tests carried out with this sample, the "magnetic-fraction" and "nonmagnetic-fraction" have a relative difference in phosphorus content between them of less than 1% at 0.2 T, and about 7% at 0.1 T, indicating that using a weaker magnetic field for HGMS separation is better for increasing the recovery of phosphorus in the "nonmagnetic-fraction".

Lastly, the flotation of the *"best-performing nonmagnetic-fraction"* (the fraction obtained when the magnetic field was set up to 0.1 T) was carried out using SDS and MIBK at pH 10 and yielded a further relative difference of 19% in phosphorus content in the froth when compared with the phosphorus contents in the tailings, showing that flotation is a suitable complement for the HGMS separation step, and could be implemented sequentially in case a higher recovery after HGMS is desired.

Therefore, evidence was found in this study indicating that using a heating step under reducing conditions and an inert atmosphere, followed by physical processing methods such as HGMS and flotation, can promote phosphorus recovery from SSA, with an overall yield in terms of phosphorus recovery from SSA close to 30%.

Chapter 3

Recovery of Phosphorus from SSA using a heat treatment and liquid-liquid separation

3.1 Introduction

The processing method proposed in this Chapter is based on the formation of two mineral species, the phosphate bearing silicocarnotite and the aluminosilicate gehlenite. Therefore, the first step taken was to study the formation of synthetic silicocarnotite and synthetic gehlenite in terms of their formation temperature and their crystallinity once synthesized.

This way, it was deduced that SSA could be used as a raw material for the *simultaneous* preparation of silicocarnotite and gehlenite after a suitable heat treatment. In this case, the resulting mix of silicocarnotite and gehlenite obtained using SSA as a precursor was named in this work as *"H-Ash"*.

In order to characterize the surface charge for pure silicocarnotite, pure gehlenite and "H-Ash", the second step was to perform the analysis of zeta potential (a good indicator of the surface properties of solids) for each one of these species. In addition, this characterization was intended to evaluate the most suitable pH value where a separation of a mixture of silicocarnotite and gehlenite could occur.

Lastly, a liquid-liquid separation technique is proposed, whereby a surfactant is adsorbed onto solid particles in a water/kerosene heterogeneous mixture and form a complex with a non-polar solvent; proceeding to cream over time and resulting in a separation. In particular, to promote the process of *selective particle capture* of the phosphate-bearing mineral silicocarnotite, the addition of a surfactant and a polymer was explored; initially for a mixture of pure materials in a 1:1 ratio (used as a *reference* for the efficacy of the process), and then for *"H-Ash"*.

3.1.1 Silicocarnotite as a source of phosphorus

The importance of silicon substituted calcium phosphates is well-documented as research on the $CaO-SiO_2-P_2O_5$ system has been performed in diverse fields. In recent times, investigations carried out in the field of biomaterials have resulted in evidence suggesting silicon substituted calcium phosphates have desirable properties for skeletal tissue engineering (Manchõn et al., 2015) such as high biocompatibility (Serena et al., 2015) and enhanced resilience (Pietak et al., 2007).

In the context of the well-stablished industry of phosphate processing, considerable attention has been devoted to the study of the specific phases present in the mineral system $CaO-SiO_2-P_2O_5$, in an attempt to develop new methods for the recovery of phosphorus and fertilizer manufacturing (Barrett and Mccaughey, 1942).

The reasoning behind such efforts is that various types of steelmaking slags have been initially studied as potential sources of P-bearing silicon substituted apatites (Lane et al., 1992). From this perspective, silicocarnotite -a crystalline phase with the general formula $Ca_5(PO_4)_2SiO_4$- appears to be of particular interest, as past reports indicate slags containing silicocarnotite can have certain suitability as fertilizer material (Taylor, 1961).

Furthermore, when bioavailability of phosphate released by fertilizing material is taken into account, fertilizers that include phosphate among "glassy" mineral phases have been considered as alternatives to traditional phosphate minerals because they are able to inhibit the bulk release of nutrients to the soil, making the phosphate release to become gradual and thus having a longer, better controlled application over time (Karapetyan et al., 2005).

Besides, the presence of silicon together with phosphates has proven beneficial to the phosphorus uptake of crops such as lettuce, mimosa, corn and others (Roy, 1969; Teranishi, 1968), suggesting that a Si-P loaded phase may be useful for its inclusion onto fertilizer formulations. Therefore, it can be concluded silicocarnotite is attractive as a valuable product, due to the beneficial properties discussed in the previous paragraphs, along with the fact that silicocarnotite can be synthesized quickly at moderately high temperatures via different methods (Bulina et al., 2016).

3.1.2 Gehlenite as a byproduct of recycling techniques

On the other hand, gehlenite -chemical formula: $Ca_2Al_2SiO_7$)-is the aluminium-rich member of the melilite group and has been repeatedly studied in the context of the $CaO-Al_2O_3-SiO_2$ system and its role as an aggregate in ceramics (Traoré et al., 2003) and cement (Palou et al., 2005). According to Fig. 3.1, this particular phase can be found with formulations located near to that of anorthite, at temperatures in the range 1200 -1500 °C.

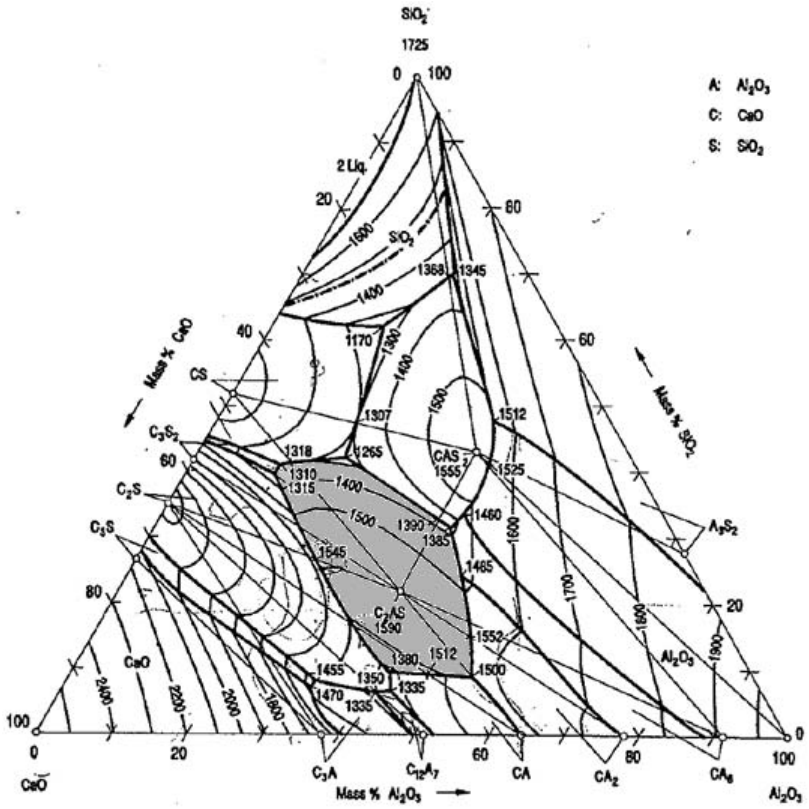

Figure 3.1: Ternary diagram for the $CaO-Al_2O_3-SiO_2$ system at high temperatures, with the gehlenite region highlighted. From Stahleisen. and Verein Deutscher Eisenhuttenleute (R.F.A) (1995).

In the context of the present work, the most relevant attribute from gehlenite is that it is a phase commonly found as part of recycling techniques that seek to obtain useful materials from solid leftovers like slag and fly ash using thermochemical methods (Francis, 2004; Guerrero et al., 1999), pointing out its prevalence as a byproduct in the process of recovery for more valuable materials.

3.1.3 Obtaining silicocarnotite and gehlenite from SSA

When phosphate containing species are heated alongside elements like calcium, silicon and iron, it is possible to obtain glass-type phases, which are commonly known as "phosphate glasses". In a simplified manner, it is considered that the basic building blocks of these "glasses" are the tetrahedral entities composed of the phosphate $(PO_4)^{3-}$ anions (Brow, 2000). These units are thought to make an arrangement of disorganized metaphosphate units able to combine with alkali, alkali earth or metallic elements and form an amorphous, glass-type structure.

In the case of SSA, and due to its composition (see Table 2.1), it is likely that glass-type phases might be formed under heating, as reports for mixtures in the $CaO-P_2O_5-Fe_2O_3$ system (Kumar and Chen, 1994), the $CaO-Al_2O_3-SiO_2$ system (Chen et al., 2017) and the $CaO-SiO_2-P_2O_5$ system (Ohura et al., 1991) have all pointed out the formation of glass phases for element concentrations similar to the ones generally reported for SSA.

Moreover, evidences of SSA forming glass-type materials have already been reported (Lynn et al., 2016; Suzuki et al., 1997) indicating that the formation of glass phases is achieved when limestone is combined with SSA and heated to temperatures close to 1400 °C, resulting in the development of glassy ceramics commonly including crystalline phases of anorthite ($CaAl_2Si_2O_8$) and diopside ($MgCaSi_2O_6$) in their composition.

Nonetheless, even though there is a significant number of scientific literature dealing with the preparation and properties of silicocarnotite, publications referring to its potential as a revalorization product obtained from secondary materials remains scarce. Nonetheless, a recent report has suggested silicon substituted apatites could be synthesized using SSA as a raw material, via the reaction of SSA with Calcium carbonate ($CaCO_3$) at temperatures higher than 1200 °C (Imai, 2019).

From the viewpoint of industrial application, one of the important takeaways from that investigation is that the *product recovered* consists of silicon substituted apatites, which are valuable as fertilizer material because they possess high bioavailability.

Additionally, if such a process is to be used industrially, not only it may be feasible to "strip" the Aluminum initially combined with Phosphorus in the SSA, but also promote the formation of materials with possible use in the cement industry such as Anorthite ($CaAl_2Si_2O_8$) or Gehlenite ($Ca_2Al_2SiO_7$). Even though this processing route for SSA holds value due to the facts mentioned above, more research is needed to find a way to properly separate the materials formed after the reaction. Therefore, the present work studies a liquid-liquid separation method using kerosene, aiming at the recovery of silicocarnotite from silicocarnotite/gehlenite mixes in a straightforward manner.

3.1.4 Surface charge of small particles and zeta potential

Small particles coming from the comminution of larger solids or from synthesis processes act in singular ways when they are dispersed in solution. The interaction of said particles with the medium and within themselves will determine the way they proceed in macromolecular scale processes such as aggregation, coagulation, phase separation, etc. Hence, proper knowledge on the forces these particles experience on their boundaries is needed to accurately understand their behavior.

Colloidal particles may possess a positive or negative electrostatic charge on their surface depending on their chemical properties. In general terms, the development of a net charge in the surface of the particles will have an effect on its immediate surroundings, attracting ions of opposite charge, which in turn will result in the formation of a double layer surrounding each particle; one inner layer with ions strongly bound to the surface of the particles, and an outer layer where ions are less firmly associated (Malvern Instruments, 2011). This is illustrated in Fig. 3.2.

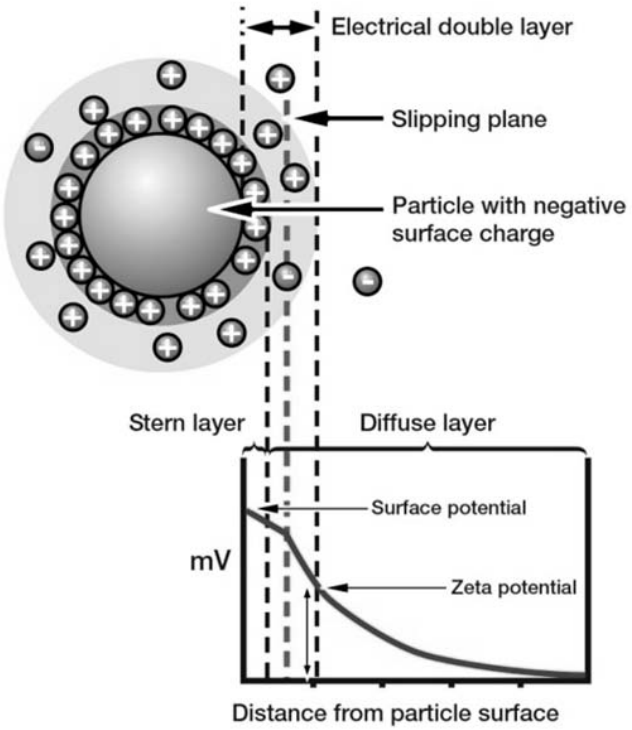

Figure 3.2: Illustration of the double layer potential on a particle. The relation of distance to zeta potential is also displayed. From Malvern Panalytical (2017)

Zeta potential is the potential at the slipping/shear plane of a colloid particle past the double layer, and in general terms gives an indication of the surface charge of the particles and their vicinity. The standard way of assessing this physical property in the laboratory is via the electrophoresis method; using a glass cell, an array of laser light, electrodes and detectors. As electrical fields are applied to the particle dispersion, the particles will migrate in the direction opposite of their surface charge (electrophoresis).

If particles are irradiated during migration, scattering of light will happen, causing a Doppler shift which is a function of the electrophoretic mobility. This data can be measured and forwarded to a computer in order to perform calculations based on the DLVO model, which is the current accepted mathematical framework for the estimation of the zeta potential (Bhattacharjee, 2016).

3.1.5 Sodium Dodecyl Sulfate, Chitosan and their interaction

Sodium Dodecyl Sulfate (SDS)

The term surfactant (short for surface active agent), designates a substance which is able to exhibit some superficial or interfacial activity. Due to their chemical composition, surfactants can be schematized as molecules that have affinity for both polar and non-polar compounds. Generally speaking, the polar portion consists of a heavily charged group or ion and it is called "hydrophilic" . Conversely, the non-polar portion is a long chain of paraffinic alkanes or cyclic compounds and is called "hydrophobic" (Salaguer, 2002).

In the case of Sodium Dodecyl Sulfate (commonly referred to as SDS), the composition of the non-polar portion is a chain of 12 linear hydrocarbon pairs (hence the name dodecyl), whereas the polar portion is a ionic pair of a sodium atom and the sulfate anion. Fig. 3.3 shows the structure of this molecule:

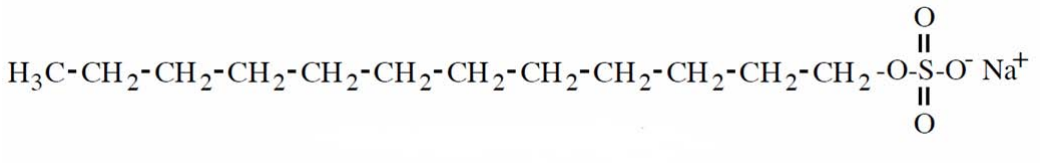

Figure 3.3: Diagram of the chemical structure of SDS, highlighting the presence of the charged $(SO_4)^{2-}$ tail. Author adapted.

Sodium dodecyl sulfate is particularly useful since it has a very good solubility in water, is not toxic and has a low cost, which makes it ubiquitous in modern society and finds a heavy use in formulation of detergents and foaming agents. For industrial purposes in the field of mineral processing, SDS is often used in the flotation technique as a surface tension modifier and collector, typically to process metal oxides (Sadowski and Polowczyk, 2004).

Chitosan

After cellulose, chitin is the second most abundant polysaccharide in nature. It is a readily available compound produced by diverse organisms and it can be obtained from crustaceans' exoskeletons. However, due to the low solubility of chitin in water, the most important product in commercial terms is Chitosan, the only known natural polysaccharide (Hamed et al., 2016).

Chitosan is prepared by the deacetylation of chitin, often performed via the reaction of chitin with 40-50% NaOH under increased temperature (see Fig. 3.4). Depending on the particular conditions, chitosan molecules may end up with a partial degree of deacetylation, which will determine the performance of the molecule as a polyelectrolyte, and needs to be stated as a property of the bulk product.

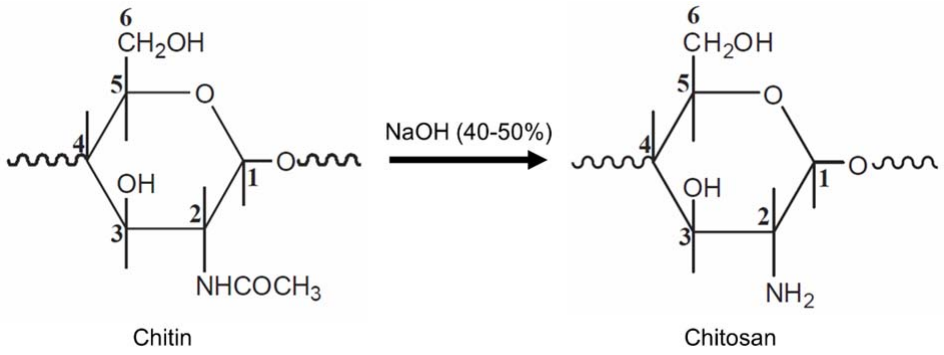

Figure 3.4: Simplified reaction for the deacetylation of chitin using NaOH for the production of chitosan. From Yang et al. (2016)

Chitosan is poorly soluble at pH = 7 but its solubility increases drastically as the pH is reduced. This is because in the presence of Hydrogen ions, the NH_2 groups get protonated and form NH_3, leading to the formation of a cationic polyelectrolyte soluble in water. In addition, experiments have shown that the best way to achieve the dissolution of chitosan without promoting degradation of the molecule under acidic conditions, is to use a weak acid like formic or acetic, usually in a 1% concentration (Sadowski and Polowczyk, 2004).

Chitosan can be used as a flocculation agent because of the charge it acquires when in solution. The mechanism of this process can be modeled as a simple charge neutralization, a charge patching, bridging or sweeping by the long chains of chitosan and small colloidal particles (Yang et al., 2016).

Interaction between SDS and chitosan

Interactions are commonly observed between surfactants and polyelectrolytes, giving rise to the formation of surfactant polyelectrolyte complexes (SPECs). These interactions are thought to be electrostatic in nature and starts at a defined concentration, called critical aggregation concentration (CAC), which is below the critical micelle concentration (CMC) of the pure surfactant (Onesippe and Lagerge, 2008).

Experimentally (see Fig. 3.5, this is tested in the following way: a diluted chitosan solution is progressively added to another solution containing SDS only, while the turbidity is constantly measured (initial turbidity of pure SDS = 1). As the concentration of chitosan rises, an increase in turbidity is observed, reflecting the presence of more and more complexes assembled by SDS-Chitosan interactions.

According to one study (Sunintaboon et al., 2012), when the surfactant content reaches the critical aggregation concentration, a transition between individual molecules associated with polymer chains and surfactant aggregates involving electrostatic and hydrophobic interactions takes place. Above this point, water insoluble complexes start to form and phase separation occurs, nonetheless, re-dissolution happens if more surfactant is added, since this leads to the formation of anionic species.

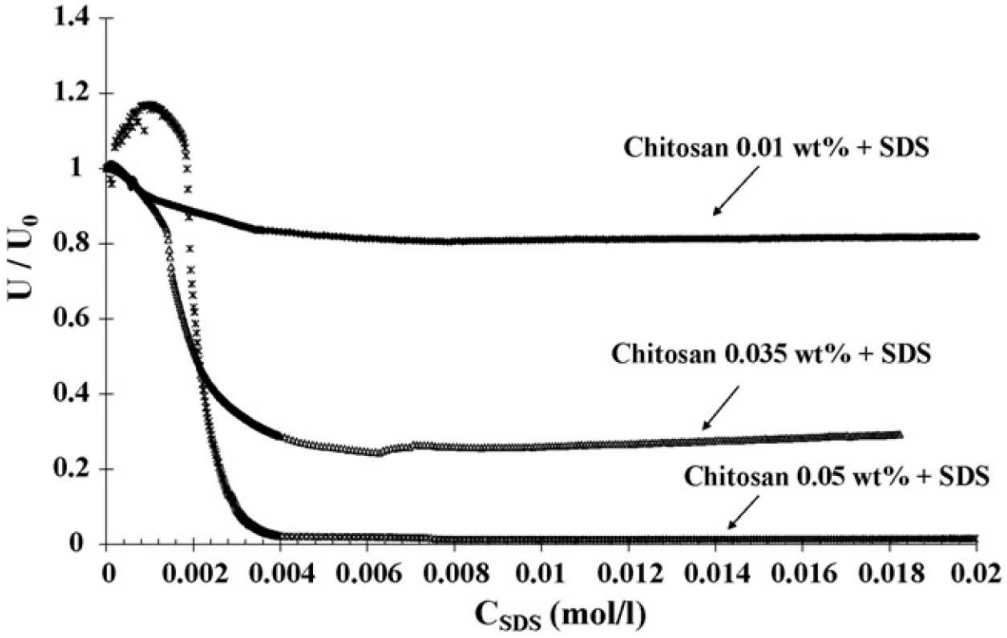

Figure 3.5: Effect of the concentration of chitosan on the turbidity of SDS solutions. From Onesippe and Lagerge (2008)

This means that the interaction and the promotion of phase separation can only materialize when the concentration is located near the CAC. Finally, there is evidence indicating no dependency on the temperature for the clustering of SDS-chitosan complexes, but being controlled by the initial pH of the solution, with stronger bonding at lower pH values. Additionally, these complexes are found to be stable if the pH is changed after their formation suggesting the irreversibility of the entire process (Thongngam and McClements, 2005).

3.1.6 Capture of solids during liquid-liquid separation

Based on the nature of their chemical bonds, solvents have been classified using the old adage "similia similibus solvuntur" , which states a compound will dissolve far more easily in a solvent possessing related functional groups than in one having a different nature (Reichardt, 2010). Broadly speaking, this means that during liquid-liquid separation, one of the phases (the solvent phase) will capture and collect solute from the other liquid phase based solely in their polar affinity.

In the case of the distribution of solids between two immiscible liquids, different phenomena arise depending on the flocculation behavior of the particles. For example, when oil is dispersed in water containing clays, a solids-stabilized oil-in-water emulsion is obtained, where a given oil droplet with diameter d is surrounded by an amount of solid particles by virtue of ther affinity to non-polar solvents, as shown in Fig.3.6. Then, a complex consisting in the oil droplet, the adsorbed particles and an associated aqueous layer, bound to control the stability of the emulsion is formed.

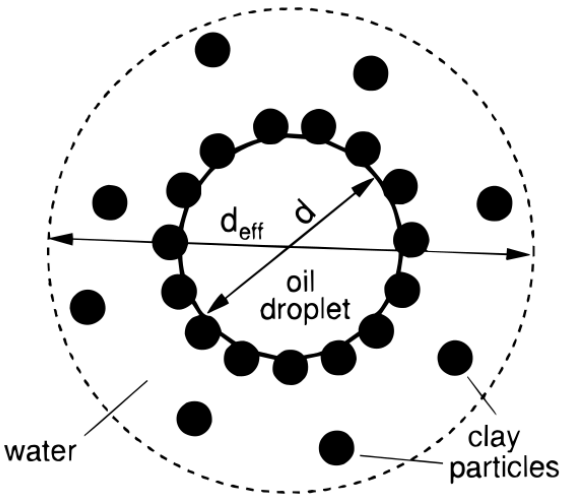

Figure 3.6: Diagram of an oil droplet surrounded by adsorbed solid particles (d = diameter of the droplet, d_{eff} = effective diameter for the droplet/solid/water complex). From Yan and Masliyah (1997)

As the settling process of the particles is now impeded by the surface interactions on top of the oil droplets, it is possible to force the process of "creaming" of emulsions. In this process, the controlling phenomena is the progressive accumulation caused by air and inmiscible droplets surrounded by adsorbed particles in the organic fraction observed as time elapses (Yan and Masliyah, 1997).

3.2 Methodology

3.2.1 Preparation of Synthetic Silicocarnotite and Gehlenite

Initially, synthetic samples of silicocarnotite and gehlenite (pure materials) were prepared using the following reagents: $Ca(OH)_2$, $Ca_3(PO_4)_2$, and SiO_2 for silicocarnotite and $Ca(OH)_2$, $Al(OH)_3$ and SiO_2 for gehlenite. All the materials were laboratory grade and provided by WAKO Pure Chemical Industries. It is postulated the desired materials undergo the reactions described by Eq.3.2 and Eq.3.1 at temperatures in the range 1100 -1300 °C.

$$2\,Ca(OH)_2 + 2\,Al(OH)_3 + SiO_2 \longrightarrow Ca_2Al_2SiO_7 + 5\,H_2O \tag{3.1}$$

$$2\,Ca(OH)_2 + Ca_3PO_4 + SiO_2 \longrightarrow Ca_5(PO_4)_2SiO_4 + 2\,H_2O \tag{3.2}$$

where Eq.3.1 refers to the formation of gehlenite ($Ca_2Al_2SiO_7$) and Eq.3.2 refers to the formation of silicocarnotite ($Ca_5(PO_4)_2SiO_4$).

Stoichiometric reagent quantities based on equations 3.1 and 3.2 were pulverized using an agate laboratory mortar and pestle (FISCHER SCIENTIFIC), and mixed carefully to ensure proper distribution. Then, small samples (around 3 g) of each one of these blends were collected and subjected to TG-DTA Analysis (RIGAKU ThermoPlus EVO TG8120) to perform an assessment of their behavior.

Afterwards, larger portions (5 g each) of the aforementioned mixes were poured inside aluminum ceramic crucibles (AS-ONE 3W, 100 mL) in order to obtain 6 aliquots of silicocarnotite mix and 6 portions of gehlenite mix separately. These samples were then heated using an electric furnace (AS-ONE HPM-1G) to temperatures in the range 900 to 1400 °C under air atmosphere, and the interval between each temperature was of 100 °C. A XRD analysis (RIGAKU SmartLab, PDXL ver. 2.3.1.0, Database: PDF-2/Release 2010 RDB) was performed on every sample in order to observe the development of the desired phases.

Subsequently, and based on the results obtained in the previous step, samples (50 g) of both silicocarnotite and gehlenite were prepared using the same equipment at 1300 °C. All the resulting materials were washed using HCl 1M (WAKO Pure Chemicals) to remove traces of unreacted $Ca(OH)_2$ after cooling down, and their mineral phases assessed using SEM/EDS analysis (JEOL JSM-6510).

3.2.2 Synthesis of "H-Ash", a mixture containing silicocarnotite and gehlenite using SSA as a precursor

As mentioned in Section 1.6, the average composition of SSA includes mineral oxides of Si, Ca, Fe, P and Al, often combined in phases that hinder its direct use as fertilizer. For instance, a pervasive mineral phase in samples of sewage sludge ash is whitlockite ($Ca_9Mg(PO_4)_6(PO_3OH)$), which has been reported to have a low phosphate bioavailability (Stemann et al., 2015).

Hence, in order to study the usage of sewage sludge ash as a precursor, a SSA sample provided by Tokyo Metropolitan Sewerage Service Corporation with a D_{50} size of 3.33 [µm] and a phosphate content of 18.5% wt. was used (Córdova Udaeta et al., 2017). Given the contents of this SSA sample, if the stoichiometric ratios expressed in both Eq. 3.1 and Eq. 3.2 are matched it is expected that the addition of a controlled amount of $Ca(OH)_2$ will lead to the formation of silicocarnotite and gehlenite after heat treatment.

For this purpose, two different blends consisting in either 50 g of $Ca(OH)_2$ and 100 g of SSA (33% $Ca(OH)_2$, 67% SSA); or 70 g of $Ca(OH)_2$ and 100 g of SSA (40% Ca(OH)2, 60% SSA) were prepared, and then heated to 1300 °C under an air atmosphere for 1 h. This sample was labeled "*H-Ash*" (meaning: heated ash) and subsequently washed with HCl 1M and its structure was validated using XRF (RIGAKU SuperMini WDXRF) and XRD (RIGAKU SmartLab, PDXL ver. 2.3.1.0, Database: PDF-2/Release 2010 RDB).

3.2.3 Experimental process for the liquid-liquid separation

Before performing the separation experiments, measuring the zeta potential is required. For this purpose, the light scattering method was used as a valid approximation for the analysis of the zeta potential of all the solids studied. To that end, 5 mM solutions using distilled water of the washed samples described earlier were prepared and evaluated using a Zeta potential and Particle Analyzer (ELS-2000, OTSUKA), using a 10mM NaCl solution to ensure proper electric flow and adjusting the pH using HCl 1M and NaOH 1M, for pH values ranging from pH 2.5 to pH 11.

For the separation experiments, 25 mL samples containing 10% wt. of solid material were prepared inside a 50 mL separation funnel (AS ONE Corporation) using desalinated water and mixed with doses of 0.14 Kg/tonne, 1.44 Kg/tonne and 14.4 Kg/tonne of sodium dodecyl sulfate (Nacalai Tesque Inc.).

Then, since prior literature reported a positive interaction of SDS and Chitosan, resulting in the formation of insoluble complexes (McCLements and Masubon Thongngam, 2004), a stock solution of Chitosan (Concentration: $5x10^{-3}$ g/mL, deacetylation degree >0.8, Manufacturer: Nacalai Tesque Inc.) was prepared using acetic acid 1M (WAKO Pure Chemicals). Accordingly, the samples in the funnels were conditioned to have a final concentration of 0, 100 and 200 g/tonne chitosan respectively, in order to assess the effect of Chitosan on the capture of materials in the organic phase.

The final steps were the incorporation of kerosene (15 mL) to the aforementioned mixtures in a 2:5 ratio, and the thorough mixing of the resultant blends for 30 minutes. After 30 minutes of settling time, both fractions (organic and inorganic) were collected separately and centrifuged for 5 mins at 2000 RPM, filtered, dried for 24 h at 70 °C, their weights recorded, and lastly analyzed using XRF to assess the P_2O_5 content on each fraction.

The separation procedure was carried out at two different initial pH values. The first value (pH = 5.5), was selected based on the result of the zeta potential analysis, specifically, the point of zero charge of silicocarnotite. The second value (pH = 4.0) was selected based on the increased solubility of hydroxyapatite (and other calcium phosphates) below this pH (Pan and Darvell, 2009), which will have an undesired effect as the amount of silicocarnotite recovered will be reduced by dissolution. Hence, table 3.1 shown below summarizes this information:

Table 3.1: Summary of the experiments carried out for liquid-liquid separation.

Sample	**Detected phases**	**Initial pH before extraction**	**SDS concentration [Kg/-tonne]**	**Chitosan concentration [g/-tonne]**
Pure Silicocarnotite	$Ca_5(PO_4)_2SiO_4$	4.0, 5.5	0.14, 1.44, 14.4	0, 100, 200
Pure Gehlenite	$Ca_2Al_2SiO_7$			
Mix 1:1 of Silicocarnotite and Gehlenite	$Ca_5(PO_4)_2SiO_4$, $Ca_2Al_2SiO_7$			
H-Ash	$Ca_5(PO_4)_2SiO_4$, $Ca_2(Mg_{0.25}Al_{0.75})(Si_{1.25}Al_{0.75})$			

Additionally, Fig.3.7 schematizes the experimental setup used for the experiments. In the case of pure samples, the heating step represents the formation of synthetic silicocarnotite and synthetic gehlenite. On the other hand, in the case of samples using SSA as a precursor, the heating step refer to the preparation of "H-Ash".

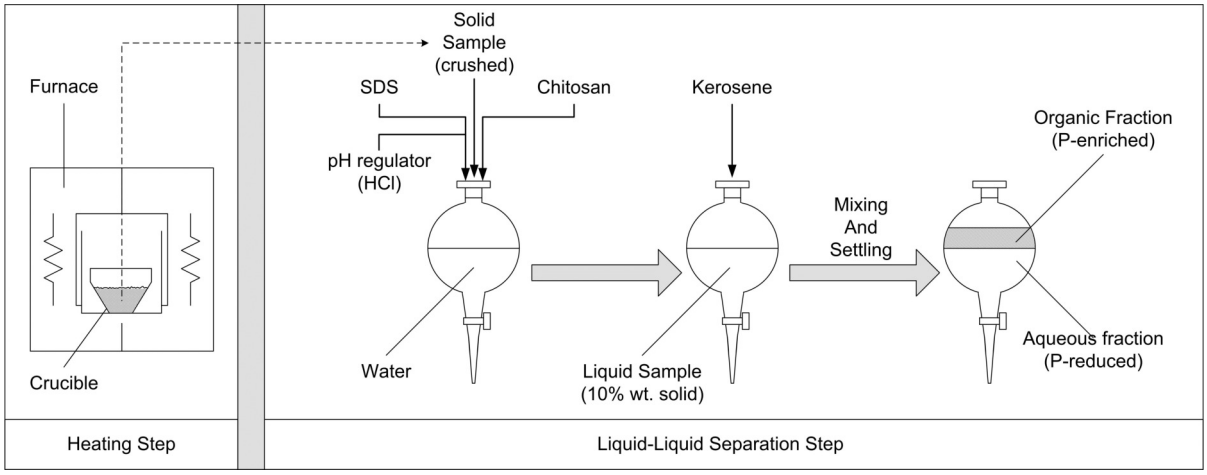

Figure 3.7: Schematic representation of the experimental procedure.

3.3 Results and Discussion

3.3.1 Preparation of synthetic silicocarnotite and synthetic gehlenite

For the synthesis of silicocarnotite, data obtained from the TG-DTA curve suggested the process of silicon substitution on the calcium phosphate phases starts at temperatures in the range 1100 -1200 °C for the proposed synthesis route. In addition, the data also indicates that before reaching said temperature range no significant substitution occurs, as can be seen in Fig. 3.8.

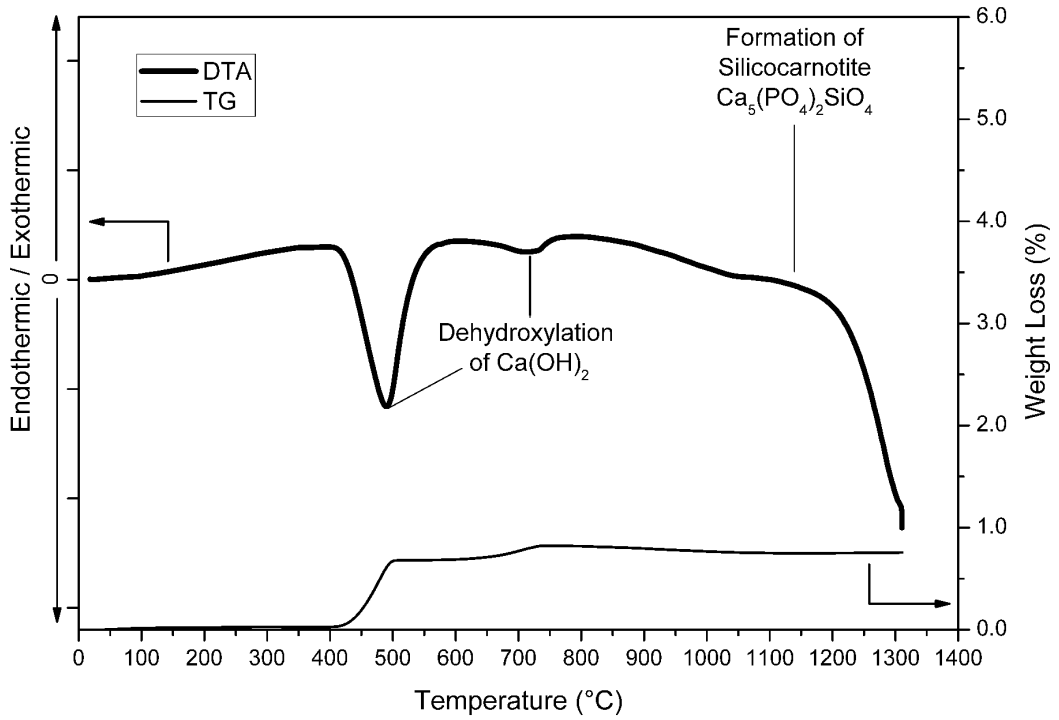

Figure 3.8: Thermogravimetric (TG-DTA) results for synthetic silicocarnotite.

Starting from 1100 °C, SiO_2 starts to coalesce with hydroxyapatite and substitution proceeds accordingly. This process continued along the temperature range of our experiment, and it is expected to yield silicocarnotite as the stable phase until temperatures close to 1400 °C where it is thought combined phases of α-2 $CaO \cdot SiO_2$ and α-3 $CaO \cdot P_2O_5$ start to form (Stahleisen. and Verein Deutscher Eisenhuttenleute (R.F.A), 1995).

XRD analyses also reflect this line of reasoning as it can be seen in Fig. 3.9, which shows the peaks due to the presence of silicon substitution start to appear in the diagram at 1100 °C and continue onwards, reaching a completely defined state at 1400 °C. In addition, our results highlight the phase of quartz (SiO_2) is no longer showing the presence of diffraction peaks at this temperature.

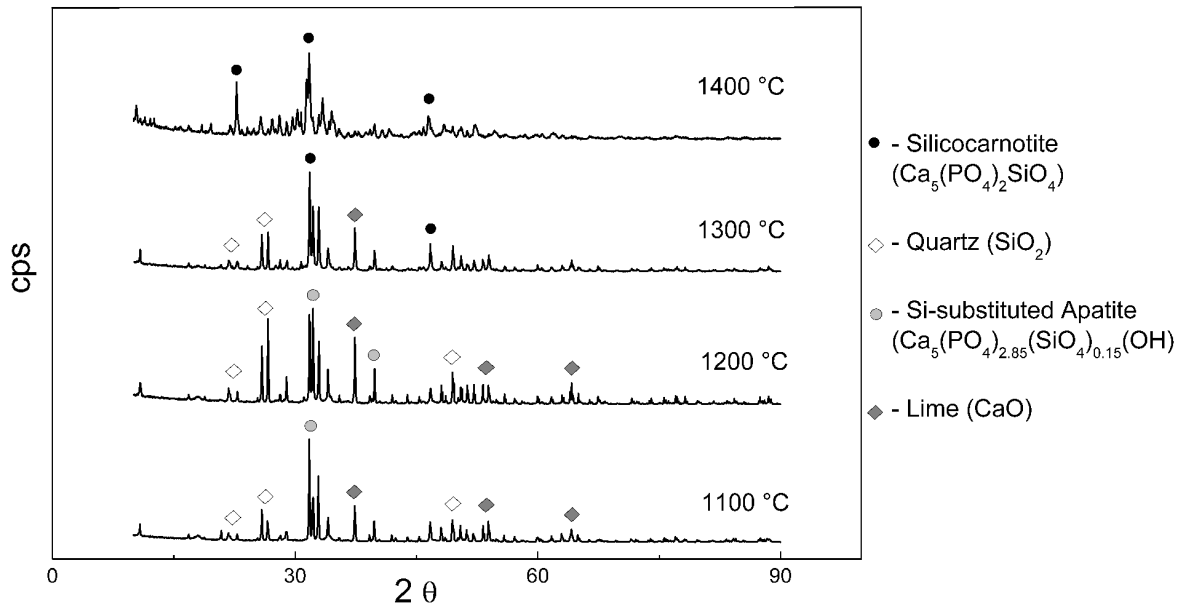

Figure 3.9: XRD results for the synthesis of silicocarnotite at different temperatures.

In the case of gehlenite (see Fig. 3.10), and in concordance with previous results found in the literature (Ptáček et al., 2013), the slump in the DTA curve projected indicates that the lowest temperature for its formation under the experimental conditions is 1200 °C, whereby an endothermic process starts and keeps on sustaining at higher temperatures of reaction.

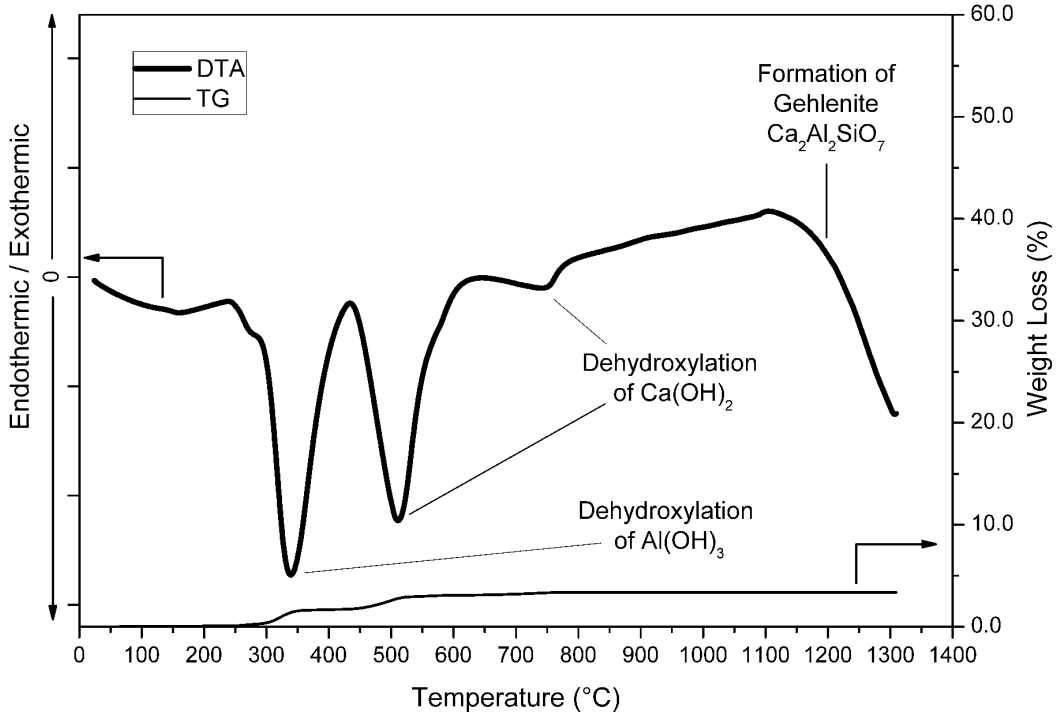

Figure 3.10: Thermogravimetric (TG-DTA) results for synthetic gehlenite.

It can also be observed that starting from 1200 °C and toward higher temperatures of reaction, calcium aluminosilicates such as mayenite ($Ca_{12}Al_{14}O_{33}$) start to form, progressively changing to gehlenite, which in turn appears more sharply defined as the temperature gets higher and higher, as it is shown by the XRD results presented in Fig. 3.11.

This can be explained due to the SiO_2 initially present as quartz, starting to react with the combined phases of calcium and aluminum that had already been formed (as mayenite) and gradually incorporate to form gehlenite, consuming energy in the process.

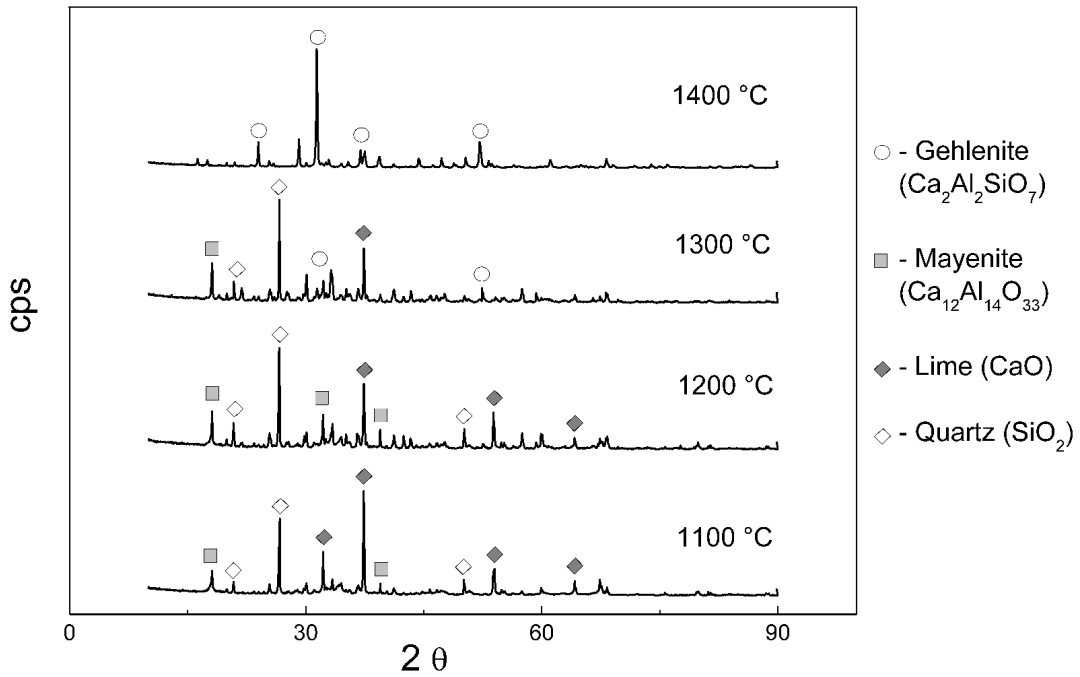

Figure 3.11: XRD results for the synthesis of gehlenite at different temperatures.

Accordingly, SEM-EDS analysis performed on samples of silicocarnotite and gehlenite synthesized at 1300 °C have also confirmed the formation of these phases for each sample. In that regard, Fig. 3.12a) shows the existence of silicocarnotite crystals as Si, Al and P emission spectra overlap is observed. On the other hand, the close-up of particles shown in Fig. 3.12b), displays a unequivocal overlap of Ca, Al and Si spectra, which is an indicator of the presence of gehlenite crystals.

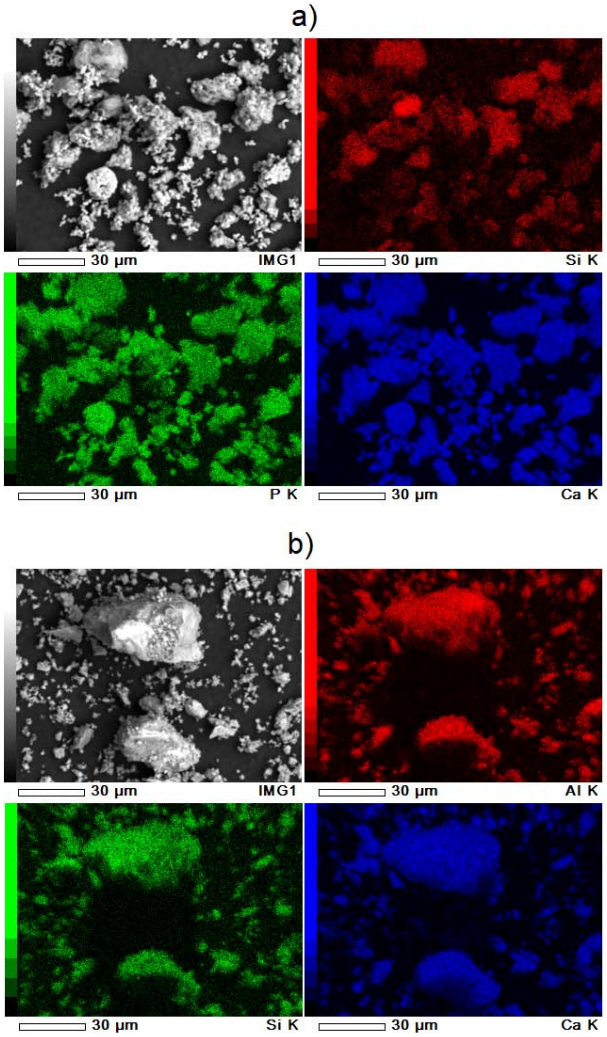

Figure 3.12: SEM/EDS images for the samples synthesized at 1300 °C. a) Silicocarnotite, b) Gehlenite.

In light of these results, it can be inferred that if the mass ratios of the precursors are matched, there is a region of temperature overlap for simultaneous formation of both silicocarnotite and gehlenite. This region is deemed to start at 1200 °C and reach a maximum temperature of around 1400 °C before changing to a different phase due to the constraints imposed by silicocarnotite formation. (Borsa et al., 2008) Therefore, in order to achieve the highest yield for the transformation while keeping the temperature expense to a minimum, the temperature chosen for the further preparation of synthetic samples of silicocarnotite and gehlenite used in the subsequent experiments carried out in this research was 1300 °C.

3.3.2 Preparation of H-Ash

In the case of H-Ash preparation, it can be seen in the TG-DTA plots presented in Fig. 3.13 that both conditions succeed in the dehydroxylation of $Ca(OH)_2$ and keep reacting similarly until a temperature of approximately 1200 °C is reached. However, only the mixture containing 40% of $Ca(OH)_2$ shown in Fig. 3.13b) end up generating a secondary shoulder peak at higher temperatures, indicating that energy is being consumed in order to form a Ca-Si-P phase. Conversely, the sample containing 33% $Ca(OH)_2$ (Fig. 3.13a)) does not exhibit the aforementioned shoulder peak at any point, hinting that the phase formation stage was already completed.

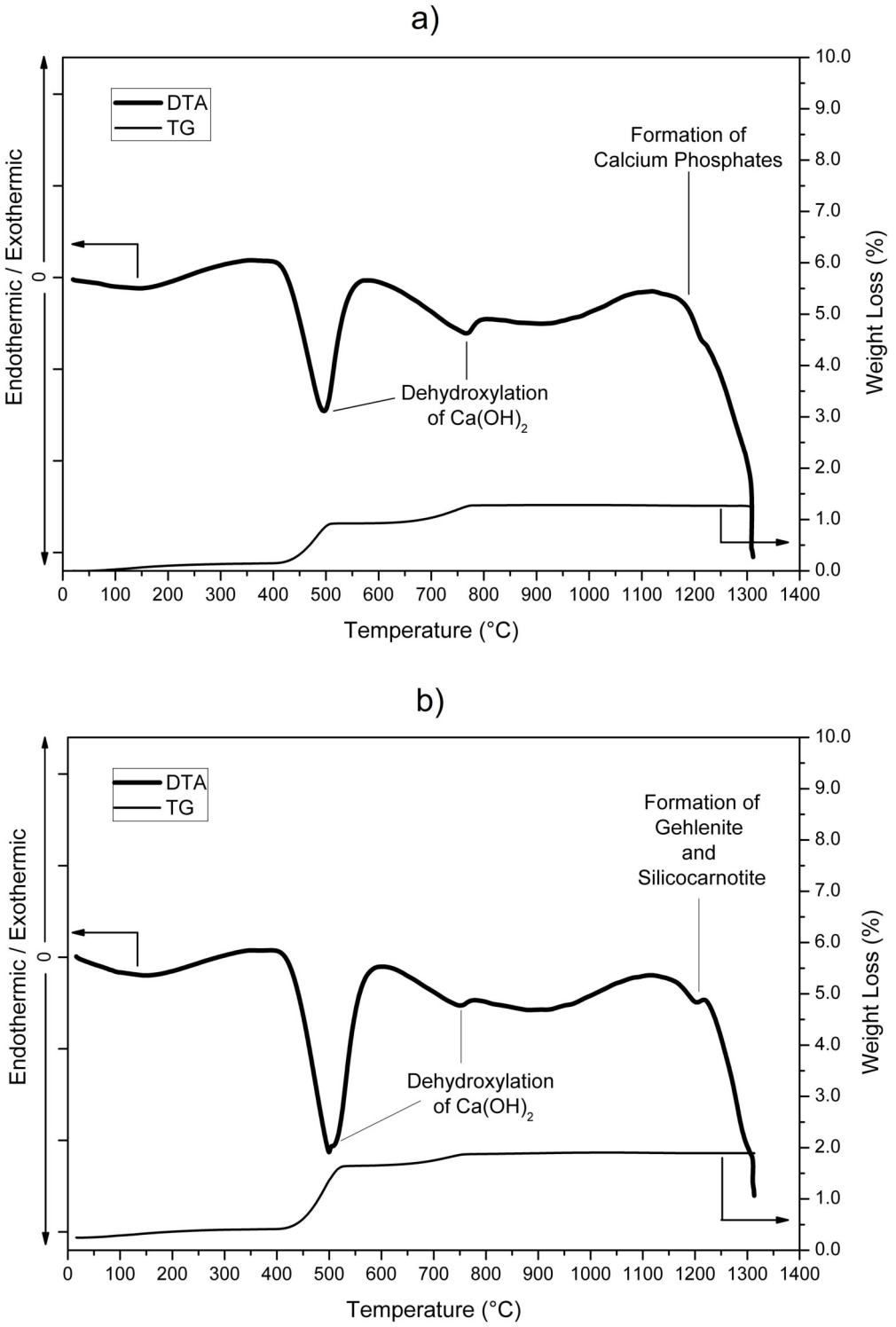

Figure 3.13: TG-DTA for the H-Ash preparations. a) 33% $Ca(OH)_2$ b) 40% $Ca(OH)_2$

This line of reasoning is reinforced by the results obtained from the XRD analysis. In that case, it was observed that the sample containing 33% of $Ca(OH)_2$ is not able to incorporate Si atoms into the phosphate structure but instead promotes the formation of phases similar to calcium iron phosphate ($Ca_{19}Fe_2(PO_4)_{14}$) alongside calcium phosphates (expressed in the analysis as decacalcium phosphate oxide ($Ca_{10}(PO_4)O$)), meaning that the amount of CaO during the transformation needs to be in excess in order to effectively "flux out" the iron atoms.

In sharp contrast, since it is known that a larger concentration of CaO favors the formation of Ca-Si-P phases at high temperatures (Lynch, 2009), the sample that had 40% $Ca(OH)_2$ as part of the mixture showed no combined phase for iron and instead resulted in the appearance of well-defined peaks indicating a complete transformation into silicocarnotite and gehlenite, as can be seen in Fig.3.14.

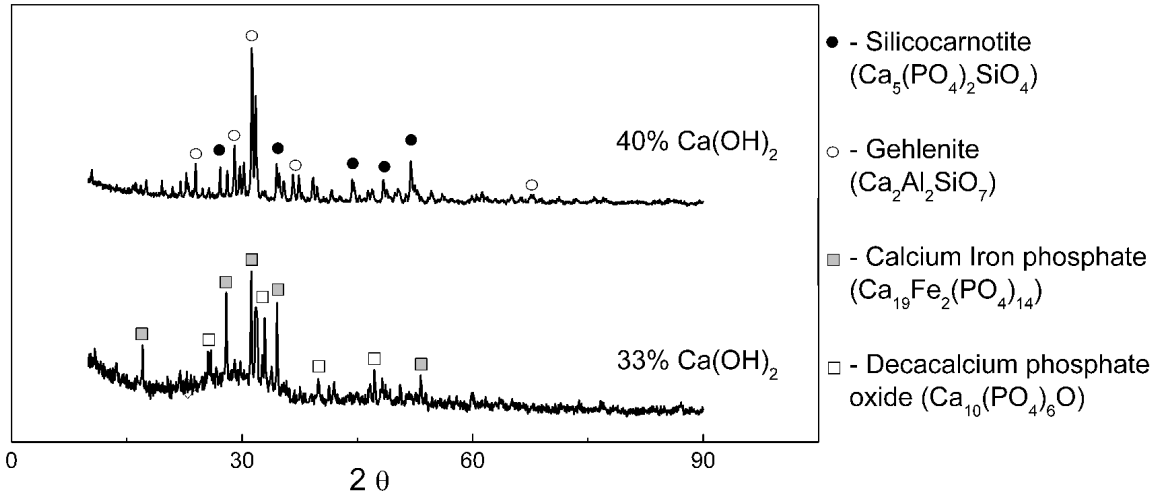

Figure 3.14: XRD results for the 2 different ratios for $Ca(OH)_2$ and SSA, synthesized at 1300 °C.

These results point out the possibility of obtaining silicocarnotite and gehlenite using SSA as a precursor when the content of $Ca(OH)_2$ added before the heat treatment is equal to 40%, which is thought to guarantee the separation of the phosphate atoms from the Al phases, and their incorporation onto Ca-Si-P phases.

3.3.3 Zeta potential of synthetic silicocarnotite, synthetic gehlenite and H-Ash

Our results show that both synthetic silicocarnotite and synthetic gehlenite behave similarly in terms of their surface charge for the most part of the pH range, showing essentially negative zeta potentials at pH values higher than 6. However, the zeta potential measured for silicocarnotite becomes more positive as the amount of H+ ions increases, reaching its point of zero charge (PZC) at pH 5.5. These results are in accordance with prior research, since zeta potential studies on a Si-substituted hydroxyapatite showed a similar shift towards the acidic region resulting in a PZC close to pH = 5 (Botelho et al., 2002).

Conversely, results for synthetic gehlenite indicate this substance remains having a negative zeta potential throughout the pH range studied (from pH=2.5 to pH=11), never reaching its PZC under our experimental conditions. Here, concordance with prior art was also achieved since evidence found elsewhere suggests that a slag with gehlenite as its main crystalline phase (Borsa et al., 2008), and even anorthite -which is thought to share similarities with gehlenite- (Lynch, 2009), have the same behavior referring to their zeta potential (Botelho et al., 2002). These results can be seen in Fig. 3.15.

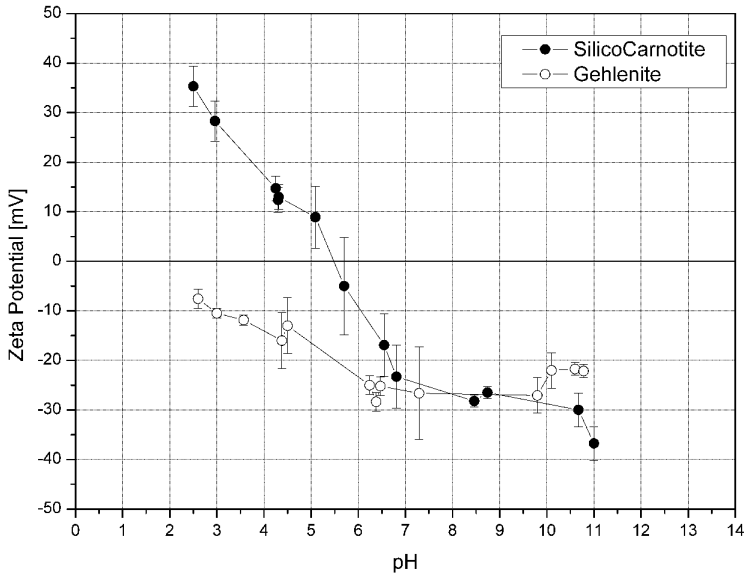

Figure 3.15: Zeta potential measurements for synthesized silicocarnotite and gehlenite.

The outcome of these experiments suggest that it would be possible to promote the adsorption of an anionic surfactant, for example sodium dodecyl sulfate ($CH_3(CH_2)_{11}SO_4Na$) onto the valuable phase of silicocarnotite at pH below 6. At the same time, the adsorption of SDS onto gehlenite will be reduced because of the negative nature of its zeta potential. This will result in silicocarnotite and being the only species capable of forming an agglomerated entity, which can be recovered afterwards using kerosene.

Correspondingly, when H-Ash was subjected to analysis, it was seen that the values for its zeta potential remain negative (around -45 mV) at pH values higher than 6.5, which is estimated as the point of zero charge (PZC) for this sample. Then, as the pH decreases the zeta potential turns gradually more positive and reaches an approximate value of +35mV at pH 3.5. In a rather interesting way, the behavior exhibited can be associated to that of pure silicocarnotite, which may imply the influence of this molecule in the overall surface potential for H-Ash, as can be seen in Fig. 3.16.

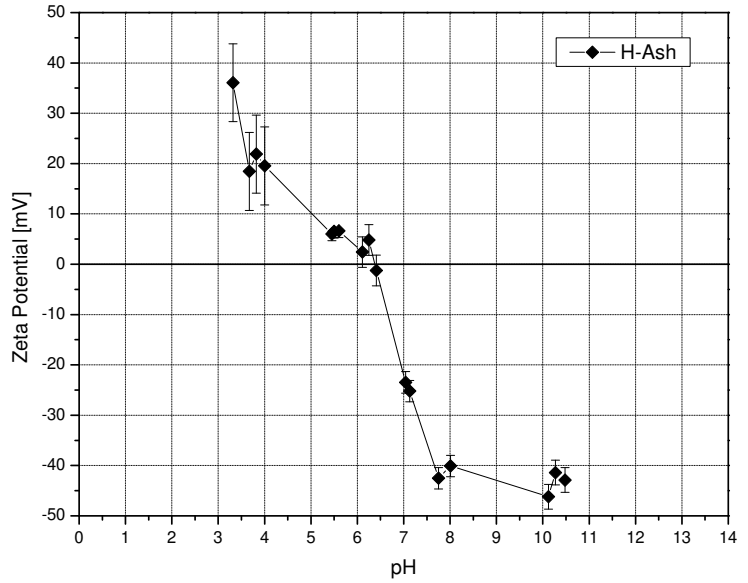

Figure 3.16: Zeta potential measurements for H-Ash.

By virtue of the similarity of the zeta potential of silicocarnotite and H-Ash, an analogous reasoning can be made for the recovery of valuable phosphate. Therefore, it is proposed that, if the conditions of the physical separation are adequate, the process previously described in Fig. 3.7 should be able to promote the capture of the phosphate-bearing phases present in H-Ash, and yield a larger concentration of phosphorus in the organic fraction, when compared to the aqueous fraction.

3.3.4 Separation of pure materials from water and kerosene mixtures

Individual separation of synthetic silicocarnotite and synthetic gehlenite

The experiments pointed out that SDS is effective at binding itself with silicocarnotite as predicted by the analysis of zeta potential. When the separation process is carried out at pH 5.5, the amount of solids captured in the organic fraction increases as the SDS dose increases as shown in Fig. 3.17a), reaching a maximum value of 53.8% collected when the dose is equal to 1.44 kg SDS/tonne. Also, considering the negative tendency observed past this SDS dose, it can be said that a larger amount of SDS does not result in more material captured in the organic fraction.

In terms of the effect of chitosan addition at this pH, a concentration of 100 g chitosan/tonne (Fig. 3.17b)) appears to have a negative effect on the capture of material. Moreover, at 200 g chitosan/tonne (Fig.3.17 c)) the percentage of silicocarnotite found in the organic fraction stagnates under 50% at both SDS contents of 1.44 and 14.4 kg/tonne.

On the other hand, if the pH before separation is set to 4.0 (Fig.3.17 d)), the maximum value for silicocarnotite captured in the organic fraction reaches a maximum of around 70% of the initial amount at 1.44 kg SDS/tonne, and remains over 50% even at higher doses of SDS, hinting the effect of a more positively charged surface on the particles.

When chitosan was added at this pH (Fig.3.17 e) and Fig.3.17 f)), the effect observed was of a reduction in the material captured at 1.44 kg SDS/tonne, but a noticeable increase in the capture at 14.4 kg SDS/tonne for 200 g chitosan/tonne. In that case, it is thought that the formation of interlinked complexes is predominant compared to the attachment of surfactant alone, thus forming a SDS-silicocarnotite-chitosan “mesh”, susceptible of transfer towards the organic fraction.

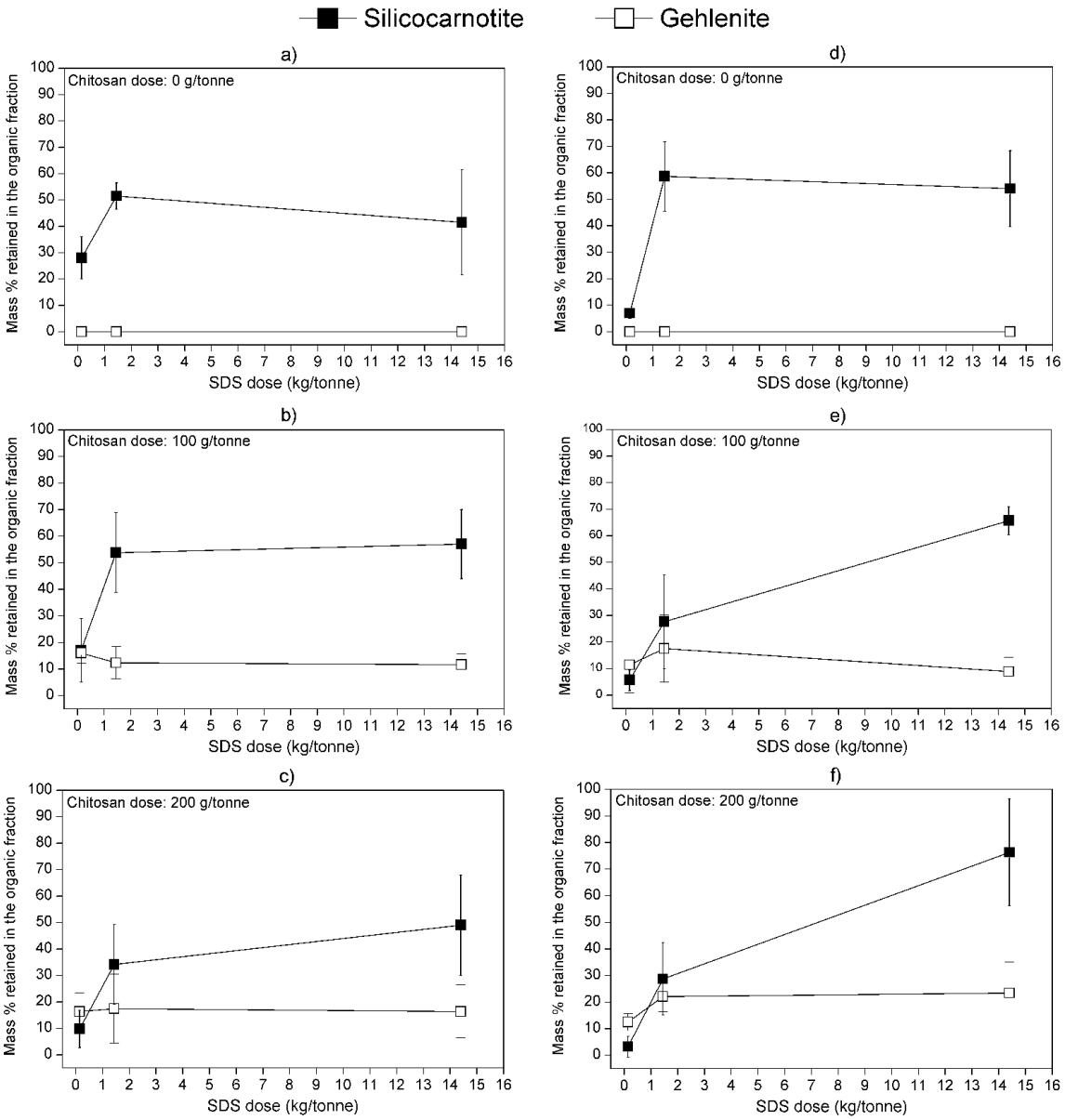

Figure 3.17: Amount of material captured in the organic fraction for synthetic silicocarnotite and synthetic gehlenite under different conditions. pH = 5.5 for a), b), c); and pH = 4.0 for d), e) and f).

Referring to the capture of gehlenite under these experimental conditions, Fig.3.17 a) and Fig.3.17 b) show that for a pH equal to 5.5, the capture of gehlenite in the organic fraction is very limited, with 0% captured when no chitosan is present, and less than 20% when 100 g/tonne chitosan is added. In the same vein, the maximum capture for gehlenite was of 30% for a dose of 1.44 kg SDS/tonne combined with 200 g chitosan/tonne (Fig. 3.17c)). This small increase indicates a fraction of the chitosan is being bound both to gehlenite and SDS resulting in a conglomerate non-polar enough to be captured by kerosene.

Comparison of the capture efficiency for synthetic silicocarnotite

In order to compare the results of the previous experiments in terms of silicocarnotite retention, we define the "*Silicocarnotite Capture Efficiency*" (SCE) for each set of conditions (SDS content and chitosan content) as described by Eq.3.3.

$$SCE = \frac{S}{100}\left(\frac{S-G}{S+G}\right) \tag{3.3}$$

where S refers to the % of silicocarnotite retained in the organic fraction, and G is the % of gehlenite captured in the same fraction. Using this equation, it is possible to directly observe which experimental conditions promote the largest capture of silicocarnotite taking into account the capture of gehlenite that would occur under the same experimental setup.

For example, if certain conditions promote a large capture of silicocarnotite S, the calculated SCE will be large. However, if the same conditions also promote some capture of gehlenite G, the denominator term of the equation will increase, and the value of the SCE for that particular set of conditions will be reduced. In consequence, experimental conditions promoting more silicocarnotite and less gehlenite captured in the organic fraction will have the SCE larger and closer to 1.0, which is the ideal case where the capture for S is 100% and the capture for G is 0%.

Threfore, Fig.3.18 was prepared after calculating the SCE value for the experiments in Section 3.3.4, and plotting the results in order to highlight the differences between different experimental conditions in terms of the SCE value.

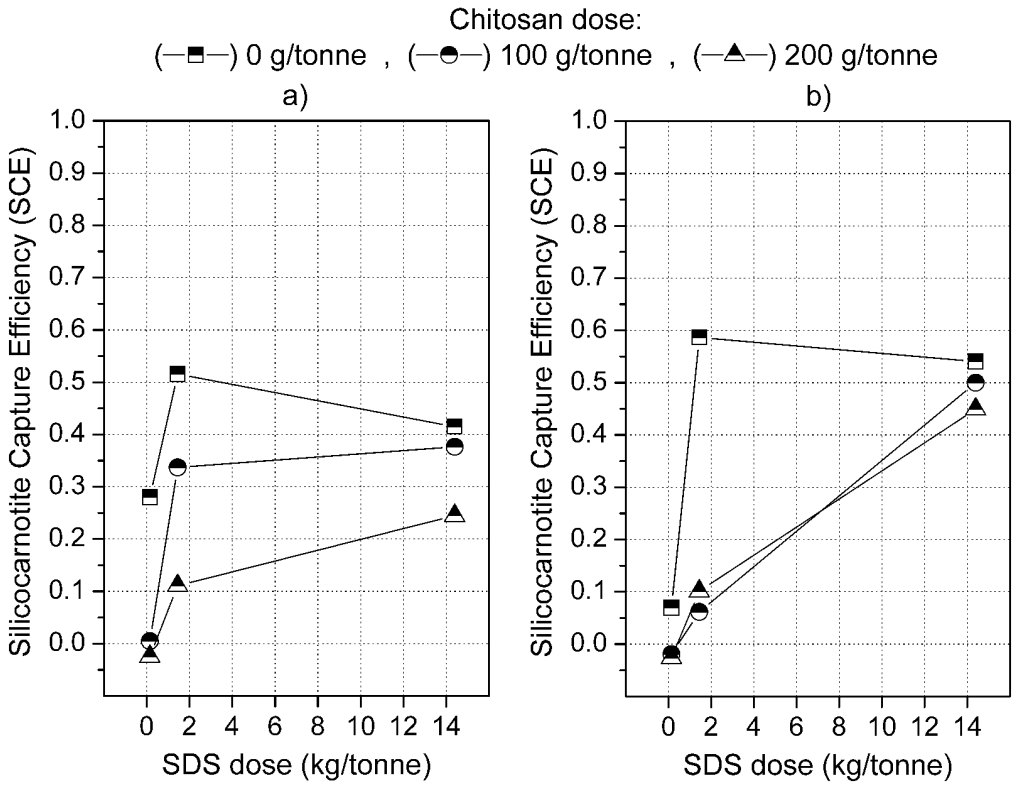

Figure 3.18: SCE values for the experiments performed using synthetic samples of silicocarnotite and gehlenite. a) pH = 5.5, b) pH = 4.0.

Fig.3.18 a) shows that the highest SCE (around 0.50) is obtained for a chitosan dose of 0 g/tonne and a dose of 1.44 kg SDS/tonne if the pH is set to 5.5. Conversely, larger doses of chitosan seem to reduce the SCE as the values for 100 g/tonne chitosan are close to 0.3, and less than 0.4 at 200 g/tonne. This could be explained in terms of the inclination of SDS to pair directly with the comparatively more positive chitosan molecules, resulting in less interaction with silicocarnotite particles.

Similarly, at pH = 4.0 (see Fig.3.18b)) the highest SCE value is achieved once again for a chitosan dose of 0g/tonne at 1.44 kg SDS/tonne, reaching a SCE close to 0.6. This hints to a higher interaction between SDS and silicocarnotite at lower pH values in agreement with the prediction based on zeta potential measurements presented in Fig.3.15. Interestingly, the SCE values at 14.4 kg SDS/tonne are all in the range 0.45 ⁻0.7 pointing out that a larger dose of SDS at this pH promotes a significant capture of silicocarnotite, suggesting that the major driving force behind agglomeration is due to the surfactant and not due to the polyelectrolyte.

Separation of a sample of Silicocarnotite and Gehlenite mixed in a 1:1 ratio as a reference for their simultaneous separation

Based on the results for pure materials, a mechanism for the *simultaneous* separation of silicocarnotite and gehlenite mixtures was derived. Accordingly, the mechanism of the proposed separation technique are illustrated in Fig.3.19 and operate as follows:

Starting with an aqueous suspension of both silicocarnotite and gehlenite, the addition of SDS (anionic surfactant) leads to the formation of reverse micelles with silicocarnotite, which has a net positive charge on the surface. On the other hand, since gehlenite is negatively charged, SDS will not interact and micelles will not be formed. When kerosene is added in the next step, it is expected from the reverse micelles encapsulating silicocarnotite to migrate towards the organic fraction and separation to be achieved.

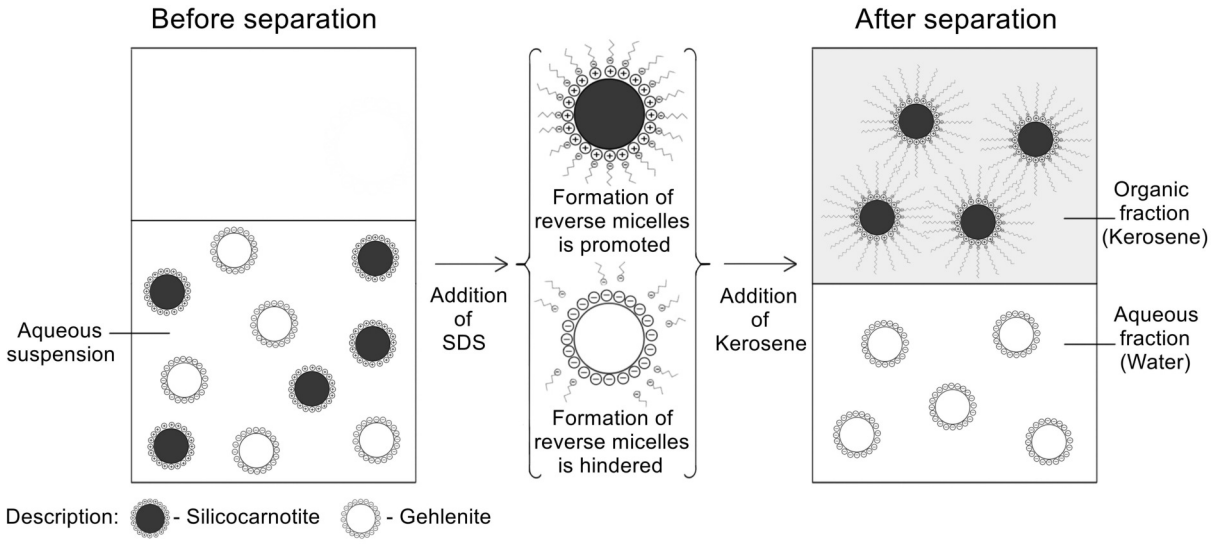

Figure 3.19: Schematic representation of the liquid-liquid separation mechanism.

The results of the experiments with the 1:1 blend of silicocarnotite and gehlenite are shown in Fig.3.20 It was revealed that using a concentration of 1.44 kg SDS/tonne yields the largest capture of material in the organic fraction, irrespective of the pH value. Still, when the dose is as high as 14.4 kg SDS/tonne, the capture is comparatively large only at large doses of chitosan. This could be due to SDS predominantly forming micellar structures instead of binding to the solids' surface. This way, it is possible complexes consisting of solids-SDS-chitosan are being formed and some material continues to be captured.

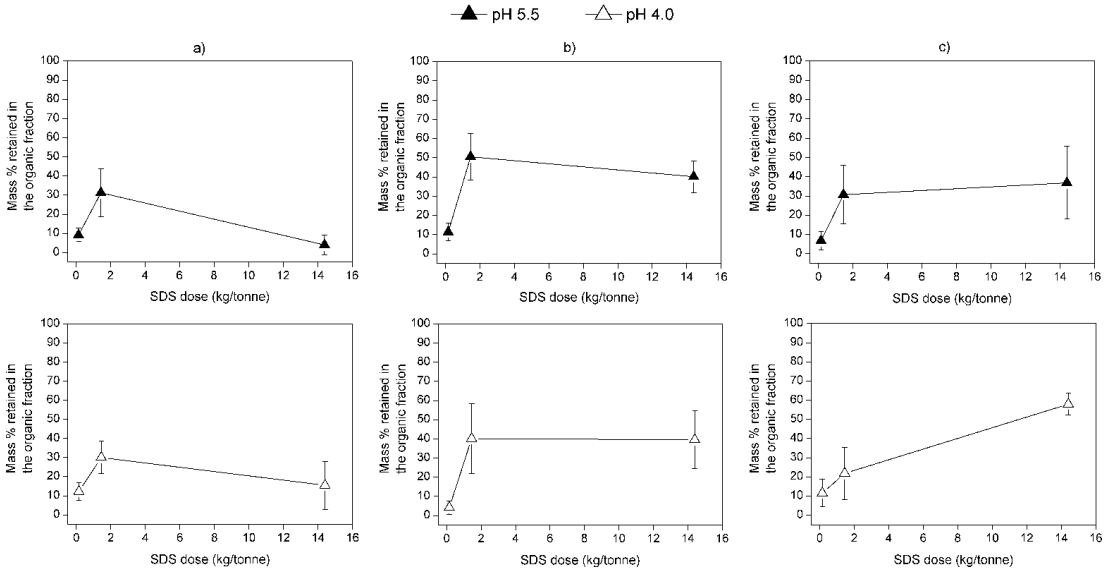

Figure 3.20: Amount of material retained in the organic fraction for a blend of 1:1 silicocarnotite and gehlenite under different pH conditions. Chitosan dose: a) 0 g/tonne, b) 100 g/tonne, c) 200 g/tonne.

Given that silicocarnotite is the only phosphate-bearing substance in the 1:1 blend, P_2O_5 content was used as a performance indicator of the separation. Accordingly, Fig.3.21 shows the general tendency for the organic fraction to be enriched in P_2O_5 compared to the aqueous fraction regardless of the conditions tested. That being said, the SDS dose resulting in the largest difference in P_2O_5 content was 1.44 kg SDS/tonne, with the sample having 0 g chitosan/tonne resulting in the largest amount of P_2O_5 in the organic fraction, and the lowest amount of P_2O_5 in the aqueous fraction.

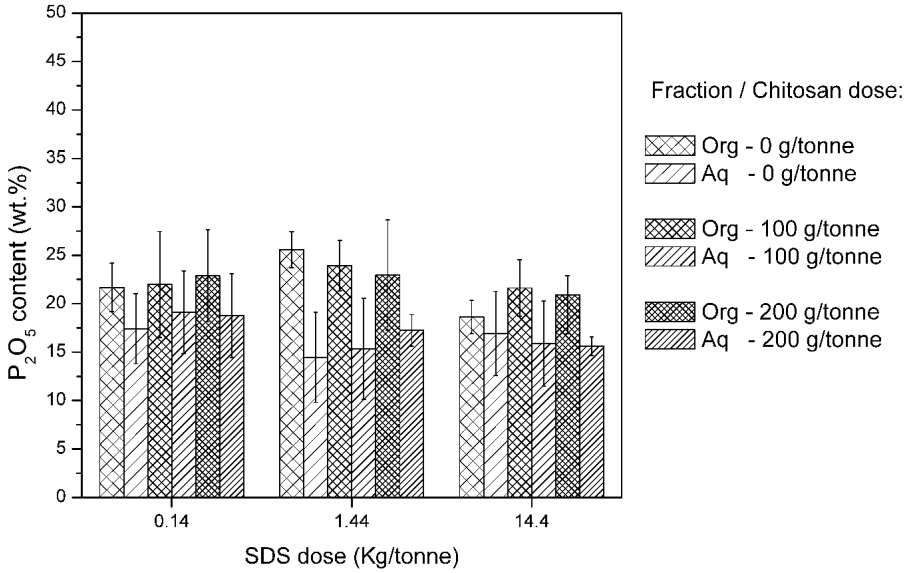

Figure 3.21: P_2O_5 content for the organic (Org) and the aqueous (Aq) fractions after liquid-liquid separation at pH = 5.5.

Additionally, Fig.3.22 shows that the effect of pH on the concentration of materials appears to be very small as the difference in P_2O_5 content between the organic and the aqueous fractions is rather similar to the ones reported at pH = 5.5 (shown in Fig.3.21), displaying the prevalence of 1.44 kg SDS/tonne as the dose with the largest difference in P_2O_5 concentration between the organic and the aqueous fractions.

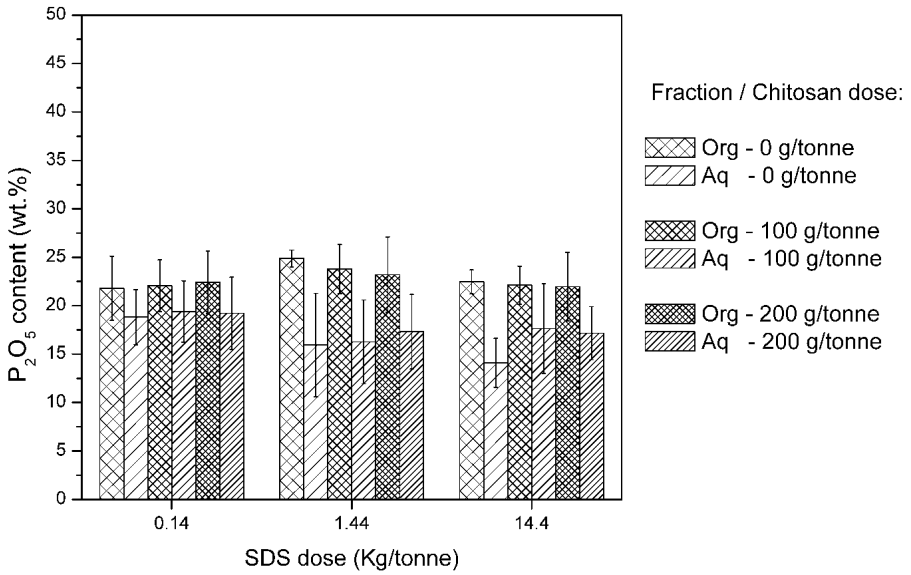

Figure 3.22: P_2O_5 content for the organic (Org) and the aqueous (Aq) fractions after liquid-liquid separation at pH = 4.0.

Finally, when the total amount of material captured is taken into account in conjunction with the P_2O_5 content of each fraction, results show that a dose of 1.44 kg SDS/tonne combined with a concentration of 100 g chitosan/tonne at either pH 5.5 or 4.0 will promote the highest overall efficiency of the separation process.

3.4 Separation of phosphate phases from H-Ash

When the separation technique was tested on H-Ash at pH = 5.5 (Fig.3.23), the results generally behave in a similar way as the combined sample of silicocarnotite and gehlenite. In spite of that, the amount of material retained is a little higher for H-Ash samples, having a maximum of 46.51%, 50.65% and 74.07% when the SDS content is 1.44 Kg/tonne and the chitosan content is 0 g/tonne, 100 g/tonne and 200 g/tonne, respectively.

At pH = 4.0, similar behaviors were observed. When no chitosan is added, the material retained in the organic fraction is rather low starting at 11.77% at 0.144 Kg SDS/tonne, and increases reaching a maximum -55.13%- as the SDS concentration is increased to 1.44 Kg/tonne and finally descends to 32.61% when 14.4 Kg SDS/tonne is used.

These results suggest the interaction of SDS-chitosan at 1.44 Kg SDS/tonne appears to positively affect the retention capacity at both the pH values tested, hinting that under these conditions, the critical aggregation concentration (CAC) is reached.

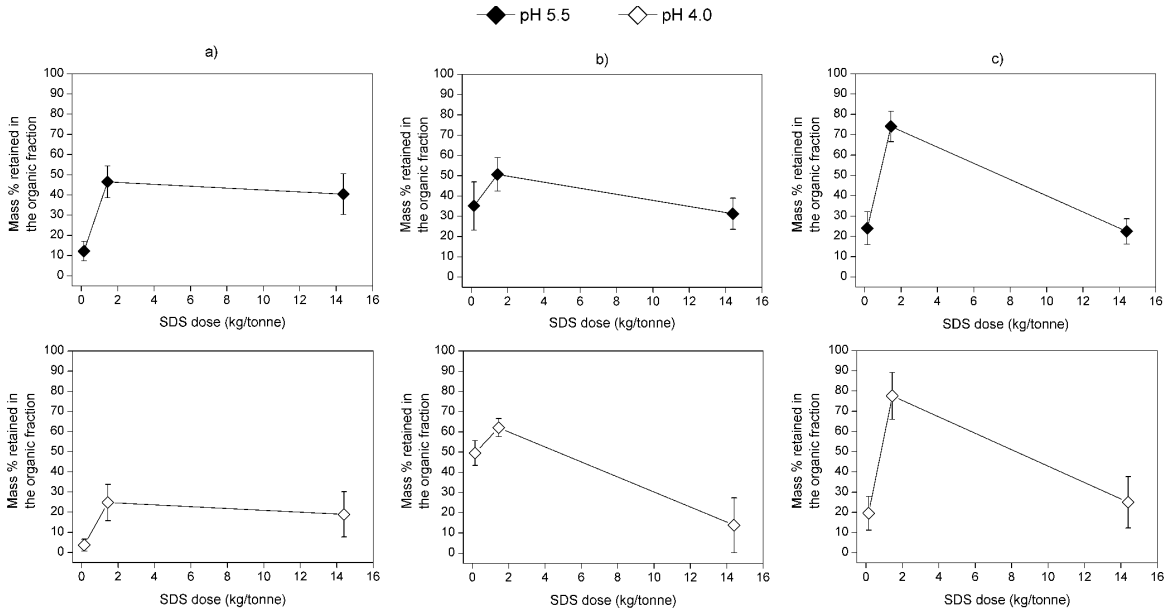

Figure 3.23: Amount of material retained in the organic fraction for H-Ash under different conditions.

As for the difference in P_2O_5 content between fractions (see Fig.3.24 and Fig.3.25), it was seen that the effectiveness of the separation process is greatly diminished, resulting in a very diffuse margin of enrichment (around 10%).

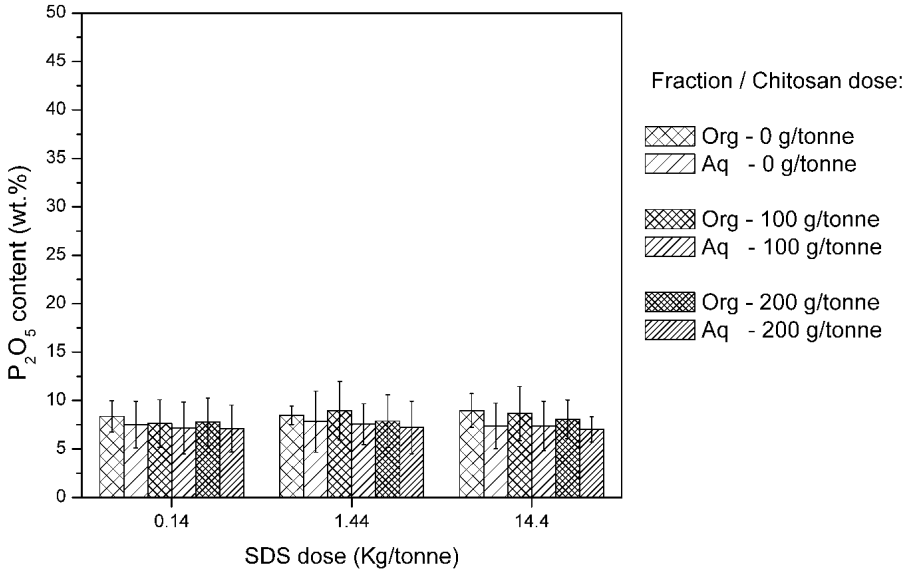

Figure 3.24: P_2O_5 content for the organic (Org) and the aqueous (Aq) fractions after separation of H-Ash at pH = 5.5.

This is probably due to the presence of Fe_2O_3, which accounts for 16% wt. of the original SSA (see Table 2.1). The reason could be the hematite (Fe_2O_3) particles remain combined within H-Ash grains, influencing the surface behavior as hematite particles are known to have positive zeta potential values (Parks, 1965). In that case, it is possible SDS is not only binding to silicocarnotite as desired, but also to the positively charged surface of Fe_2O_3-influenced *H-Ash*. This hypothesis could also explain why the material capture for H-Ash is relatively large, regardless of their phosphate content.

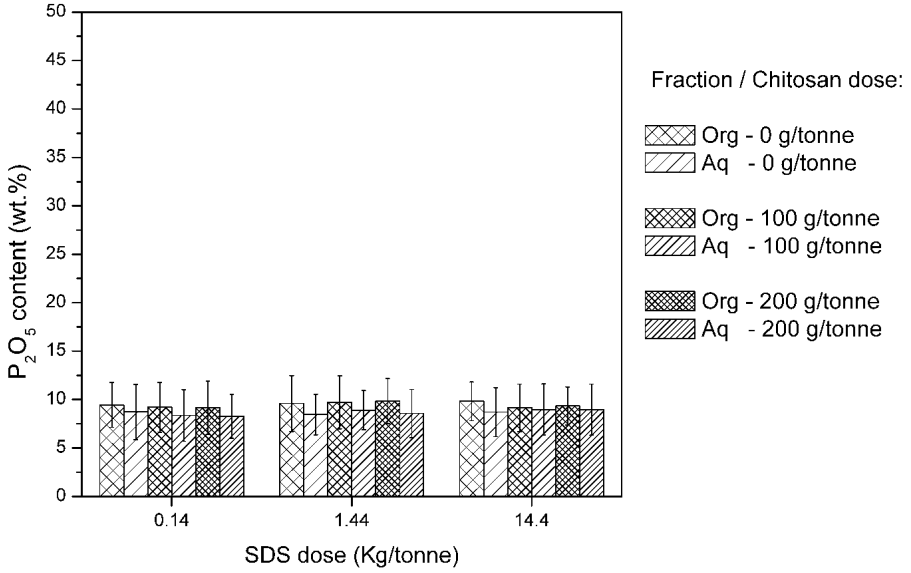

Figure 3.25: P_2O_5 content for the organic (Org) and the aqueous (Aq) fractions after separation of H-Ash at pH = 4.0.

3.5 Conclusions

Our results show the viability of promoting the simultaneous formation of silicocarnotite ($Ca_5(PO_4)_2SiO_4$) and gehlenite ($Ca_2Al_2SiO_7$) when stoichiometric amounts of raw materials react at 1300 °C, as our TG-DTA and XRD analyses indicated both phases are predominant under such conditions. Also, the feasibility of obtaining silicocarnotite and gehlenite *simultaneously* using SSA and $Ca(OH)_2$ as precursors was also demonstrated via the preparation of the material we called "H-Ash".

In terms of the surface properties of the prepared materials, the zeta potential of silicocarnotite is negative at pH values higher than 6, and the estimated point of zero charge was found to occur at pH = 5.5. In a similar fashion, H-Ash was found to have the point of zero charge at pH = 6. Contrarily, our measurements suggested the zeta potential of gehlenite remains negative under the range pH = 2.5 to pH = 11.

As for the liquid-liquid separation process using kerosene and sodium dodecyl sulfate (SDS) our results indicated SDS promotes the clustering of silicocarnotite particles in the organic fraction, but it does not affect gehlenite in an appreciable manner.

Referring to the separation process, the most effective dose was found to be 1.44 Kg SDS/-tonne, attaining more than 70% of the original silicocarnotite captured in the organic fraction at pH 4.0. This particular result is interesting as it illustrates the effectiveness of using anionic surfactants for the capture of silicon-laden phosphates for physical separations.

On the other hand, it was shown that the effect of chitosan is to reduce the amount of silicocarnotite captured and to promote the agglomeration of gehlenite in the organic fraction, indicating the interaction between positively charged chitosan and negatively charged gehlenite is electrostatic in nature.

Additionally, when the separation process was tested on a blend composed of 1 part silicocarnotite and 1 part gehlenite (1:1 mixture), the results revealed it is possible to capture around 60% of the original material in the organic fraction if the separation is performed using a dose of 1.44 Kg SDS/tonne and if 100 g/tonne chitosan is added as an agglomeration aid. Further analysis on the obtained fractions determined that the P_2O_5 concentration (21.12%) in the organic fraction was approximately 2 times higher than the one found in the aqueous fraction (10.13%), indicating silicocarnotite (a P_2O_5 bearing material), was enriched by this separation technique.

Conversely, less conducive results were obtained when "H-Ash" was subjected to the separation process. Even though the capture of material in the organic phase remained consistent at values 46.51% (0 g/tonne chitosan), 50.65% (100 g/tonne chitosan) and 74.07% (200 g/tonne chitosan) for 1.44 Kg SDS/tonne at pH = 5.5, the difference in P_2O_5 content was reduced when compared to the results obtained for pure materials, resulting in a comparative yield staying in the vicinity of 10% on a relative basis. It is possible the high concentration of Fe_2O_3 originally found in the SSA is the reason for these results, as the Fe_2O_3 particles within the original SSA sample are notoriously small (see 2.10) and the zeta potential of iron oxides is often positive and close to the zeta potential of silicocarnotite, which could explain their interference during the separation.

Chapter 4

General Discussion

The current situation of scarcity and the increasing demand for phosphorus resources around the world make it necessary to find ways to recycle this element as much as possible, since there are several evidences pointing out that the ongoing process of mineral exploitation of phosphate rock resources is unsustainable in the long run and may lead to a critical situation of phosphorus shortage in the future. In this regard, the efforts made by reseachers aimed at the reuse of urban sources of phosphorus like Sewage Sludge Ash (SSA) have recently been gaining attention as the generation of waste in urban settings is constantly increasing due to overpopulation and migration to cities.

Then, recycling phosphorus from SSA is advantageous because access to this waste product is straightforward, as wastewater processing plants that rely on incineration for the final disposal of the wastewater sludge in urban settings already gather large amounts of SSA to comply with environmental regulations, and are actively looking out for alternatives for the disposal of SSA after processing. This is done in order to add value to an otherwise useful product that may go towards landfills or end up as a low-value filler for the cement industry if left untreated. In addition, the comparatively large amount of phosphates normally found in SSA (around 20%), makes it attractive as a target material for phosphorus recycling.

Considering that the current methods used for phosphorus recycling from SSA focus on the recovery of phosphate phases *only* suitable for the fertilizers industry, it is safe to say the main requirements for any phosphorus-laden species coming after the processing of SSA are: an acceptable soil-solubility for the phosphorus coming from SSA, and a low content of heavy metals for any solid coming from SSA, which can sometimes be found in large quantities in untreated SSA. As such, Section 1.7 presented an overview of the recent research trends in this topic, highlighting the methods that use thermochemical and leaching processes to comply with the aforementioned requirements.

Although these traditional methods are able to obtain a large amount of phosphorus from SSA, they may require large amounts of energy (as in the case of thermochemical methods), or the constant spending of chemical reagents (in the case of leaching/crystallization methods), that may reduce their sustainability and increase their cost if implemented on a large scale.

It follows that, even if the traditional methods are effective in recovering phosphorus from SSA, the downsides of high energy consumption, and the requirement of a large amount of chemicals are factors that needed to be improved by alternative ways for the processing of SSA. This is one of the reasons why the novel physical methods for phosphorus recovery from SSA, explained in Chapter 2 and Chapter 3 are presented in this work. Hence, the author considers the developed techniques to be useful as alternatives for the traditional methods, and to be suitable as contributions to the scientific community in terms of exploring the performance of physical methods that do not rely on high temperatures or a large dosage of reagents for the purpose of recovering phosphorus from SSA.

In this regard, Chapter 2 presented the case for a physical separation method where the magnetic properties of the iron present in SSA are utilized. This approach is promising since iron oxides are almost always detected in SSA as remnants coming from the iron salts commonly used for the treatment process of urban wastewater, and any method that is sufficiently effective for iron removal could be extremely useful for SSA processing. For example, once the iron content is reduced, any other traditional technique (e.g. acid leaching) could be implemented avoiding the dissolution of iron ions, which are usually considered as interferences in solution.

This way, the method presented in Chapter 2, which is the recovery of phosphorus from SSA using a carbothermic reaction followed by High Gradient Magnetic Separation and Flotation, introduced the contribution of a novel approach that takes advantage of the magnetic properties of iron for its capture and separation from SSA, and then is followed by the enrichment of the *non-magnetic fraction* in terms of phosphorus content using a flotation process.

Our results showed that the direct capture of iron particles from SSA is a rather difficult feat since the iron atoms initially present in the SSA are in the crystalline phase of hematite (Fe_2O_3), which is not very magnetic and can only achieve a small percentage of capture when subjected to a physical separation process using magnetization (for example HGMS separation). This is the reason why the thermal treatment of carbothermic reduction was proposed, in order to achieve the chemical reduction of hematite to the more magnetic magnetite (Fe_3O_4), resulting in an overall increase (around 60% more than the original) in the magnetization value of iron in SSA.

Similarly, as the requirements for nutrient bioavailability from the fertilizer industry demand phosphorus to be in a soil-soluble phase, it was shown in Section 2.3 that the addition of Fe_2O_3 to SSA prior to carbothermic reduction promotes the formation of the phase of *stanfieldite* ($Ca_3Mg_3(PO_4)_4$), which has been shown to have good soil-solubility properties (Schnug and De Kok, 2016). In general terms, this is favorable since it not only implies the improvement of the magnetization properties of hematite through magnetite, but also ensures the formation of a soil-soluble mineral phase for phosphorus, overall resulting in an "enhanced SSA" with larger magnetization and higher phosphorus soil-solubility.

In order to separate the products from "enhanced SSA", the physical method of flotation was proven useful as there was an enrichment in terms of phosphorus content when the "non-magnetic" fraction was treated. Here, the results suggested that carrying out the physical separation using flotation at a high pH (pH = 10), leads to phosphorus being more concentrated in the froth (around 19% more concentrated) when compared to the tailings. This indicates that once the "enhanced SSA" is prepared, increasing the concentration of the phosphate species can be achieved using only a physical method, reducing the need for further chemical processing.

Therefore, the process flow diagram presented in Fig.4.1 illustrates the flow of a potential implementation of the method proposed in Chapter 2, suitable for incineration facilities capable of heating materials at temperatures close to 700°C.

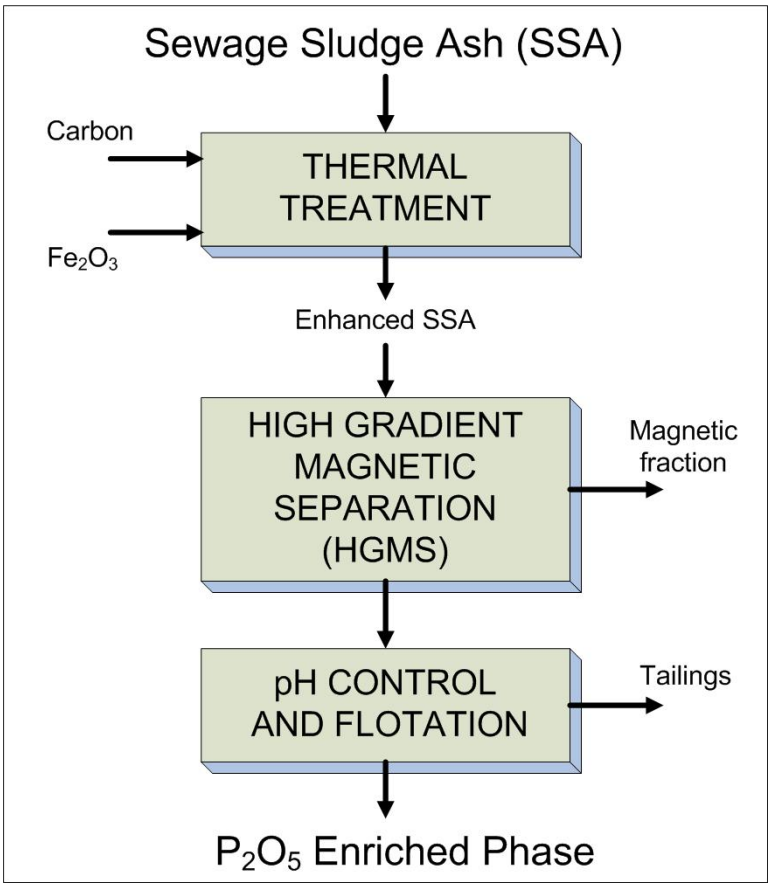

Figure 4.1: Proposed process diagram for Method 1

Even though the overall yield in terms of phosphorus is comparatively low (around 30% of the original phosphorus is recovered), it is thought this method could be easily implemented as a pre-treatment option for SSA samples containing large amounts of iron oxides in their composition, and still be useful for interested parties dealing with processing and disposal of SSA.

On the other hand, because the thermochemical processing of SSA could be a viable option for installations able to heat SSA (Ohtake and Okano, 2015), Chapter 3 presented the case for a processing method involving the simultaneous formation of the soil-soluble phase of *silicocarnotite* ($Ca_5(PO_4)_2SiO_4$) and the aluminum phase of *gehlenite* ($Ca_2Al(AlSiO_7)$) through a one-step thermochemical transformation.

Hence, the results presented in Section 3.3 showed that it is possible to promote the simultaneous formation of the soil-soluble (Anderson et al., 1992) phosphate phase of *silicocarnotite* ($Ca_5(PO_4)_2SiO_4$), and the aluminosilicate phase *gehlenite* ($Ca_2Al(AlSiO_7)$), when stoichiometric amounts of pure reactants react at 1300 °C. This highlights the feasibility of "stripping out" the aluminum initially combined with phosphorus in SSA (e.g as $AlPO_4$), and "relocating it" as an aluminosilicate in gehlenite ($Ca_2Al(AlSiO_7)$). Incidentally, these results also pointed out that this process will cause phosphate to combine with silicon and calcium forming a crystal phase considered to be more favorable (Akiyama, 1988) in terms of bioavailability for crops.

Accordingly, the process of obtaining silicocarnotite and gehlenite using SSA and $Ca(OH)_2$ as precursors was also demonstrated via the preparation of "H-Ash" (heated ash) in Section 1.6.2, where the main phases of *silicocarnotite and gehlenite* were detected at 1300 °C as expected. In this case, the addition of a low cost reagent like $Ca(OH)_2$ should be suitable for the implementation of the process at a large scale, as this reagent is commonly used in many industrial processes as "slaked lime" (Oates, 2010).

Since our results (see Section 3.3.3) also showed that there are notorious differences in the surface behavior (based on zeta potential measurements) between *silicocarnotite* and *gehlenite* when the pH value is in the range pH = 4 to pH = 6, the author considers that other physical processes, which could be practical for the enrichment of silicocarnotite could be employed; as it follows that any physical separation based on the differences of surface charge for these two materials may me effective for separation.

In line with the observations made for zeta potential, this work focused on the physical process of liquid-liquid separation using kerosene and sodium dodecyl sulfate (SDS), presenting the results in Section 3.3.4. In this case, the anionic nature of SDS promoted the clustering of silicocarnotite in the organic fraction, without affecting the negatively charged gehlenite in an appreciable manner. Hence, the P_2O_5 concentration in the organic fraction (21.12%) was approximately 2 times the value of the P_2O_5 concentration found in the aqueous fraction (10.13%), indicating that silicocarnotite was enriched via a physical method in the organic fraction by the technique proposed. In addition, since the separation was carried out based on the differences of surface charge for the materials, it is proposed that facilities could for example, perform the physical process of anionic flotation for silicocarnotite/gehlenite mixtures to enrich the concentration of silicocarnotite in the froth.

However, less conducive results were obtained when "H-Ash" was subjected to the same liquid-liquid separation process. In this case, even though the capture of material in the organic phase remained consistent (between 45 - 75 %) at pH = 5.5, the difference in P_2O_5 content between the *organic* and the *aqueous* fractions was not so noticeable, staying in the vicinity of 10% on a relative basis.

In order to improve the difference in P_2O_5 content between the fractions, the author suggests that the separation method should be carried out in a sequential manner, using a series of mixing stages as it is common practice (Müller et al., 2008) for installations working with liquid-liquid separation. Also, as silicocarnotite particles are not dissolved, but only bound physically to the organic solvent (kerosene), it should be possible to recycle the organic solvent after each cycle of separation as shown in Fig.4.2, where a proposed flow diagram for the overall process described in Chapter 3 is presented.

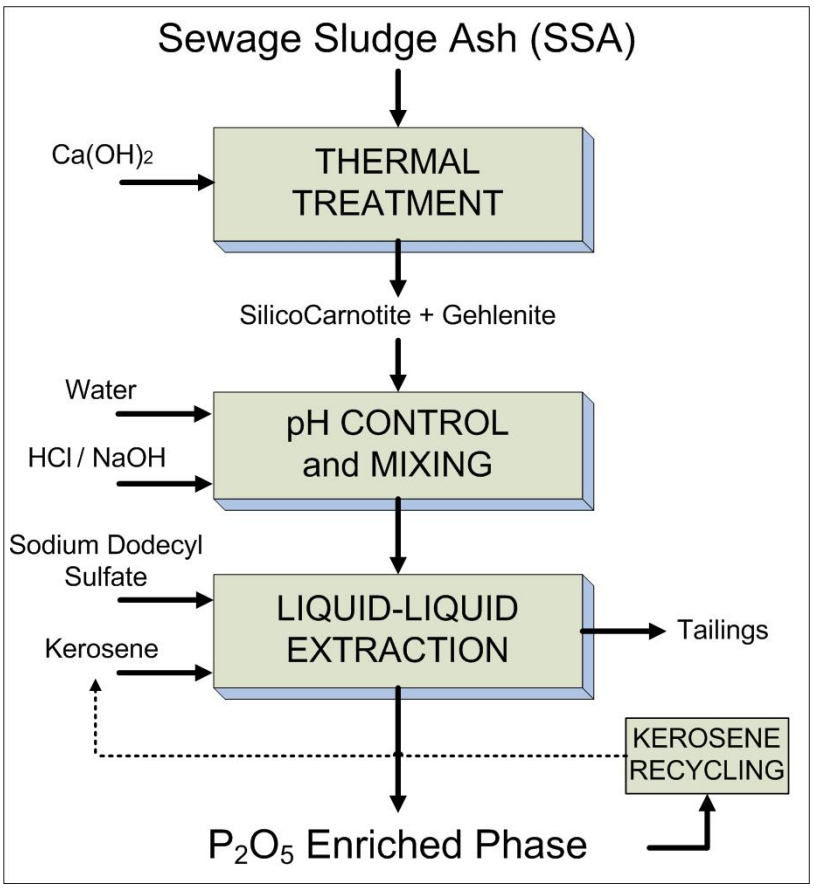

Figure 4.2: Proposed process diagram for Method 2

Nonetheless, considering that the magnetic separation method presented in Chapter 2 introduced a process for the removal of iron in SSA, it might be possible to combine this approach as a "pretreatment" before performing heat treatment followed by liquid-liquid separation. In this case, the best way would be to heat SSA at 680 °C using carbon, subject the mixture to HGMS separation and after that, use the heating treatment at 1300 °C using $Ca(OH_2)$ for the "non-magnetic rich fraction" to obtain the target phases of *silicocarnotite* and *gehlenite* simultaneously. Accordingly, the last step could be the liquid-liquid separation which will benefit from the reduced amount of Fe_2O_3 found in the "non-magnetic rich fraction", and thus achieve a higher phosphorus recovery.

Consequently, it is suggested that any given SSA can undergo thermal treatment and this way modify its phosphate phase to obtain *silicocarnotite* and likewise, modify its aluminum phase to obtain gehlenite, making possible the physical separation process shown in Fig.4.2 and yield an "organic fraction" enriched in phosphorus content, useful for the industry of fertilizers.

In order to compare the traditional methods for SSA processing to the two original methods introduced lines above, Table 4.1 was prepared. This table shows that traditional methods like thermochemical processing and leaching have rather high "yields in terms of phosphorus recovery", whereas physical methods are comparatively less effective in this case.

Table 4.1: Comparison[†] of traditional methods for phosphorus recovery from SSA and the methods presented in this work

	Yield	Soil solubility	Energy demand	Reagent demand	Impact on the environment due to byproducts	Current state of development
Thermochemical methods	High (∼70%) (Mattenberger et al., 2008)	High (Herzel et al., 2016)	High (1000-2000 °C) (Petzet et al., 2012)	Low (Chloride salts)(Rapf, 2012)	Yes (Volatile metal chlorides) (Adam et al., 2009)	Pilot plant (Rapf, 2012)
Leaching methods	High (70-90%) (Donatello et al., 2010)	High (∼90%) (Fang et al., 2018)	Low (T = 30°C)(Biswas et al., 2009)	High ($CaCl_2$, HCl) (Liu and Qu, 2016)	High (Disposal of acidic waste)(Fang et al., 2020)	Pilot plant (Fang et al., 2020)
Other methods	Medium (∼60%) (Guedes et al., 2016)	High (Ebbers et al., 2015)	High (50mA for 7 days) (Ottosen et al., 2014)	Medium (Guedes et al., 2014)	Low (Ottosen et al., 2014)	Lab scale (Ebbers et al., 2015)
Carbothermic reaction followed by High Gradient Magnetic Separation and Flotation (Chapter 2)	Low (∼20%)	High (Adam et al., 2009)	Medium (HGMS, Flotation cell)	Low (Physical methods)	Low (no residue for HGMS, only surfactants for flotation)	Lab scale
Heat treatment and liquid-liquid separation (Chapter 3)	Low (∼10%)	High (Karapetyan et al., 2005)	High (1200-1300 °C)	Low (Physical methods)	Low (no residue for heating, only surfactants for liquid separation)	Lab scale

[†]Table prepared considering the data available in the literature for traditional methods. Soil solubility for the separation methods presented in Chapter 2 and Chapter 3 is based on data from literature references describing similar materials, and is expressed using the citrate-solubility protocol for phosphates shown in Appendix C.

Regardless, it can be argued that there are several advantages of using the physical methods of this work. The first advantage is to have a low demand of reagents, as the processing methods only use physical properties like magnetization and surface charge to attain the recovery of phosphorus. This implies a second advantage, since the methods presented practically do not

generate byproducts as the few reagents required are only used to change the magnetization of SSA and to improve the soil solubility of the phosphate phase in the case of the method presented in Chapter 2; and likewise to promote the formation of silicocarnotite (considered to have good soil solubility) for the technique introduced in Chapter 3.

Another point that could be considered advantageous is the relatively low requirement of energy for both methods when compared to the thermochemical methods. Here, the carbothermic reaction presented in Chapter 2 is particularily attractive as the temperature required for this transformation is less than 700 °C. Conversely, the temperature of 1300 °C required for the heat treatment presented in Chapter 3 is less favorable, as it represents a smaller benefit when compared to traditional thermochemical reactions which are known to require temperatures in the range 1000 - 2000 °C.

In terms of "yield", defined in this document as the percentage of phosphorus being recovered from SSA which can be useful for fertilizers (see Section 1.7); the major downside of using physical methods is the comparatively low value of "yield" obtained for phosphorus concentrations. Conversely, traditional techniques have an advantage as their reported yields for recovery are in the range 60 - 90 %, whereas the present research work achieved yields in the range 10 - 20 %. Nonetheless, the author considers this could be improved if the physical methods could be applied sequentially several times in order to maximize the capture of unwanted elements, and improve the concentration of phosphorus in the froth for the flotation process presented in Fig.4.1, and the concentration of silicocarnotite in the organic fraction for the method outlined in Fig.4.2.

Considering that the direct utilization of recovered phosphate using any available technique requires careful evaluation due to the risk of unwanted heavy metals that may still be present in the solids, it is important to mention that, although the original SSA had a comparatively low percentage of heavy metals (see Table 2.1), the solids obtained by the methods presented in this work may still have the presence of unwanted elements (namely Cu, Zn, Cr and Ni).

However, it might be possible to use the products recovered as an auxiliary source of phosphorus, meaning that it could be possible to combine traditional phosphate fertilizers with a percentage (e.g. 20-30%) of the product recovered from SSA. This way, treated SSA could serve as a supplementary source of phosphate and still be able to comply with the current regulations guiding the application of phosphate fertilizers in Japan, which in general terms (Herawati et al., 2000; K.Kumazawa, 1997; Ministry of Agriculture Forestry and Fisheries (MAFF), 2018; Zunaidi et al., 2020) indicate the set limit for Zn content to be less than 1800 mg/Kg, for Cu to be less than 600 mg/Kg, whereas the limit for Cr content is to be a maximum of 0.05% for each 1.0% of P_2O_5 and Ni content to be a maximum of 0.005% for each 1.0 % of P_2O_5.

In summary, Chapters 2 and 3 of this research work presented two alternative methods based on the use of physical separation techniques, which can constitute ways to obtain supplementary phosphorus from a recycled material like SSA and be of use for the implementation in incineration facilities; being these results suggested as incremental improvements in the research field of phosphorus recycling from SSA.

Final remarks and future prospects

The processing methods presented in this work are aimed at the improvement of the current state of the art on the recovery of phosphorus from SSA and constitute alternatives for interested entities (e.g. urban sewage management organizations, recycling companies) currently running incineration plants for the final treatment of sewage streams.

Using HGMS and flotation as shown in Method 1 and using liquid-liquid separation as shown in Method 2, introduced the possibility of including physical separations for phosphorus recovery and could be employed as *pre-treatment steps* for the enrichment of phosphorus used at treatment installations concerned with the environmental impact of using traditional techniques.

Appendices

Appendix A

Table A.1: Common sources of dietary phosphorus. Adapted from Noori et al. (2010)

Source		**Serving**	**Phosphorus [mg]**	**Phosphorus-Protein ratio [mg/g]**	**Gastro-intestinal Absorption [%]**
Animal protein					
	Milk, skim	8 ounces	247	29	40 to 60
	Yogurt, plain		385	27	40 to 60
	Cheese		131	20	40 to 60
	Egg	1 large	86	14	40 to 60
	Beef (cooked)		173	7	40 to 60
	Chicken	3 ounces	155	8	40 to 60
	Turkey	3 ounces	173	8	40 to 60
	Fish, halibut	3 ounces	242	9.3	40 to 60
	Fish, salmon	3 ounces	282	13.4	40 to 60
Vegetarian protein					
	Bread, whole wheat	1 slice	57	Varies	10 to 30
	Bread, enriched white	1 slice	25	Varies	10 to 30
	Almonds	12 ounces	134	23	10 to 30
	Peanuts	1 ounce	107	15	10 to 30
	Lentils (cooked)	Half a cup	178	20	10 to 30
	Chocolate	1.4 ounces	142 to 216	27	10 to 30
Inorganic/Preservatives					
	Carbonated cola drink	12 ounces		Not applicable	80 to 100

Appendix B

The concept of *carbon equivalent* (C_{eq}) defined in this text refers to the ratio of carbon added to each mixture compared to the amount of carbon theoretically required to achieve the reduction of Fe_2O_3 to metallic iron via the following reactions:

$$3\,Fe_2O_3 + C \longrightarrow 2\,Fe_3O_4 + CO \tag{B.1}$$

$$Fe_3O_4 + 4\,CO \longrightarrow 3\,Fe + 4\,CO_2 \tag{B.2}$$

Therefore, the value of C_{eq} is:

$$Ceq = \frac{C_{\text{added}}}{C_{\text{theoretical}}} \tag{B.3}$$

where C_{added} refers to the amount of C added to the mix in g, and $C_{\text{theoretical}}$ refers to the theoretical amount of C required in g. Then, since the Fe_2O_3 content in SSA was found to be approximately 16.5 g Fe_2O_3, it follows that:

$$Ceq = \frac{C_{\text{added}}}{3.3} \tag{B.4}$$

which is the final equation used for the calculation of C_{eq} used in the text.

Appendix C

In order to determine the agronomic performance, and to establish the effective bioavailability of phosphorus in fertilizers, the parameter of "soil solubility" of phosphorus is commonly used. This solubility is normally considered a proxy for the simulation of the extraction ability of plant roots in terms of phosphate uptake via the rhizome (Santos et al., 2019). In this light, the typical assessment for phosphate availability from a given fertilizer is carried out using a solution of neutral ammonium citrate to extract phosphorus from the solid, and then use this liquid to fertilize a series of plants. Naturally, the study of dependent and independent variables is arranged using an experimental design (for example, factorial design) to obtain reliable results (Prochnow et al., 1998; Rafael et al., 2018; Santos et al., 2019).

For reference, a summarized version of the protocol for the determination of citrate-soluble phosphorus via the ammonium vanadomolybdate absorptiometric method, described by the Ministry of Agriculture, Forestry and Fisheries (Kimura, 2016) is presented below.

Method for the determination of citrate-soluble phosphoric acid, using the ammonium vanadomolybdate absorptiometric analysis

Summary:

This test method is applicable to the fertilizers that do not contain the matter not colored by the hydrolysis with nitrate acids such as phosphonic acid. Extract by adding a citric acid solution to an analytical sample. Heat after adding nitric acid (1+1), hydrolyze non-orthophosphoric acid to orthophosphate ion and measure the absorbance of phosphovanadomolybdate salt formed by the reaction with ammonium vanadate (V), hexaammonium heptamolybdate and nitric acid to obtain citrate soluble phosphoric acid (C-P_2O_5) in an analytical sample.

Reagents:

- Nitric acid: A JIS Guaranteed Reagent (HNO_3 60 % (mass fraction)) specified in JIS K8541 or a reagent of equivalent quality.
- Citric acid solution[(1)]: Dissolve 20 g of citric acid monohydrate specified in JIS K8283 in water to make 1000 mL.
- Coloring reagent solution[(1),(2)]: Dissolve 1.12 g of ammonium vanadate (V)[(3)] specified in JIS K8747 in water, add 150 mL of nitric acid, then add 50 g of hexaammonium heptamolybdate tetrahydrate[(4)] specified in JIS K8905 while dissolving in water, and further add water to make 1000 mL[(5)].

[(1)] This is an example of preparation; prepare an amount as appropriate.
[(2)] This corresponds to reagent "b" solution in the Official Methods of Analysis of Fertilizers (1992).
[(3)] This corresponds to ammonium metavanadate in the Official Methods of Analysis of Fertilizers (1992).
[(4)] This corresponds to ammonium molybdate in the Official Methods of Analysis of Fertilizers (1992).
[(5)] Store in an amber bottle. However the reagent solution does not tolerate long term preservation.

- Phosphoric acid standard solution (P_2O_5 10 mg/mL)[(1)]: Heat potassium dihydrogen phosphate specified in JIS K9007 at 105 °C ± 2 °C for about 2 hours, let it stand to cool in a desiccator, and weigh 19.17 g to a weighing dish. Dissolve with a small amount of water, transfer to a 1000 mL volumetric flask, add 2 mL - 3 mL of nitric acid, and add water up to the marked line.
- Phosphoric acid standard solution (P_2O_5 0.5 mg/mL)[(1)]: Transfer 50 mL of phosphoric acid standard solution (P_2O_5 10 mg/mL) to a 1000 mL volumetric flask, add 2 mL - 3 mL of nitric acid, and add water up to the marked line.

Instruments:

- Constant-temperature rotary shaker: A constant-temperature rotary shaker that can rotate a 250 mL volumetric flask, set up in a thermostat adjustable to 30 °C ± 1 °C,upside down at 30 - 40 revolutions/min.
- Hot plate: A hot plate whose surface temperature can be adjusted up to 250 °C.
- Spectrophotometer: A spectrophotometer specified in JIS K0115.

Procedures:

- Extraction: Conduct extraction as shown below.
  - Weigh 1 g of an analytical sample to the order of 1 mg, and put it in a 250 mL volumetric flask.
  - Add 150 mL of citric acid solution heated up to about 30 °C, and shake to mix at 30 - 40 revolutions/min (30 °C ± 1 °C) for 1 hour.
  - After standing to cool, add water up to the marked line.
  - Filter with Type 3 filter paper to make the sample solution.
- Coloring: Conduct coloring as follows:
  - Transfer a predetermined amount (the equivalents of 0.5 mg - 6 mg as P_2O_5 and no more than the equivalents of 17 mL of the citric acid solution) of the sample solution to a 100-mL tall beaker.
  - Add the citric acid solution to make the equivalents of 17 mL of the citric acid solution (20 mg/mL).
  - Add 4 mL of nitric acid (1+1)[(6)], and heat to boil[(7)].
  - After standing to cool, transfer to a 100 mL volumetric flask with water[(8)].
  - Add 20 mL of coloring reagent solution, and further add water up to the marked line, and then leave at rest for about 30 minutes.
- Measurement: Conduct measurement according to JIS K0115 and as shown below. Specific measurement procedures are according to the operation method of the spectrophotometer used in measurement.

[(6)] When the solution is muddled by adding nitric acid (1+1), conduct centrifugation after the last procedure.

[(7)] When it does not contain non-orthophosphate, the boil operation is not necessary.

[(8)] The volume of the solution after transferring should be up to about 60 mL.

- Measurement conditions for the spectrophotometer: Set up the measurement conditions for the spectrophotometer considering the detection wavelength equal to 420 nm.
- Calibration curve preparation:
  * Transfer 1 mL - 12 mL of phosphoric acid standard solution (P_2O_5 0.5 mg/mL) to 100 mL volumetric flasks step-by-step.
  * Add 17 mL of citric acid solution, then add 4 mL of nitric acid (1+1), further add a proper amount of water[9] and conduct the same procedure to make the P_2O_5 0.5 mg/100 mL - 6 mg/100 mL phosphoric acid standard solution for the calibration curve preparation.
  * Conduct the same procedures as the previous step for another 100 mL volumetric flask to make the blank test solution for the calibration curve preparation.
  * Measure absorbance at a wavelength of 420 nm of the phosphoric acid standard solutions for the calibration curve preparation using the blank test solution for the calibration curve preparation as the control[10].
  * Prepare the calibration curve of the phosphoric acid concentration and absorbance of the phosphoric acid standard solutions for the calibration curve preparation.
- Sample measurement:
  * Regarding the solution at the last step of coloring, measure the absorbance by the same procedure as the measurement of absorbance for phosphoric acid standard at a wavelenght of 420 nm[10].
  * Obtain the phosphoric acid (P_2O_5) content from the calibration curve, and calculate citrate soluble phosphoric acid (C-P_2O_5) in the analytical sample.

[9] If no water is added, precipitate is produced in some cases when a coloring reagent solution is added.
[10] Measure within 2 hours after adding the coloring reagent solution.

References

Acelas, N. Y., López, D. P., Wim Brilman, D. W., Kersten, S. R., and Kootstra, A. M. J. 2014. Supercritical water gasification of sewage sludge: Gas production and phosphorus recovery. *Bioresource Technology* 174:167–175. https://doi.org/10.1016/j.biortech.2014.10.003.

Adam, C., Peplinski, B., Michaelis, M., Kley, G., and Simon, F. G. 2009. Thermochemical treatment of sewage sludge ashes for phosphorus recovery. *Waste Management* 29(3):1122–1128. https://doi.org/10.1016/j.wasman.2008.09.011.

Akiyama, T. 1988. Calcination Reaction of Brazilian Aluminum Phosphate Ore with Calcium Carbonate. *Japanese Journal of Soil Science and Plant Nutrition* 59(3):260–265. https://doi.org/10.20710/dojo.59.3_260.

Amann, A., Zoboli, O., Krampe, J., Rechberger, H., Zessner, M., and Egle, L. 2018. Environmental impacts of phosphorus recovery from municipal wastewater. *Resources, Conservation and Recycling* 130(December 2017):127–139. https://doi.org/10.1016/j.resconrec.2017.11.002.

Amrullah, A. and Matsumura, Y. 2018. Supercritical water gasification of sewage sludge in continuous reactor. *Bioresource Technology* 249(September 2017):276–283. https://doi.org/10.1016/j.biortech.2017.10.002.

Anderson, D. L., Snyder, G. H., and Warren, J. D. 1992. Availability of phosphorus in calcium silicate slag. *Communications in Soil Science and Plant Analysis* 23(9-10):907–918. https://doi.org/10.1080/00103629209368638.

Angelova, V., Ivanova, R., Delibaltova, V., and Ivanov, K. 2004. Bio-accumulation and distribution of heavy metals in fibre crops (flax, cotton and hemp). *Industrial Crops and Products* 19(3):197–205. https://doi.org/10.1016/j.indcrop.2003.10.001.

Arrhenius, G., Sales, B., Mojzsis, S., and Lee, T. 1997. Entrophy and charge in molecular evolution - the case of phosphate. *J. theor. Biol.* 187:503–522.

Asano, T. 2007. *Water reuse : issues, technologies, and applications.* McGraw-Hill, New York.

Askiitians.com. 2020. Allotropes of phosphorus with physical properties. Available at: `https://files.askiitians.com/cdn1/images/2017125-182154602-1807-1-phosphorus-allotropic-forms.jpg`.

Averbuch-Pouchot, M.-T. and Durif, A. 1996. *Topics in Phosphate Chemistry.* WORLD SCIENTIFIC. https://doi.org/doi:10.1142/3076.

Bailey, R. 2019. Learn about nucleic acids and their function. Available at: `https://www.thoughtco.com/nucleic-acids-373552`.

Barrett, R. L. and Mccaughey, W. J. 1942. The System CaO-SiO_2-P_2O_5. *American Mineralogist* 27(10):680–695. http://dx.doi.org/.

Bhattacharjee, S. 2016. DLS and zeta potential - What they are and what they are not? *Journal of Controlled Release* 235:337–351. https://doi.org/10.1016/j.jconrel.2016.06.017.

Biswas, B. K., Inoue, K., Harada, H., Ohto, K., and Kawakita, H. 2009. Leaching of phosphorus from incinerated sewage sludge ash by means of acid extraction followed by adsorption on orange waste gel. *Journal of Environmental Sciences* 21(12):1753–1760. https://doi.org/http://dx.doi.org/10.1016/S1001-0742(08)62484-5.

Bogaard, A., Fraser, R., Heaton, T. H. E., Wallace, M., Vaiglova, P., Charles, M., Jones, G., Evershed, R. P., Styring, A. K., Andersen, N. H., Arbogast, R.-M., Bartosiewicz, L., Gardeisen, A., Kanstrup, M., Maier, U., Marinova, E., Ninov, L., Schäfer, M., and

Stephan, E. 2013. Crop manuring and intensive land management by Europe's first farmers. *Proceedings of the National Academy of Sciences* 110(31):12589 LP – 12594. https://doi.org/10.1073/pnas.1305918110.

Bolsover, S., Hyams, J., and Shepard, E. 2003. Energy Trading within the Cell. In *Cell Biology*, Wiley Online Books, pages 257–280. https://doi.org/doi:10.1002/047146158X.ch12.

Bongaarts, J. 2016. Development: Slow down population growth. *Nature* 530(7591):409–412. https://doi.org/10.1038/530409a.

Borsa, R., Freche, M., Cosmeleata, G., Lacout, J.-L., and Ciuca, S. 2008. *High temperature preparation of silicon containing apatite*, volume 70.

Botelho, C. M., Lopes, M. A., Gibson, I. R., Best, S. M., and Santos, J. D. 2002. Structural analysis of Si-substituted hydroxyapatite: zeta potential and X-ray photoelectron spectroscopy. *Journal of Materials Science: Materials in Medicine* 13(12):1123–1127. https://doi.org/10.1023/A:1021177601899.

Brow, R. K. 2000. Review: the structure of simple phosphate glasses. *Journal of Non-Crystalline Solids* 263:1–28. https://doi.org/10.1016/S0022-3093(99)00620-1.

Buehler, M. J. 2007. Molecular nanomechanics of nascent bone: Fibrillar toughening by mineralization. *Nanotechnology* 18(29). https://doi.org/10.1088/0957-4484/18/29/295102.

Bulina, N. V., Chaikina, M. V., Gerasimov, K. B., Ishchenko, A. V., and Dudina, D. V. 2016. A novel approach to the synthesis of silicocarnotite. *Materials Letters* 164:255–259. https://doi.org/10.1016/j.matlet.2015.10.047.

Chandrajith, R. and Dissanayake, C. 2009. Phosphate mineral fertilizers, trace metals and human health. *Journal of the National Science Foundation of Sri Lanka* 37(3):153. https://doi.org/10.4038/jnsfsr.v37i3.1219.

Chang, A. R. and Anderson, C. 2017. Dietary Phosphorus Intake and the Kidney. *Annual Review of Nutrition* 37(1):321–346. https://doi.org/10.1146/annurev-nutr-071816-064607.

Chang, Y., Cho, B., Kim, S., and Kim, J. 2019. Direct conversion of fibroblasts to osteoblasts as a novel strategy for bone regeneration in elderly individuals. *Experimental & Molecular Medicine* 51(5):54. https://doi.org/10.1038/s12276-019-0251-1.

Chen, L., Yang, R., Guan, C., Zeng, J., Shao, Y., and Huang, L. 2016. Enhanced pulsating HGMS of fine hematite with combinative rod matrix. *Separation Science and Technology* 51(3):564–568. https://doi.org/10.1080/01496395.2015.1088871.

Chen, M. and Graedel, T. E. 2016. A half-century of global phosphorus flows, stocks, production, consumption, recycling, and environmental impacts. *Global Environmental Change* 36:139–152. https://doi.org/10.1016/j.gloenvcha.2015.12.005.

Chen, W., Chang, A. C., and Wu, L. 2007. Assessing long-term environmental risks of trace elements in phosphate fertilizers. *Ecotoxicology and Environmental Safety* 67(1):48–58. https://doi.org/10.1016/j.ecoenv.2006.12.013.

Chen, X., Karpukhina, N., Brauer, D. S., and Hill, R. G. 2017. High chloride content calcium silicate glasses. *Physical Chemistry Chemical Physics* 19(10):7078–7085. https://doi.org/10.1039/c6cp07905a.

Cheremisinoff, N. P. 2002. Chapter 12 - Treating the Sludge. Butterworth-Heinemann, Woburn, pages 496–600. https://doi.org/https://doi.org/10.1016/B978-075067498-0/50015-2.

Childers, D. L., Corman, J., Edwards, M., and Elser, J. J. 2011. Sustainability Challenges of Phosphorus and Food: Solutions from Closing the Human Phosphorus Cycle. *BioScience* 61(2):117–124. https://doi.org/10.1525/bio.2011.61.2.6.

Cooper, J., Lombardi, R., Boardman, D., and Carliell-Marquet, C. 2011. The future distribution and production of global phosphate rock reserves. *Resources, Conservation and Recycling* 57:78–86. https://doi.org/http://dx.doi.org/10.1016/j.resconrec.2011.09.009.

Cordell, D. and Neset, T. S. S. 2014. Phosphorus vulnerability: A qualitative framework for assessing the vulnerability of national and regional food systems to the multidimensional stressors of phosphorus scarcity. *Global Environmental Change* 24(1):108–122. https://doi.org/10.1016/j.gloenvcha.2013.11.005.

Cordell, D., Drangert, J. O., and White, S. 2009. The story of phosphorus: Global food security and food for thought. *Global Environmental Change* 19(2):292–305. https://doi.org/10.1016/j.gloenvcha.2008.10.009.

Cordell, D. and White, S. 2015. Tracking phosphorus security: indicators of phosphorus vulnerability in the global food system. *Food Security* 7(2):337–350. https://doi.org/10.1007/s12571-015-0442-0.

Córdova Udaeta, M., Dodbiba, G., Ponou, J., Sone, K., and Fujita, T. 2017. Recovery of phosphorus from Sewage Sludge Ash (SSA) by heat treatment followed by high gradient magnetic separation and flotation. *Advanced Powder Technology* 28(3):755–762. https://doi.org/10.1016/j.apt.2016.11.023.

Cornish, P. S. 2009. Research directions: Improving plant uptake of soil phosphorus, and reducing dependency on input of phosphorus fertiliser. http://dx.doi.org/10.1071/CP08920.

Daintith, J. 2009. Phosphorus. https://doi.org/10.1093/acref/9780199204632.013.3197.

Desport, B., Carpena, J., Lacout, J. L., Borschneck, D., and Gattacceca, J. 2011. Characterization of a calcium phospho-silicated apatite with iron oxide inclusions. *Journal of Crystal Growth* 316(1):164–171. https://doi.org/10.1016/j.jcrysgro.2010.12.054.

Donatello, S., Tong, D., and Cheeseman, C. R. 2010. Production of technical grade phosphoric acid from incinerator sewage sludge ash (ISSA). *Waste Management* 30(8-9):1634–1642. https://doi.org/10.1016/j.wasman.2010.04.009.

Donatello, S. and Cheeseman, C. R. 2013. Recycling and recovery routes for incinerated sewage sludge ash (ISSA): A review. *Waste Management* 33(11):2328–2340. https://doi.org/10.1016/j.wasman.2013.05.024.

Ebbers, B., Ottosen, L. M., and Jensen, P. E. 2015. Comparison of two different electrodialytic cells for separation of phosphorus and heavy metals from sewage sludge ash. *Chemosphere* 125:122–129. https://doi.org/https://doi.org/10.1016/j.chemosphere.2014.12.013.

El-Geassy, A. A., Halim, K. S. A., Bahgat, M., Mousa, E. A., El-Shereafy, E. E., and El-Tawil, A. A. 2013. Carbothermic reduction of Fe ₂ O ₃ /C compacts: comparative approach to kinetics and mechanism. *Ironmaking & Steelmaking* 40(7):534–544. https://doi.org/10.1179/1743281212Y.0000000076.

Elser, J. and Bennett, E. 2011. Phosphorus cycle: A broken biogeochemical cycle. *Nature* 478(7367):29–31. https://doi.org/10.1038/478029a.

Everaert, M. 2018. *PhD Thesis: Layered double hydroxides as slow-release phosphorus fertilizer*. Ph.D. thesis, KU Leuven.

E.Y.Tsymbal. 2005. Section 16 : Magnetic properties of materials (continued). *The University of Nebraska* Physics 92(section 16):1–19.

Fang, L., shan Li, J., Donatello, S., Cheeseman, C. R., Wang, Q., Poon, C. S., and Tsang, D. C. 2018. Recovery of phosphorus from incinerated sewage sludge ash by combined two-step extraction and selective precipitation. *Chemical Engineering Journal* 348(April):74–83. https://doi.org/10.1016/j.cej.2018.04.201.

Fang, L., Wang, Q., shan Li, J., Poon, C. S., Cheeseman, C. R., Donatello, S., and Tsang, D. C. 2020. Feasibility of wet-extraction of phosphorus from incinerated sewage sludge ash (ISSA) for phosphate fertilizer production: A critical review. *Critical Reviews in Environmental Science and Technology* 0(0):1–33. https://doi.org/10.1080/10643389.2020.1740545.

Farrokhpay, S. 2011. The significance of froth stability in mineral flotation - A review. *Advances in Colloid and Interface Science* 166(1-2):1–7. https://doi.org/10.1016/j.cis.2011.03.001.

Ferrasse, J. H., Seyssiecq, I., and Roche, N. 2003. Thermal gasification: A feasible solution for sewage sludge valorisation? *Chemical Engineering and Technology* 26(9):941–945. https://doi.org/10.1002/ceat.200301813.

Filippelli, G. M. 2008. The Global Phosphorus Cycle: Past, Present, and Future. *Elements* 4(2):89–95. https://doi.org/10.2113/GSELEMENTS.4.2.89.

Fleischer, M. 1954. The abundance and distribution of the chemical elements in the earth's crust. *Journal of Chemical Education* 31(9):446. https://doi.org/10.1021/ed031p446.

Foner, S. 1959. Versatile and sensitive vibrating-sample magnetometer. *Review of Scientific Instruments* 30(7):548–557. https://doi.org/10.1063/1.1716679.

Fonts, I., Kuoppala, E., and Oasmaa, A. 2009. Physicochemical properties of product liquid from pyrolysis of sewage sludge. *Energy and Fuels* 23(8):4121–4128. https://doi.org/10.1021/ef900300n.

Fortes, M. C., Silva, A. A., Guimarães, R. C., Ataíde, C. H., and Barrozo, M. A. 2007. Preseparation of siliceous gangue in apatite flotation. *Industrial and Engineering Chemistry Research* 46(21):7027–7029. https://doi.org/10.1021/ie070841f.

Francis, A. A. 2004. Conversion of blast furnace slag into new glass-ceramic material. *Journal of the European Ceramic Society* 24(9):2819–2824. https://doi.org/10.1016/j.jeurceramsoc.2003.08.019.

Franz, M. 2008. Phosphate fertilizer from sewage sludge ash (SSA). *Waste Management* 28(10):1809–1818. https://doi.org/10.1016/j.wasman.2007.08.011.

Frauenkron, M., Scherer, H. W., Mengel, K., Kluge, G., and Severin, K. 2009. Fertilizers, 1. General. *Ullmann's Encyclopedia of Industrial Chemistry* pages 405–428. https://doi.org/doi:10.1002/14356007.a10_323.pub3.

Froelich, P. N., Bender, M. L., Luedtke, N. A., Heath, G. R., and DeVries, T. 1982. The marine phosphorus cycle. *Am. J. Sci* 282(4):474–511.

Fujita, T. and Iwasaki I. 1989. Phosphorus Removal from Steelmaking Slags Slow-Cooled in a Non-Oxidizing Atmosphere by Magnetic Separation / Flotation. *Iron Steelmaker* 16(1):47–55.

Fytili, D. and Zabaniotou, A. 2008. Utilization of sewage sludge in EU application of old and new methods-A review. *Renewable and Sustainable Energy Reviews* 12(1):116–140. https://doi.org/10.1016/j.rser.2006.05.014.

Gad, S. C. 2005. Metals. Elsevier, New York, volume 34, page 49. https://doi.org/https://doi.org/10.1016/B0-12-369400-0/00599-8.

Gao, X., Matsuura, H., IlSohn, Wang, W., Min, D. J., and Tsukihashi, F. 2013. Phase Relationship for the CaO-SiO2-FeO-5 mass% P2O5 System with Oxygen Partial Pressure of 10-8 atm at 1673 and 1623 K. *Materials Transactions2* 54(4):544–552. https://doi.org/10.2320/matertrans.M-M2013801.

George, T. S., Hinsinger, P., and Turner, B. L. 2016. Phosphorus in soils and plants ‐facing phosphorus scarcity. *Plant and Soil* 401(1-2):1–6. https://doi.org/10.1007/s11104-016-2846-9.

Griffith, E. J., Ponnamperuma, C., and Gabel, N. W. 1977. Phosphorus, a key to life on the primitive earth. *Origins of life* 8(2):71–85. https://doi.org/10.1007/BF00927976.

Groß, B., Eder, C., Grziwa, P., Horst, J., and Kimmerle, K. 2008. Energy recovery from sewage sludge by means of fluidised bed gasification. *Waste Management* 28(10):1819–1826. https://doi.org/10.1016/j.wasman.2007.08.016.

Guedes, P., Couto, N., Ottosen, L. M., and Ribeiro, A. B. 2014. Phosphorus recovery from sewage sludge ash through an electrodialytic process. *Waste Management* 34(5):886–892. https://doi.org/10.1016/j.wasman.2014.02.021.

Guedes, P., Couto, N., Ottosen, L. M., Kirkelund, G. M., Mateus, E., and Ribeiro, A. B. 2016. Valorisation of ferric sewage sludge ashes: Potential as a phosphorus source. *Waste Management* 52:193–201. https://doi.org/10.1016/j.wasman.2016.03.040.

Guerrero, A., Goñi, S., Macías, A., and Luxán, M. P. 1999. Hydraulic activity and microstructural characterization of new fly ash-belite cements synthesized at different temperatures. *Journal of Materials Research* 14(6):2680–2687. https://doi.org/10.1557/JMR.1999.0359.

Gupta, D. K., Chatterjee, S., Datta, S., Veer, V., and Walther, C. 2014. Role of phosphate fertilizers in heavy metal uptake and detoxification of toxic metals. *Chemosphere* 108:134–144. https://doi.org/10.1016/j.chemosphere.2014.01.030.

Habashi, F. and Awadalla, F. T. 1988. In Situ and Dump Leaching of Phosphate Rock. *Industrial and Engineering Chemistry Research* 27(11):2165–2169. https://doi.org/10.1021/ie00083a035.

Halka, M., Halka, M., and Nordstrom, B. 2010. *Periodic Table of the Elements*. Facts On File Inc.

Hamed, I., Özogul, F., and Regenstein, J. M. 2016. Industrial applications of crustacean by-products (chitin, chitosan, and chitooligosaccharides): A review. *Trends in Food Science and Technology* 48:40–50. https://doi.org/10.1016/j.tifs.2015.11.007.

Herawati, N., Suzuki, S., Hayashi, K., Rivai, I. F., and Koyama, H. 2000. Cadmium, copper, and zinc levels in rice and soil of Japan, Indonesia, and China by soil type. *Bulletin of Environmental Contamination and Toxicology* 64(1):33–39. https://doi.org/10.1007/s001289910006.

Herzel, H., Krüger, O., Hermann, L., and Adam, C. 2016. Sewage sludge ash - A promising secondary phosphorus source for fertilizer production. *Science of the Total Environment* 542:1136–1143. https://doi.org/10.1016/j.scitotenv.2015.08.059.

Holford, I. C. 1997. Soil phosphorus: Its measurement, and its uptake by plants. *Australian Journal of Soil Research* 35(2):227–239. https://doi.org/10.1071/S96047.

Hong Tian, Z., hai LI, B., ming ZHANG, X., and hang JIANG, Z. 2009. Double Slag Operation Dephosphorization in BOF for Producing Low Phosphorus Steel. *Journal of Iron and Steel Research International* 16(3):6–14. https://doi.org/10.1016/S1006-706X(09)60036-4.

Imai, T. 2019. Calcination Technology for Manufacturing Mineral Fertilizer Using CaO-Enriched Sewage Sludge Ash. In Ohtake, H. and Tsuneda, S., editors, *Phosphorus Recovery and Recycling*, Springer, Singapore. https://doi.org/10.1007/978-981-10-8031-9_11.

Jaffer, Y., Clark, T. A., Pearce, P., and Parsons, S. A. 2002. Potential phosphorus recovery by struvite formation. *Water Research* 36(7):1834–1842. https://doi.org/10.1016/S0043-1354(01)00391-8.

Jantzen, H., Schugerl, K., and Helmrich, H. 1979. Improvement of the production of Rhenania phosphate fertilizer by means of investigations in a laboratory rotary kiln reactor. *Powder Technology* 23(1):1–14. https://doi.org/10.1016/0032-5910(79)85020-2.

Jiles, D. 1991. *Introduction to Magnetism and Magnetic Materials*. Taylor & Francis, 3rd edition. https://doi.org/10.1007/978-1-4615-3868-4.

Kabata-Pendias, A. 2011. *Trace elements in soils and plants*. https://doi.org/10.1201/b10158-25.

Karapetyan, K. G., Senichenkov, V. A., Zenin, G. S., and Ryabova, M. N. 2005. Kinetics of dissolution of glassy fertilizers. *Russian Journal of Applied Chemistry* 78(9):1383–1385. https://doi.org/10.1007/s11167-005-0522-6.

Kawatra, S. and Eisele, T. 1992. 1 Froth Flotation - Fundamental Principles. *Recovery of Pyrite in Coal Flotation: Entrainment or Flotation* pages 1–30.

Keyzer, M. 2010. Towards a Closed Phosphorus Cycle. *De Economist* 158(4):411–425. https://doi.org/10.1007/s10645-010-9150-5.

Kimura, M. 2016. Testing Methods for Fertilizers. *Incorporated Administrative Agency, Food and Agricultural Materials Inspection Center (FAMIC)* pages 1–370.

King, R. 2001. *Modeling and Simulation of Mineral Processing Systems*. Butterworth-Heinemann. https://doi.org/https://doi.org/10.1016/C2009-0-26303-3.

K.Kumazawa. 1997. Use of Sewage Sludge for Agriculture in Japan. *Proceedings of consultants meetings* (4(1)):111–127.

Klug, A. 1968. Rosalind Franklin and the discovery of the structure of DNA. *Nature* 219(5156):808–844. https://doi.org/10.1038/219808a0.

Koizumi, S., Miki, T., and Nagasaka, T. 2016. Enrichment of Phosphorus Oxide in Steelmaking Slag by Utilizing Capillary Action. *Journal of Sustainable Metallurgy* 2(1):38–43. https://doi.org/10.1007/s40831-015-0035-3.

Koppelaar, R. H. and Weikard, H. P. 2013. Assessing phosphate rock depletion and phosphorus recycling options. *Global Environmental Change* 23(6):1454–1466. https://doi.org/10.1016/j.gloenvcha.2013.09.002.

Kraft, M. D. 2015. Phosphorus and calcium: A review for the adult nutrition support clinician. *Nutrition in Clinical Practice* 30(1):21–33. https://doi.org/10.1177/0884533614565251.

Krüger, O., Grabner, A., and Adam, C. 2014. Complete survey of German sewage sludge ash. *Environmental Science and Technology* 48(20):11811–11818. https://doi.org/10.1021/es502766x.

Kumar, B. and Chen, C. H. 1994. Magnetic properties of materials in the CaO-P2O 5-Fe2O3 system. *Journal of Applied Physics* 75(10):6760–6762. https://doi.org/10.1063/1.356845.

Lane, G. A., Barnes, M. W., Klimkiewicz, M., and Brown, P. W. 1992. Hydration in the System Ca2SiO4‐Ca3(PO4)2 at 90°C. *Journal of the American Ceramic Society* 75(6):1423–1429. https://doi.org/10.1111/j.1151-2916.1992.tb04204.x.

Lazoryak, B. I., Belik, A. A., Kotov, R. N., Leonidov, I. A., Mitberg, E. B., Karelina, V. V., Kellerman, D. G., Stefanovich, S. Y., and Avetisov, A. K. 2003. Reduction and re-oxidation behavior of calcium iron phosphate, Ca9Fe(PO4)7. *Chemistry of Materials* 15(3):625–631. https://doi.org/10.1021/cm010851l.

Lema, J. and Suarez, S. 2017. *Innovative Wastewater Treatment & Resource Recovery Technologies: Impacts on Energy, Economy and Environment*, volume 16. https://doi.org/10.2166/9781780407876.

Li, W.-K., Zhou, G.-D., and Wai Mak, T. C. 2008. Structural Chemistry of Group 15 Elements. In *Advanced Structural Inorganic Chemistry*, Oxford University Press, Oxford. https://doi.org/10.1093/acprof:oso/9780199216949.003.0015.

Lin, L., Bao, Y.-p., Wang, M., Jiang, W., and Zhou, H.-m. 2014. Separation and Recovery of Phosphorus from P-bearing Steelmaking Slag. *Journal of Iron and Steel Research International* 21(5):496–502. https://doi.org/10.1016/S1006-706X(14)60077-7.

Liu, C., Zhang, W., and Li, H. 2019. Selective flotation of apatite from calcite using 2-phosphonobutane-1,2,4-tricarboxylic acid as depressant. *Minerals Engineering* 136(December 2018):62–65. https://doi.org/10.1016/j.mineng.2019.03.003.

Liu, Y. and Qu, H. 2016. Design and optimization of a reactive crystallization process for high purity phosphorus recovery from sewage sludge ash. *Journal of Environmental Chemical Engineering* 4(2):2155–2162. https://doi.org/10.1016/j.jece.2016.03.042.

Lofthouse, C. H. 1981. Intensity Magnetic Separator. *IEEE Transaction on Magnetics* MAG-17(6):3302–3304.

Lynch, D. 2009. Winning the global race for solar silicon. https://doi.org/10.1007/s11837-009-0166-8.

Lynn, C. J., Dhir, R. K., and Ghataora, G. S. 2016. Sewage sludge ash characteristics and potential for use in bricks, tiles and glass ceramics. *Water Science and Technology* 74(1):17–29. https://doi.org/10.2166/wst.2016.040.

Lynn, C. J., Dhir, R. K., Ghataora, G. S., and West, R. P. 2015. Sewage sludge ash characteristics and potential for use in concrete. *Construction and Building Materials* 98:767–779. https://doi.org/10.1016/j.conbuildmat.2015.08.122.

Maciá, E. 2005. The role of phosphorus in chemical evolution. *Chemical Society Reviews* 34(8):691–701. https://doi.org/10.1039/b416855k.

Malvern Instruments. 2011. Zeta potential: An Introduction in 30 minutes. *Zetasizer Nano Serles Technical Note. MRK654-01* 2:1–6. https://doi.org/10.1017/CBO9781107415324.004.

Malvern Panalytical. 2017. Investigating the Impact of Particle Characteristics on Suspension Rheology. https://www.azom.com/article.aspx?ArticleID=13727.

Manchõn, A., Alkhraisat, M., Rueda-Rodriguez, C., Torres, J., Prados-Frutos, J. C., Ewald, A., Gbureck, U., Cabrejos-Azama, J., Rodriguez-González, A., and Lõpez-Cabarcos, E. 2015. Silicon calcium phosphate ceramic as novel biomaterial to simulate the bone regenerative properties of autologous bone. *Journal of Biomedical Materials Research - Part A* 103(2):479–488. https://doi.org/10.1002/jbm.a.35196.

Mattenberger, H., Fraissler, G., Brunner, T., Herk, P., Hermann, L., and Obernberger, I. 2008. Sewage sludge ash to phosphorus fertiliser: Variables influencing heavy metal removal during thermochemical treatment. *Waste Management* 28(12):2709–2722. https://doi.org/10.1016/j.wasman.2008.01.005.

McBride, M. B., Richards, B. K., and Steenhuis, T. 2004. Bioavailability and crop uptake of trace elements in soil columns amended with sewage sludge products. *Plant and Soil* 262(1-2):71–84. https://doi.org/10.1023/B:PLSO.0000037031.21561.34.

McCLements, D. J. M. C. C. and Masubon Thongngam. 2004. Characterization of Interactions between Chitosan and an Anionic Surfactant. *Journal of Agricultural and Food Chemistry* 52:987–991.

Mclaughlin, M., Tiller, K., Naidu, R., and Stevens, D. 1996. Review: the behaviour and environmental impact of contaminants in fertilizers. *Australian Journal of Soil Research* 34(1):1. https://doi.org/10.1071/SR9960001.

Menad, N., Kanari, N., and Save, M. 2014. Recovery of high grade iron compounds from LD slag by enhanced magnetic separation techniques. *International Journal of Mineral Processing* 126:1–9. https://doi.org/10.1016/j.minpro.2013.11.001.

Mesa, D. and Brito-Parada, P. R. 2019. Scale-up in froth flotation: A state-of-the-art review. *Separation and Purification Technology* 210(April 2018):950–962. https://doi.org/10.1016/j.seppur.2018.08.076.

Metson, G. S., Bennett, E. M., and Elser, J. J. 2012. The role of diet in phosphorus demand. *Environmental Research Letters* 7(4). https://doi.org/10.1088/1748-9326/7/4/044043.

Minerals Education Coalition. 2020. Picture of phosphorus rock. Available at: `https://mineralseducationcoalition.org/wp-content/uploads/Phosphorite_136389572.jpg`.

Ministry of Agriculture Forestry and Fisheries (MAFF). 2018. Regulations for Compound Fertilizer. Retrieved from: `https://chemycal.com/news/a754c633-aaeb-4fd9-bdec-ab7b6437cf06/Japan{_}amends{_}Standards{_}for{_}normal{_}fertilizers`.

Miyazaki, T. and Jin, H. 2012. *The Physics of Ferromagnetism*, volume 158 of *Springer Series in Materials Science*. Springer Berlin Heidelberg. https://doi.org/10.1524/zkri.1990.190.3-4.315.

Molnar, C. and Gair, J. 2013. The structure of DNA. In *Concepts of Biology - 1st Canadian Edition*, chapter 3. https://opentextbc.ca/biology/.

Morita, K., Guo, M., Oka, N., and Sano, N. 2002. Resurrection of the iron and phosphorus resource in steel-making slag. *Journal of Material Cycles and Waste …* pages 93–101. http://link.springer.com/article/10.1007/s10163-001-0067-6.

Müller, E., Berger, R., Blass, E., Sluyts, D., and Pfennig, A. 2008. Liquid-Liquid Extraction https://doi.org/doi:10.1002/14356007.b03_06.pub2.

Murakami, T., Suzuki, Y., Nagasawa, H., Yamamoto, T., Koseki, T., Hirose, H., and Okamoto, S. 2009. Combustion characteristics of sewage sludge in an incineration plant for energy recovery. *Fuel Processing Technology* 90(6):778–783. https://doi.org/https://doi.org/10.1016/j.fuproc.2009.03.003.

Mussig, C. 2013. ATP-ADP cycle. Available at `https://commons.wikimedia.org/wiki/File:ADP_ATP_cycle.png`.

Nair, A. K., Gautieri, A., Chang, S. W., and Buehler, M. J. 2013. Molecular mechanics of mineralized collagen fibrils in bone. *Nature Communications* 4:1724–1729. https://doi.org/10.1038/ncomms2720.

Nanzer, S., Oberson, A., Berger, L., Berset, E., Hermann, L., and Frossard, E. 2014. The plant availability of phosphorus from thermo-chemically treated sewage sludge ashes as studied by 33P labeling techniques. *Plant and Soil* 377(1-2):439–456. https://doi.org/10.1007/s11104-013-1968-6.

Navarro-Alarcon, M., Zambrano, E., Moreno-Montoro, M., Agil, A., and Olalla, M. 2012. Duplicate portion sampling combined with spectrophotometric analysis affords the most accurate results when assessing daily dietary phosphorus intake. *Nutrition Research* 32(8):573–580. https://doi.org/10.1016/j.nutres.2012.06.013.

Nipattummakul, N., Ahmed, I. I., Kerdsuwan, S., and Gupta, A. K. 2010. Hydrogen and syngas production from sewage sludge via steam gasification. *International Journal of Hydrogen Energy* 35(21):11738–11745. https://doi.org/10.1016/j.ijhydene.2010.08.032.

Noori, N., Sims, J. J., Kopple, J. D., Shah, A., Mehrotra, R., and Kovesdy, C. P. 2010. ch (April).

Oates, T. 2010. Lime and Limestone pages 1–53. Available at: `https://doi.org/10.1002/0471238961.1209130507212019.a01.pub3`.

Ohtake, H. and Okano, K. 2015. Development and Implementation of Technologies for Recycling Phosphorus in Secondary Resources in Japan 19(1):1–31.

Ohura, K., Nakamura, T., and Yamamuro, T. 1991. Bone-bonding ability of Pz05-Free CaO SiOz glasses 25:357–365.

Onesippe, C. and Lagerge, S. 2008. Study of the complex formation between sodium dodecyl sulfate and chitosan. *Colloids and Surfaces A: Physicochemical and Engineering Aspects* 317(1-3):100–108. https://doi.org/10.1016/j.colsurfa.2007.10.002.

Ottosen, L. M., Jensen, P. E., and Kirkelund, G. M. 2014. Electrodialytic Separation of Phosphorus and Heavy Metals from Two Types of Sewage Sludge Ash. *Separation Science and Technology (Philadelphia)* 49(12):1910–1920. https://doi.org/10.1080/01496395.2014.904347.

Palou, M., Majling, J., Dovál, M., Kozanková, J., and Mojumdar, S. C. 2005. Formation and stability of crystallohydrates in the non-equilibrium system during hydration of sab cements. *Ceramics - Silikaty* 49(4):230–236.

Pan, H.-B. and Darvell, B. W. 2009. Calcium Phosphate Solubility: The Need for Re-Evaluation. *Crystal Growth & Design* 9(2):639–645. https://doi.org/10.1021/cg801118v.

Parks, G. A. 1965. The Isoelectric Points of Solid Oxides, Solid Hydroxides, and Aqueous Hydroxo Complex Systems. *Chemical Reviews* 65(2):177–198. https://doi.org/10.1021/cr60234a002.

Partridge, A. and Smith, G. 1971. Flotation and Adsorption Characteristics of the Hematite-Dodecylamine-Starch System. *Canadian Metallurgical Quarterly* 10(3):229–234. https://doi.org/10.1179/cmq.1971.10.3.229.

Pasek, M. A. 2008. Rethinking early Earth phosphorus geochemistry. *Proceedings of the National Academy of Sciences* 105(3):853 LP – 858. https://doi.org/10.1073/pnas.0708205105.

Paytan, A. and McLaughlin, K. 2007. The oceanic phosphorus cycle. *Chemical Reviews* 107(2):563–576. https://doi.org/10.1021/cr0503613.

Peirce, J. J., Weiner, R. F., and Vesilind, P. A. 1998. Chapter 8 - Wastewater Treatment. Butterworth-Heinemann, Woburn, pages 105–123. https://doi.org/https://doi.org/10.1016/B978-075069899-3/50009-2.

Peralta-Videa, J. R., Lopez, M. L., Narayan, M., Saupe, G., and Gardea-Torresdey, J. 2009. The biochemistry of environmental heavy metal uptake by plants: implications for the food chain. *The international journal of biochemistry & cell biology* 41(8-9):1665–1677. https://doi.org/10.1016/j.biocel.2009.03.005.

Petzet, S., Peplinski, B., and Cornel, P. 2012. On wet chemical phosphorus recovery from sewage sludge ash by acidic or alkaline leaching and an optimized combination of both. *Water Research* 46(12):3769–3780. https://doi.org/10.1016/j.watres.2012.03.068.

Pietak, A. M., Reid, J. W., Stott, M. J., and Sayer, M. 2007. Silicon substitution in the calcium phosphate bioceramics. *Biomaterials* 28(28):4023–4032. https://doi.org/10.1016/j.biomaterials.2007.05.003.

Prochnow, L. I., Kiehl, J. C., and Van Raij, B. 1998. Plant availability of phosphorus in the neutral ammonium citrate fraction of Brazilian acidulated phosphates. *Nutrient Cycling in Agroecosystems* 52(1):61–65. https://doi.org/10.1023/A:1016335612914.

Ptáček, P., Opravil, T., Šoukal, F., Havlica, J., and Holešinský, R. 2013. Kinetics and mechanism of formation of gehlenite, Al-Si spinel and anorthite from the mixture of kaolinite and calcite. *Solid State Sciences* 26:53–58. https://doi.org/10.1016/j.solidstatesciences.2013.09.014.

Qian, T.-t. and Jiang, H. 2014. Migration of phosphorus in sewage sludge during different thermal treatment processes. *Sustainable chemistry & engineering* 2:1411–1419. https://doi.org/10.1021/sc400476j.

Rafael, R. B. A., Fernandez-Marcos, M. L., Cocco, S., Ruello, M. L., Weindorf, D. C., Cardelli, V., and Corti, G. 2018. Assessment of Potential Nutrient Release from Phosphate Rock and Dolostone for Application in Acid Soils. *Pedosphere* 28(1):44–58. https://doi.org/10.1016/S1002-0160(17)60437-5.

Rapf, M. 2012. RecoPhos and other thermo-chemical processes for the recovery of phosphorus from sewage sludge. In *Recy and Depotech*. Leoben, Austria, July, page 6.

Raymond, N. S., Müller Stöver, D., Richardson, A. E., Nielsen, H. H., and Stoumann Jensen, L. 2018. Biotic strategies to increase plant availability of sewage sludge ash phosphorus. *Journal of Plant Nutrition and Soil Science* pages 1–12. https://doi.org/10.1002/jpln.201800154.

Reichardt, C. 2010. Classification of Solvents. https://doi.org/10.1002/9783527632220.ch3.

Ros, A., Montes-Moran, M. A., Fuente, E., Nevskaia, D. M., and Martin, M. J. 2006. Dried sludges and sludge-based chars for H2S removal at low temperature: Influence of sewage sludge characteristics. *Environmental Science and Technology* 40(1):302–309. https://doi.org/10.1021/es050996j.

Roy, A. 1969. Phosphorus-Silicon Interactions in Soils and Plants 9981:239.

Sadowski, Z. and Polowczyk, I. 2004. Agglomerate flotation of fine oxide particles. *International Journal of Mineral Processing* 74(1-4):85–90. https://doi.org/10.1016/j.minpro.2003.09.007.

Salaguer, J.-L. 2002. SURFACTANTS Types and Uses. *Laboratory of Formulation, Interfaces, Rheology and Processes* 2:1–49. https://doi.org/10.1016/j.marpolbul.2013.12.019.

Samolada, M. C. and Zabaniotou, A. A. 2014. Comparative assessment of municipal sewage sludge incineration, gasification and pyrolysis for a sustainable sludge-to-energy management in Greece. *Waste Management* 34(2):411–420. https://doi.org/https://doi.org/10.1016/j.wasman.2013.11.003.

Santos, W. O., Mattiello, E. M., Barreto, M. S. C., and Cantarutti, R. B. 2019. Acid ammonium citrate as P extractor for fertilizers of varying solubility. *Revista Brasileira de Ciencia do Solo* 43:1–12. https://doi.org/10.1590/18069657rbcs20180072.

Sato, M. and Nakahira, A. 2013. Influence of Fe addition to hydroxyapatite by aqueous solution process. *Journal of the Ceramic Society of Japan* 121(1413):422–425. https://doi.org/10.2109/jcersj2.121.422.

Schachtman, D. P., Reid, R. J., and Ayling, S. M. 1998. Update on phosphorus uptake phosphorus uptake by plants : From soil to cell. *Molecular And General Genetics* 116(2):447–453. https://doi.org/10.1104/pp.116.2.447.

Schaum, C., Cornel, P., and Jardin, N. 2007. *Phosphorus recovery from sewage sludge ash- a wet chemical approach*.

Schnug, E. and De Kok, L. 2016. *Phosphorus in Agriculture: 100 % Zero*. Springer Netherlands. https://books.google.co.jp/books?id=lBNkDAAAQBAJ.

Schütte, T., Niewersch, C., Wintgens, T., and Yüce, S. 2015. Phosphorus recovery from sewage sludge by nanofiltration in diafiltration mode. *Journal of Membrane Science* 480:74–82. https://doi.org/10.1016/j.memsci.2015.01.013.

Serena, S., Caballero, A., De Aza, P. N., and Sainz, M. A. 2015. New evaluation of the in vitro response of silicocarnotite monophasic material. *Ceramics International* 41(8):9412–9419. https://doi.org/10.1016/j.ceramint.2015.03.319.

Shenoy, V. V. and Kalagudi, G. M. 2005. Enhancing plant phosphorus use efficiency for sustainable cropping. *Biotechnology Advances* 23(7-8):501–513. https://doi.org/http://dx.doi.org/10.1016/j.biotechadv.2005.01.004.

Sierra, H., Cordova, M., Chen, C. S. J., Rajadhyaksha, M., Sabbagh, Y., Giral, H., Caldas, Y., Levi, M., and Schiavi, S. C. 2011. Intestinal phosphate transport. *Advances in chronic kidney disease* 18(2):85–90. https://doi.org/10.1053/j.ackd.2010.11.004.

Singh, R. K. and Srinivasan, A. 2010. Apatite-forming ability and magnetic properties of glass-ceramics containing zinc ferrite and calcium sodium phosphate phases. *Materials Science and Engineering C* 30(8):1100–1106. https://doi.org/10.1016/j.msec.2010.06.003.

Sis, H. and Chander, S. 2003. Reagents used in the flotation of phosphate ores: A critical review. *Minerals Engineering* 16(7):577–585. https://doi.org/10.1016/S0892-6875(03)00131-6.

Smith, S. R. 2009. A critical review of the bioavailability and impacts of heavy metals in municipal solid waste composts compared to sewage sludge. *Environment International* 35(1):142–156. https://doi.org/10.1016/j.envint.2008.06.009.

Smol, M., Kulczycka, J., Henclik, A., Gorazda, K., and Wzorek, Z. 2015. The possible use of sewage sludge ash (SSA) in the construction industry as a way towards a circular economy. *Journal of Cleaner Production* 95:45–54. https://doi.org/10.1016/j.jclepro.2015.02.051.

Stahleisen., V. and Verein Deutscher Eisenhuttenleute (R.F.A). 1995. *Slag atlas*. Verlag Stahleisen GmbH, Dusseldorf.

Stasta, P., Boran, J., Bebar, L., Stehlik, P., and Oral, J. 2006. Thermal processing of sewage sludge. *Applied Thermal Engineering* 26(13):1420–1426. https://doi.org/10.1016/j.applthermaleng.2005.05.030.

Stemann, J., Peplinski, B., and Adam, C. 2015. Thermochemical treatment of sewage sludge ash with sodium salt additives for phosphorus fertilizer production - Analysis of underlying chemical reactions. *Waste Management* 45:385–390. https://doi.org/10.1016/j.wasman.2015.07.029.

Sunintaboon, P., Pumduang, K., Vongsetskul, T., Pittayanurak, P., Anantachoke, N., Tuchinda, P., and Durand, A. 2012. One-step preparation of chitosan/sodium dodecyl sulfate-stabilized oil-in-water emulsion of Zingiber cassumunar Roxb. oil extract. *Colloids and Surfaces A: Physicochemical and Engineering Aspects* 414:151–159. https://doi.org/10.1016/j.colsurfa.2012.07.031.

Sutherland, K. L. 1948. Physical chemistry of flotation. XI: Kinetics of the flotation process. *Journal of Physical and Colloid Chemistry* 52(2):394–425. https://doi.org/10.1021/j150458a013.

Suzuki, S., Tanaka, M., and Kaneko, T. 1997. Glass-ceramic from sewage sludge ash. *Journal of materials science* 2:1775–1779. https://doi.org/10.1023/a:1018584202392.

Svoboda, J. 2001. A realistic description of the process of high-gradient magnetic separation. *Minerals Engineering* 14(11):1493–1503. https://doi.org/10.1016/S0892-6875(01)00162-5.

Takahashi, H. 2007a. Study on Sewage Sludge Gasification. http://www.gesui.metro.tokyo.jp/english/tec_papers/technical/tp0702.pdf.

Takahashi, H. 2007b. Study on Sewage Sludge Gasification. *Proceedings of the Water Environment Federation* 2007:4265–4272. https://doi.org/10.2175/193864707787974689.

Takeda, E., Taketani, Y., Sawada, N., Sato, T., and Yamamoto, H. 2004. The regulation and function of phosphate in the human body. *BioFactors* 21(1-4):345–355. https://doi.org/10.1002/biof.552210167.

Taylor, A. W. 1961. Siliceous Materials in Plant Nutrition, Review of the Effects of Siliceous Dressings on the Nutrient Status of Soils. *Journal of Agricultural and Food Chemistry* 9(2):163–165. https://doi.org/10.1021/jf60114a022.

Teranishi, D. Y. 1968. *The effect of silicon, phosphorus and soil pH and their interactions on yield and nutrient uptake of sugar cane.* Master's thesis, University of Hawaii.

Thongngam, M. and McClements, D. J. 2005. Influence of pH, ionic strength, and temperature on self-association and interactions of sodium dodecyl sulfate in the absence and presence of chitosan. *Langmuir* 21(1):79–86. https://doi.org/10.1021/la048711o.

Traoré, K., Kabré, T. S., and Blanchart, P. 2003. Gehlenite and anorthite crystallisation from kaolinite and calcite mix. *Ceramics International* 29(4):377–383. https://doi.org/10.1016/S0272-8842(02)00148-7.

Uchiyama, S., Kondo, S., and Takayasu, M. 1976. Performance on paralell stream type magnetic filter for HGMS. *IEEE Transaction on Magnetics* MAG-12(6). https://doi.org/10.1017/CBO9781107415324.004.

United Nations Population Division. 2018. Urban population (% of total population) - Japan. Available at: `https://data.worldbank.org/indicator/SP.URB.TOTL.IN.ZS?locations=JP`.

van Dijk, K. C., Lesschen, J. P., and Oenema, O. 2016. Phosphorus flows and balances of the European Union Member States. *Science of the Total Environment* 542:1078–1093. https://doi.org/10.1016/j.scitotenv.2015.08.048.

Van Vuuren, D. P., Bouwman, A. F., and Beusen, A. H. W. 2010. Phosphorus demand for the 1970-2100 period: A scenario analysis of resource depletion. *Global Environmental Change* 20(3):428–439. https://doi.org/10.1016/j.gloenvcha.2010.04.004.

Vesilind, P. A. and Ramsey, T. B. 1996. Effect of Drying Temperature On the Fuel Value of Wastewater Sludge. *Waste Management & Research* 14(2):189–196. https://doi.org/10.1177/0734242X9601400208.

Villalba, G., Liu, Y., Schroder, H., and Ayres, R. U. 2008. Global phosphorus flows in the industrial economy from a production perspective. *Journal of Industrial Ecology* 12(4):557–569. https://doi.org/10.1111/j.1530-9290.2008.00050.x.

Vogel, C., Exner, R. M., and Adam, C. 2013. Heavy metal removal from sewage sludge ash by thermochemical treatment with polyvinylchloride. *Environmental Science and Technology* 47(1):563–567. https://doi.org/10.1021/es300610e.

Werther, J. and Ogada, T. 1999. Sewage sludge combustion. *Progress in Energy and Combustion Science* 25(1):55–116. https://doi.org/10.1016/S0360-1285(98)00020-3.

Wikimedia-Commons, . 2014. Phosphorus cycle. Available at: `https://commons.wikimedia.org/wiki/File:Phosphorus_Cycle_copy.jpg`.

Wills, B. A. and Finch, J. A. 2016. Chapter 12 - Froth Flotation. In Wills, B. A. and Finch, J. A. B. T. W. M. P. T. E. E., editors, *Wills' Mineral Processing Technology*, Butterworth-Heinemann, Boston, pages 265–380. https://doi.org/https://doi.org/10.1016/B978-0-08-097053-0.00012-1.

Withers, P., Elser, J., Hilton, J., Ohtake, H., Schipper, W., and van Dijk, K. 2015. Greening the global phosphorus cycle: how green chemistry can help achieve planetary P sustainability. *Green Chemistry* 17(4):2087–2099. https://doi.org/10.1039/C4GC02445A.

Wollmann, I., Gauro, A., Müller, T., and Möller, K. 2018. Phosphorus bioavailability of sewage sludge-based recycled fertilizers. *Journal of Plant Nutrition and Soil Science* 181(2):158–166. https://doi.org/10.1002/jpln.201700111.

Yan, N. and Masliyah, J. H. 1997. Creaming Behavior of Solids-Stabilized Oil-in-Water Emulsions. *Industrial and Engineering Chemistry Research* 36(4):1122–1129. https://doi.org/10.1021/ie960360o.

Yang, R., Li, H., Huang, M., Yang, H., and Li, A. 2016. A review on chitosan-based flocculants and their applications in water treatment. *Water Research* 95(2015):59–89. https://doi.org/10.1016/j.watres.2016.02.068.

Yaroshevsky, A. A. 2006. Abundances of chemical elements in the Earth's crust. *Geochemistry International* 44(1):48–55. https://doi.org/10.1134/S001670290601006X.

Yokoyama, K., Kubo, H., Mori, K., Okada, H., Takeuchi, S., and Nagasaka, T. 2007. Separation and recovery of phosphorus from steelmaking slags with the aid of a strong magnetic field. *ISIJ International* 47(10):1541–1548. https://doi.org/10.2355/isijinternational.47.1541.

Zunaidi, A. A., Lim, L. H., and Metali, F. 2020. Assessments of Heavy Metals in Commercially Available Fertilizers in Brunei Darussalam. *Agricultural Research* https://doi.org/10.1007/s40003-020-00500-4.